

For Reference

NOT TO BE TAKEN FROM THIS ROOM

Ex LIBRIS
UNIVERSITATIS
ALBERTAEANAE







THE UNIVERSITY OF ALBERTA

URANIUM-LEAD GEOCHRONOLOGY OF KENORAN ROCKS
AND MINERALS OF THE CHARLES LAKE AREA, ALBERTA.

BY



KUO SAY LEE, B.Eng.

A THESIS

SUBMITTED TO THE FACULTY OF GRADUATE STUDIES AND RESEARCH
IN PARTIAL FULFILMENT OF THE REQUIREMENTS FOR THE DEGREE

OF

MASTER OF SCIENCE

DEPARTMENT OF GEOLOGY

EDMONTON, ALBERTA

Spring, 1972.



THE UNIVERSITY OF ALBERTA
FACULTY OF GRADUATE STUDIES
AND RESEARCH

The undersigned certify that they have read and recommend to the Faculty of Graduate Studies and Research for acceptance, a thesis entitled 'Uranium-lead geochronology of Kenoran rocks and minerals of the Charles Lake area, Alberta' submitted by Kuo Say Lee, B. Eng., in partial fulfilment for the degree of Master of Science.

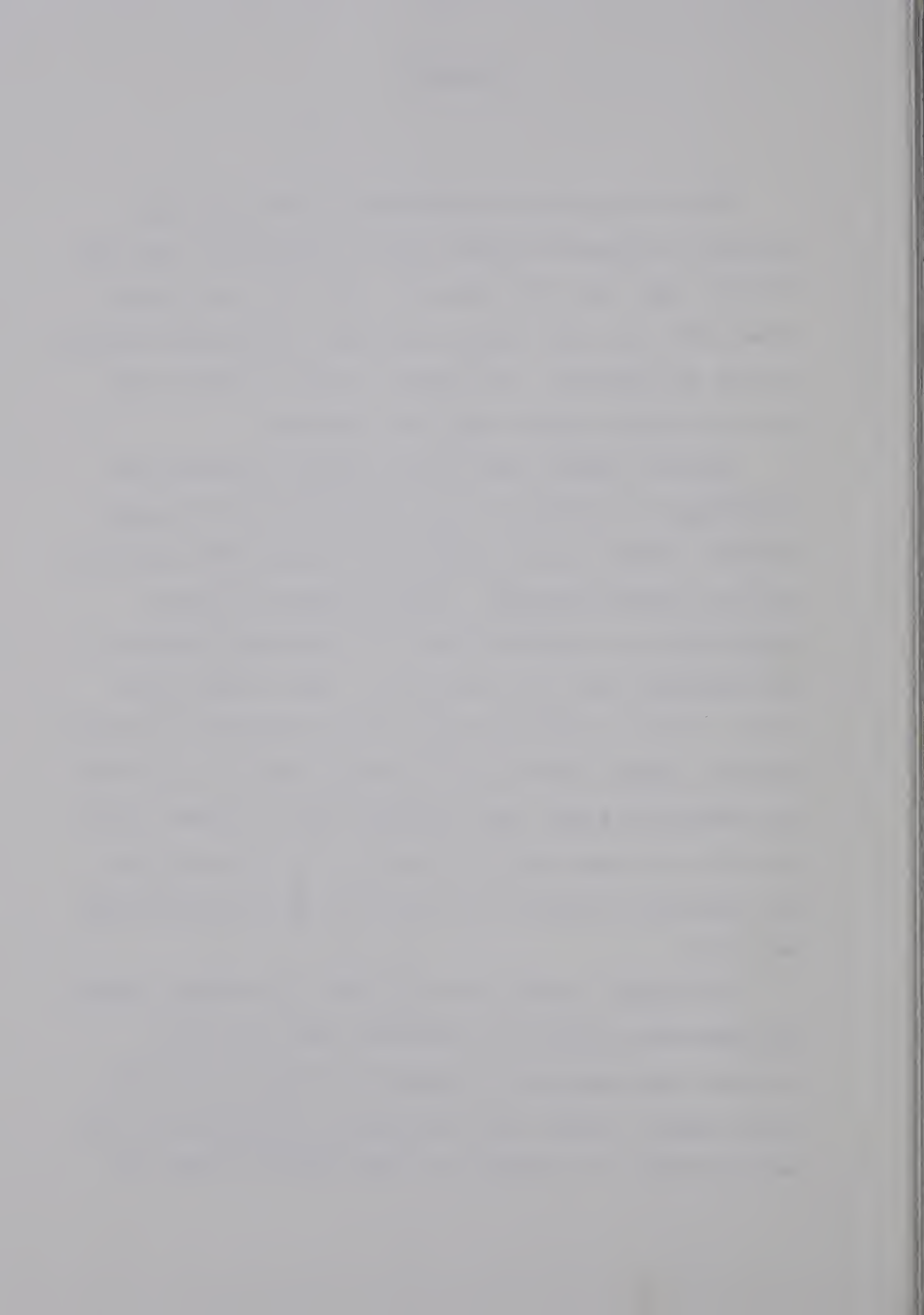


ABSTRACT

The U-Pb method of radiometric dating has been applied to probable Archean rocks and minerals from the Charles Lake area, N.E.Alberta. U-Pb ages were determined for five rock samples and their associated minerals, zircon and apatite. Pb isotopic ratios of whole rock and K-feldspar samples were also examined.

Mineral phases under study (zircon, apatite and K-feldspar) are shown to have been disturbed or isotopically "reset" by the Hudsonian Orogeny (1800—1900 m.y. ago) to varying degrees. Zircon samples have been subjected to a combined effect of continuous diffusion and episodic lead loss mechanism. Some zircons have been, in part, recrystallized during the Hudsonian event. Apatite samples tend to give younger apparent ages than the Hudsonian event, most probably due to greater uncertainties in common lead correction. Pb incorporation or resetting in apatite apparently occurred around 1800 m.y. ago.

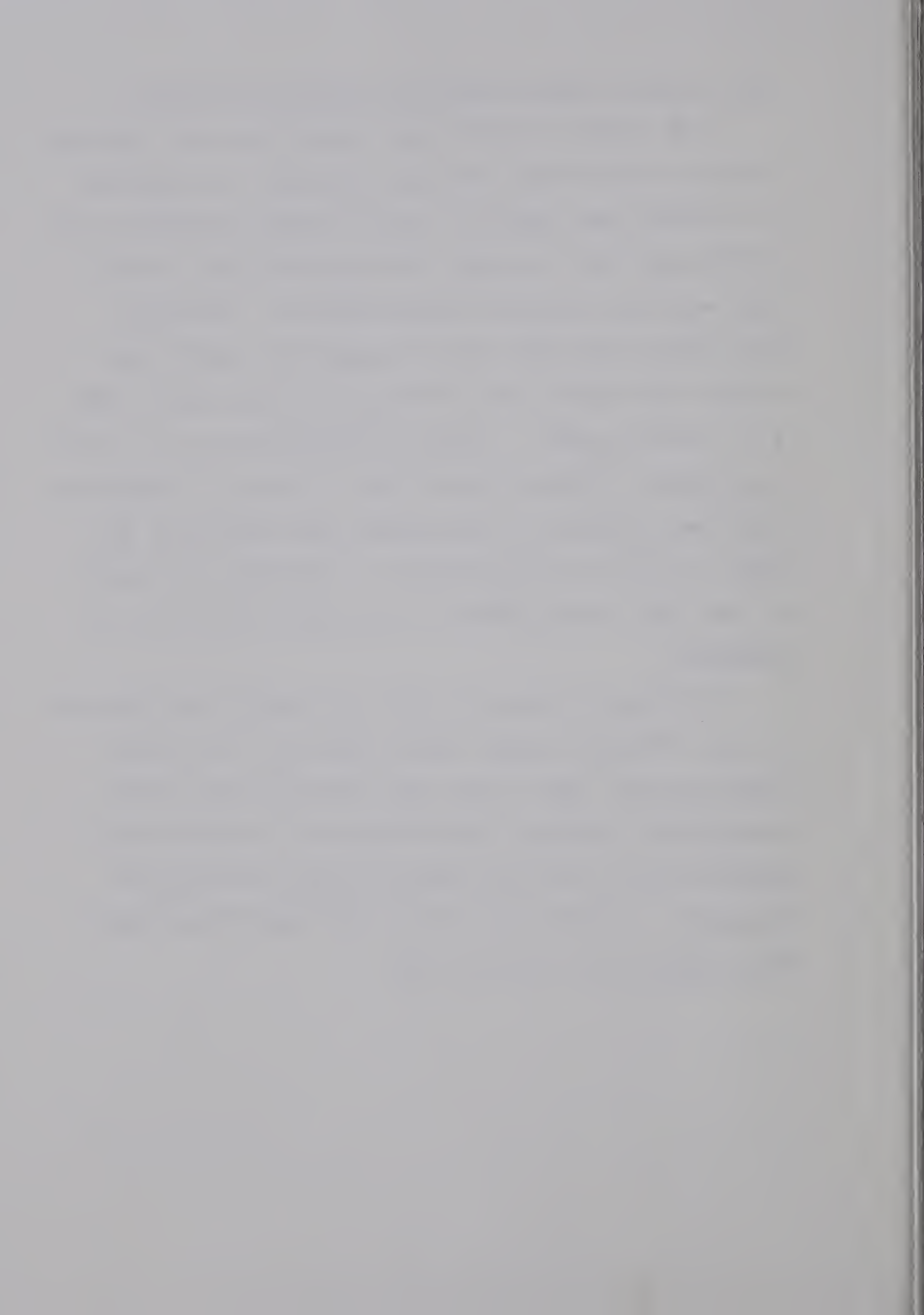
K-feldspar leads appear to have a two-stage history and generally display an anomalous lead character. Initial lead homogeneity between K-feldspar and whole rock samples (except one) existed at the Hudsonian time, most probably as a result of lead remixing within the



rock-feldspar system caused by the Hudsonian event.

U-Pb system in whole rock samples have not remained entirely closed after the rock formation, as indicated by a primary age (2500 m.y. ago or younger obtained from a U-Pb whole rock isochron interpretation and a whole rock modified concordia interpretation). (Previous Rb-Sr whole rock dates on six pegmatites cutting the present rock types give a "minimum" primary age of 2550 m.y. for the rocks). A Pb-Pb interpretation of the rock leads gives a primary age of 2500 + 100 m.y., indicating that the variation in the primary age obtained by the whole rock U-Pb interpretations is possibly the result of some open system effects in U system after the rock formation.

Pb isotopic ratios of the rock samples are compared to the K-feldspar leads, three additional rock leads from the area, and to four rock and one galena leads representing "younger" (post-kinematic) intrusion and mineralization from the adjacent Andrew Lake area to the east. A three-stage history for these rock leads best explains the isotopic data.



ACKNOWLEDGEMENTS

The writer wishes to express his deep gratefulness to his supervisor, Dr. H.Baadsgaard, who initially introduced the thesis project and patiently directed and assisted in the analytical work. His many idea-provoking discussions with the writer are also invaluable.

Dr. G.L.Cumming of the Department of Physics kindly allowed the writer to use the Mass Spectrometry facilities and a Fortran computer program written by him. His help and encouragement have proven to be very beneficial.

Three rock lead analyses using volatilization method were made by Mr. F.Tsong of the Department of Physics and were used for interpretation in the present thesis. His cooperation is gratefully acknowledged.

Technicians and graduate students of the Mass Spectrometry Laboratory, Department of Physics, provided valuable assistance and encouragement. Their friendliness and concern is deeply appreciated.

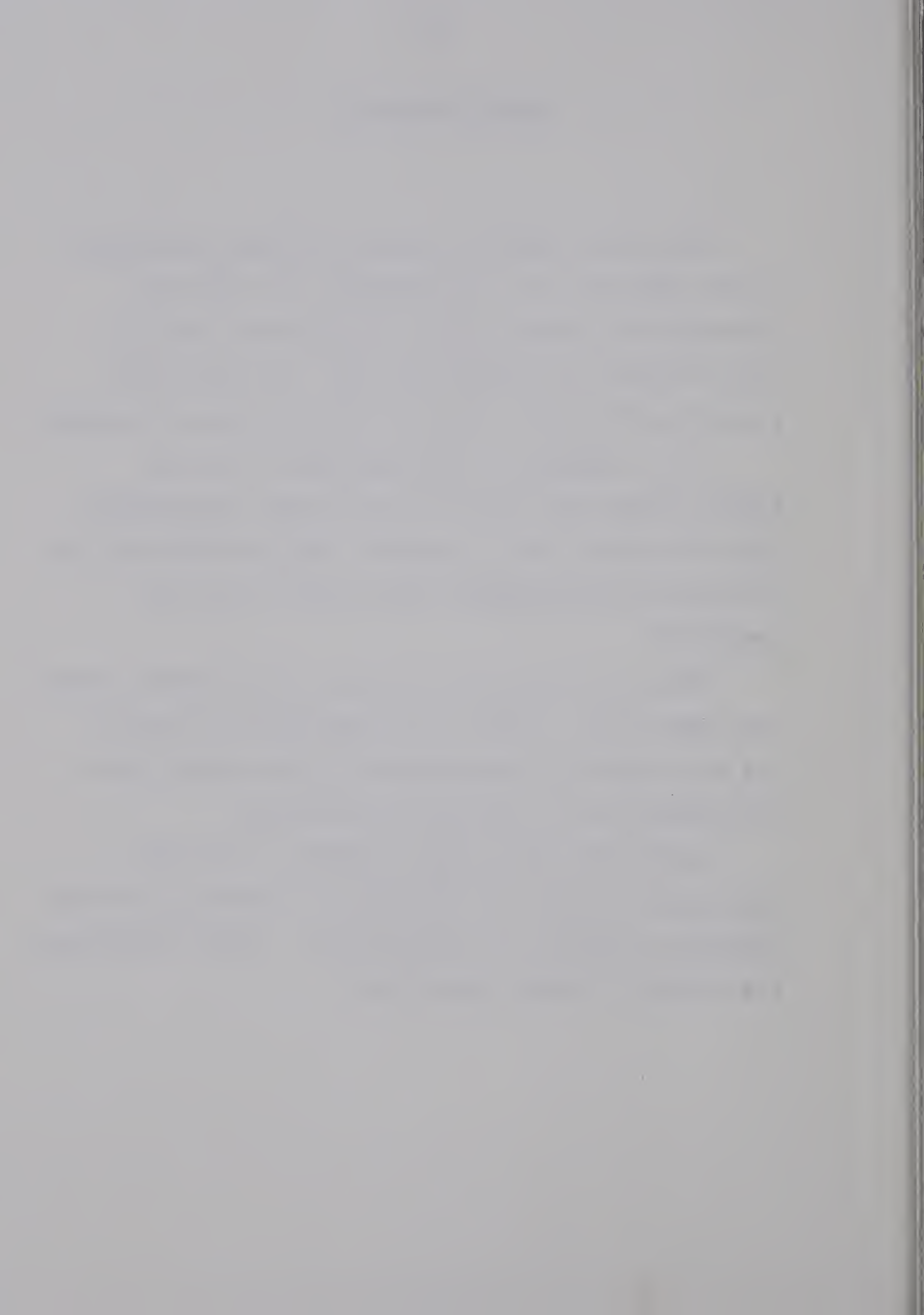
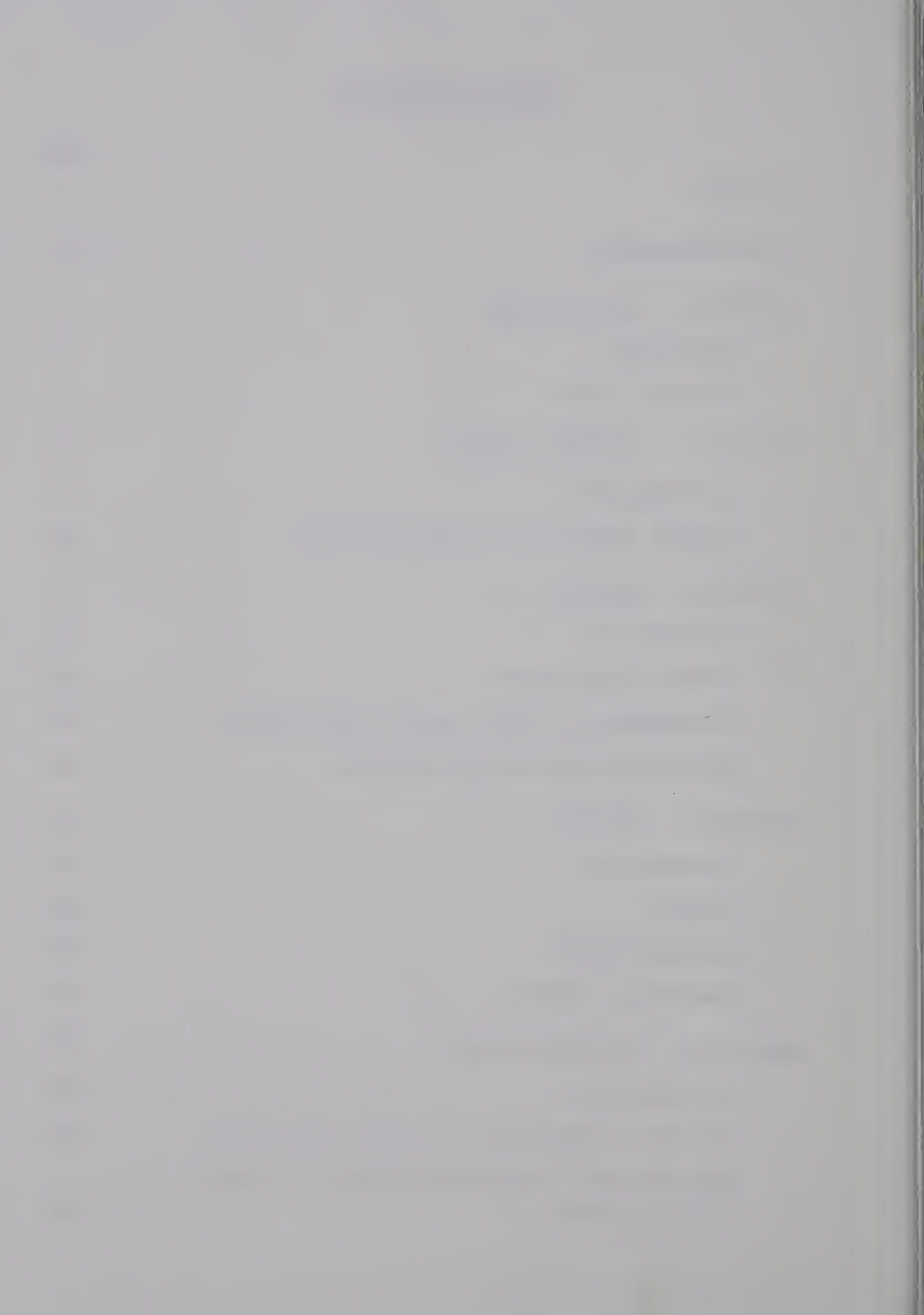
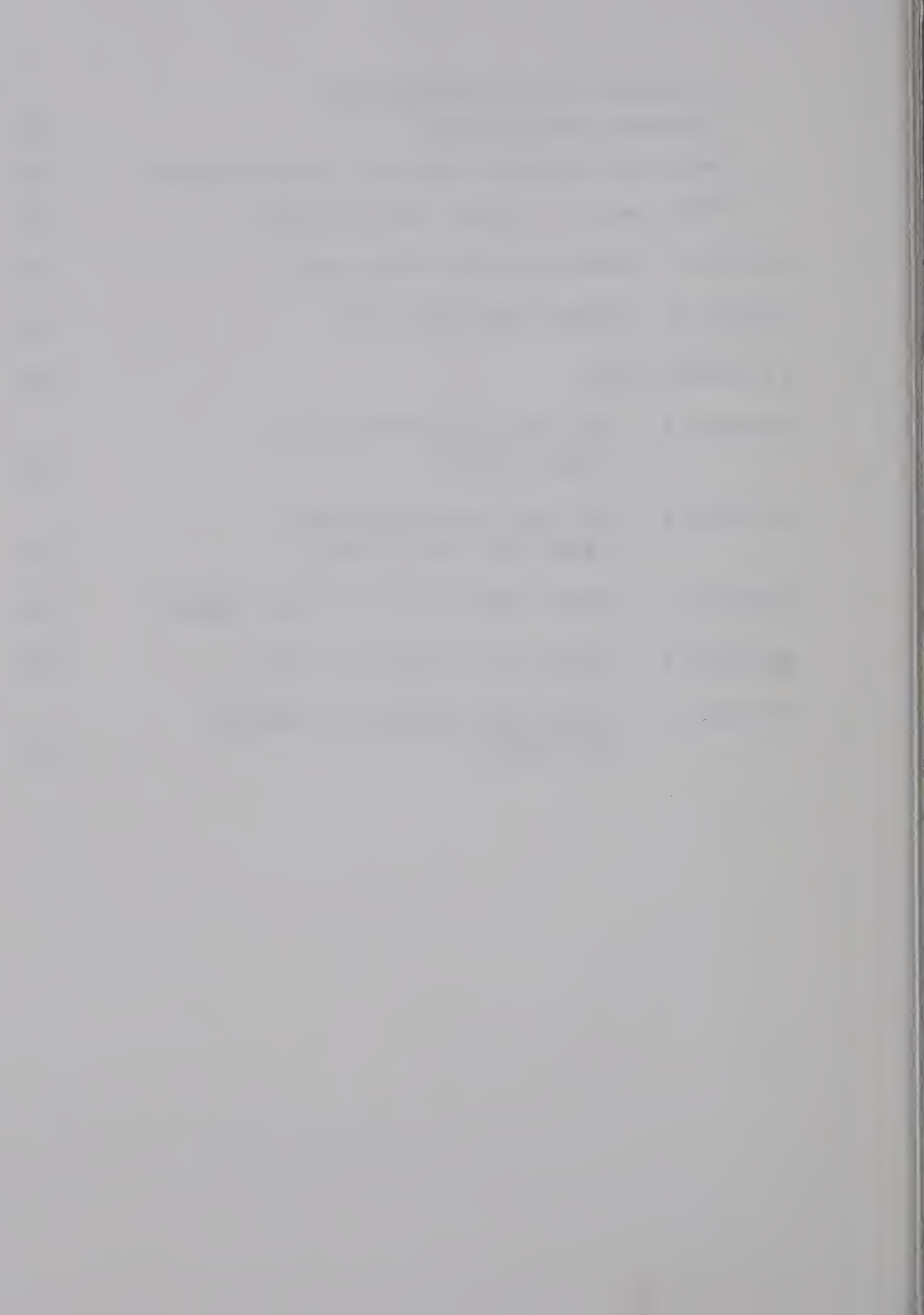


TABLE OF CONTENTS

	Page
ABSTRACT	i
ACKNOWLEDGEMENTS	iii
CHAPTER 1. INTRODUCTION	1
Objectives	1
Previous work	1
CHAPTER 2. GENERAL GEOLOGY	4
Introduction	4
Sample locations and descriptions	8
CHAPTER 3. METHODS	13
Introduction	13
Sample preparation	13
Extraction of lead, uranium and thorium	15
Mass spectrometer measurements	16
CHAPTER 4. RESULTS	19
Introduction	19
Spikes	20
Reagent blanks	21
Analytical results	22
CHAPTER 5. INTERPRETATION	32
Introduction	32
U-Th-Pb systematics in zircon and apatite	34
Apatite-rock isochron & apatite Pb isotope interpretation	46



K-feldspar Pb and feldspar-rock isochron interpretation	55
Whole rock modified concordia interpretation	70
Whole rock Pb isotope interpretation	81
CHAPTER 6. COMPARISON WITH OTHER AREAS	97
CHAPTER 7. SUMMARY AND CONCLUSIONS	101
LITERATURE CITED	109
APPENDIX A. THIN SECTION OBSERVATIONS OF 5 ROCK SAMPLES	116
APPENDIX B. THIN SECTION OBSERVATIONS OF 3 ADDITIONAL ROCK SAMPLES	119
APPENDIX C. CRYSTAL MORPHOLOGY OF ZIRCON SAMPLES	122
APPENDIX D. EXTRACTION PROCEDURE OF LEAD	125
APPENDIX E. EXTRACTION PROCEDURE OF URANIUM AND THORIUM	126



LIST OF FIGURES

FIGURE 2-1	Location of the Charles Lake area in the Western Canadian Shield	5
FIGURE 2-2	Geological map of the Charles Lake area (with rock sample locations)	7
FIGURE 5-1	Concordia plot of zircon & apatite samples	38
FIGURE 5-2a	$^{206}\text{Pb}/^{204}\text{Pb}$ versus $^{238}\text{U}/^{204}\text{Pb}$ for apatite-rock pairs 1-5 and 2-3	47
FIGURE 5-2b	$^{206}\text{Pb}/^{204}\text{Pb}$ versus $^{238}\text{U}/^{204}\text{Pb}$ for apatite-rock pairs 1-7, 3-8 and 4-1	48
FIGURE 5-3a	$^{207}\text{Pb}/^{204}\text{Pb}$ versus $^{235}\text{U}/^{204}\text{Pb}$ for apatite-rock pairs 1-5 and 2-3	49
FIGURE 5-3b	$^{207}\text{Pb}/^{204}\text{Pb}$ versus $^{235}\text{U}/^{204}\text{Pb}$ for apatite-rock pairs 1-7, 3-8 and 4-1	50
FIGURE 5-4	$^{207}\text{Pb}/^{204}\text{Pb}$ versus $^{206}\text{Pb}/^{204}\text{Pb}$ for whole rock, K-feldspar and apatite samples	54
FIGURE 5-5	$^{207}\text{Pb}/^{204}\text{Pb}$ versus $^{206}\text{Pb}/^{204}\text{Pb}$ for K-feldspar samples	59
FIGURE 5-6	$^{206}\text{Pb}/^{204}\text{Pb}$ versus $^{238}\text{U}/^{204}\text{Pb}$ for whole rock and K-feldspar samples	63
FIGURE 5-7	$^{207}\text{Pb}/^{204}\text{Pb}$ versus $^{235}\text{U}/^{204}\text{Pb}$ for whole rock and K-feldspar samples	64
FIGURE 5-8	$^{208}\text{Pb}/^{204}\text{Pb}$ versus $^{232}\text{Th}/^{204}\text{Pb}$ for whole rock and K-feldspar samples	66
FIGURE 5-9	Modified concordia plot for whole rock samples	75

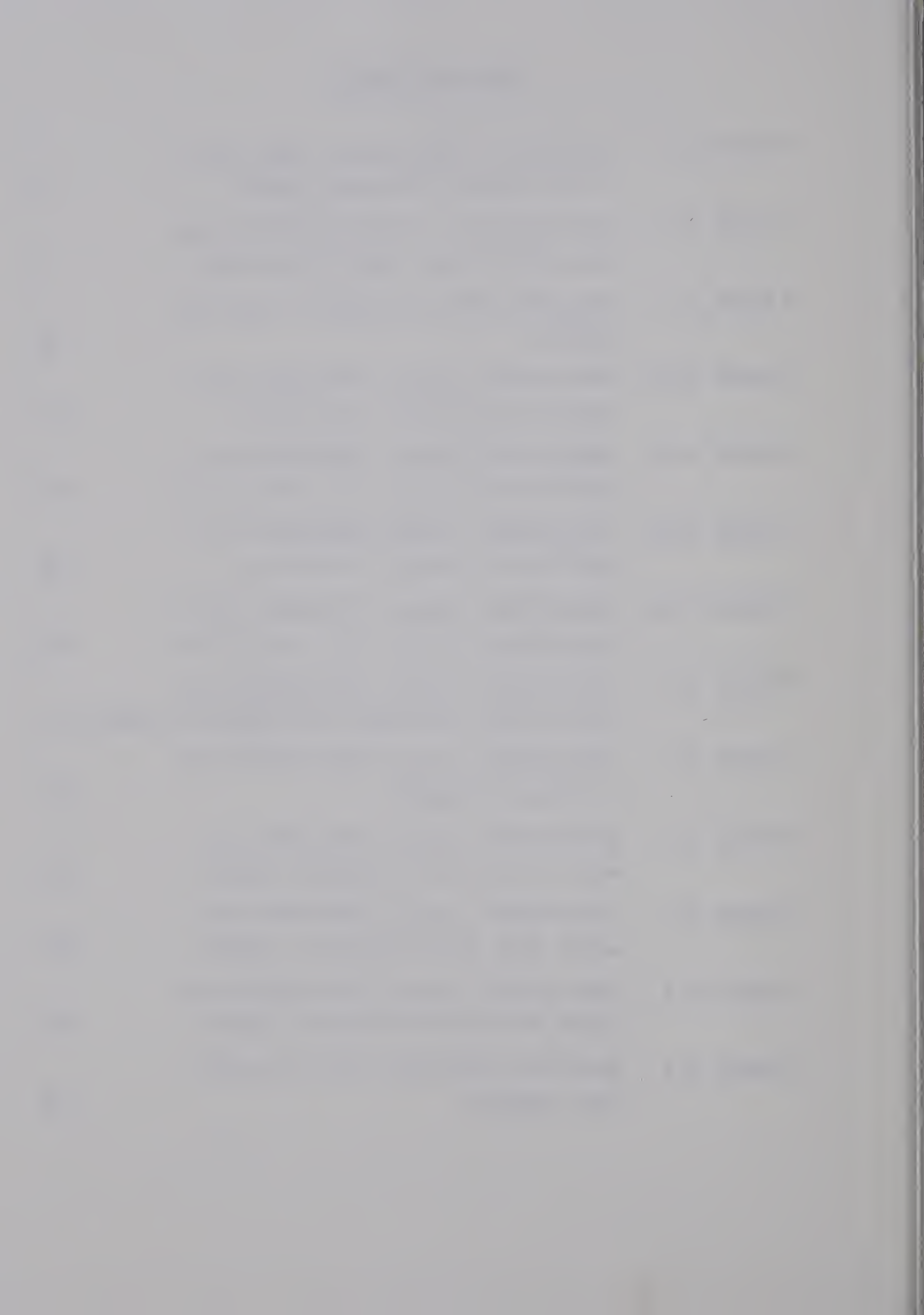


FIGURE 5-10a	$^{206}\text{Pb}/^{204}\text{Pb}$ versus time in m.y. ago for leads in whole rock and K-feldspar samples	88
FIGURE 5-10b	$^{207}\text{Pb}/^{204}\text{Pb}$ versus time in m.y. ago for leads in whole rock & K-feldspar samples	89
FIGURE 5-11	$^{207}\text{Pb}/^{204}\text{Pb}$ versus $^{206}\text{Pb}/^{204}\text{Pb}$ for whole rock and K-feldspar samples	91
FIGURE 5-12	$^{208}\text{Pb}/^{204}\text{Pb}$ versus $^{206}\text{Pb}/^{204}\text{Pb}$ for whole rock and K-feldspar samples	92

LIST OF TABLES

TABLE 4-1	Interlaboratory comparison of isotopic composition of Broken Hill Standard #1	24
TABLE 4-2	Composition of U, Th and Pb spikes and standards	25
TABLE 4-3	Interlaboratory comparison of reagent lead blanks	26
TABLE 4-4	U, Th and Pb concentrations in whole rock, zircon and apatite samples	27
TABLE 4-5	Measured and corrected lead isotope compositions for whole rock samples	28
TABLE 4-6	Measured and calculated ratios of U, Th isotopes; U-Pb, Th-Pb for whole rock, zircon and apatite samples	29
TABLE 4-7	Measured (unspiked and spiked) lead isotopic compositions for zircon and apatite samples	30
TABLE 4-8	Measured lead isotopic compositions, contamination Pb % and $^{206}\text{Pb}/^{204}\text{Pb}$ measurement errors for K-feldspar samples	31

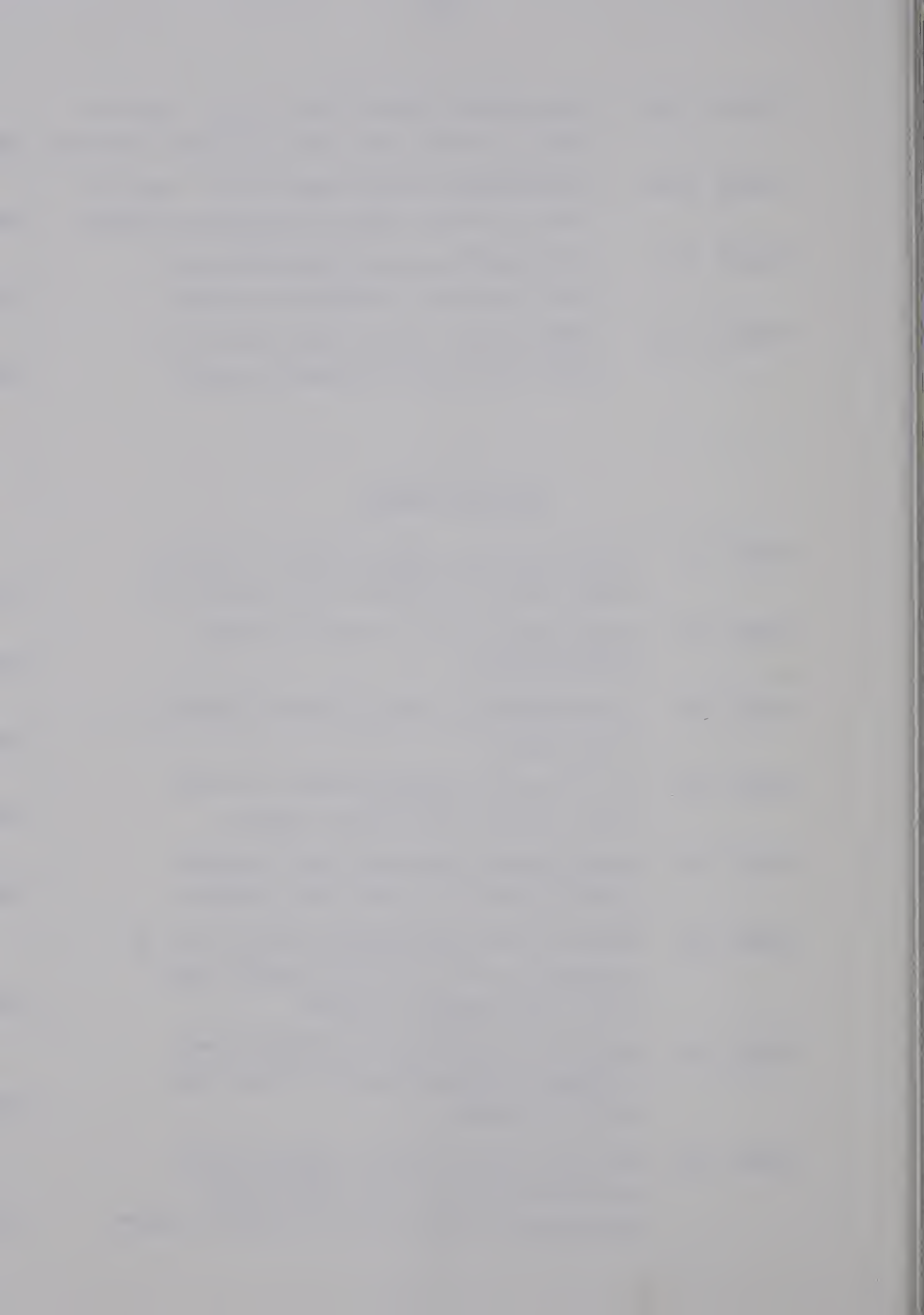
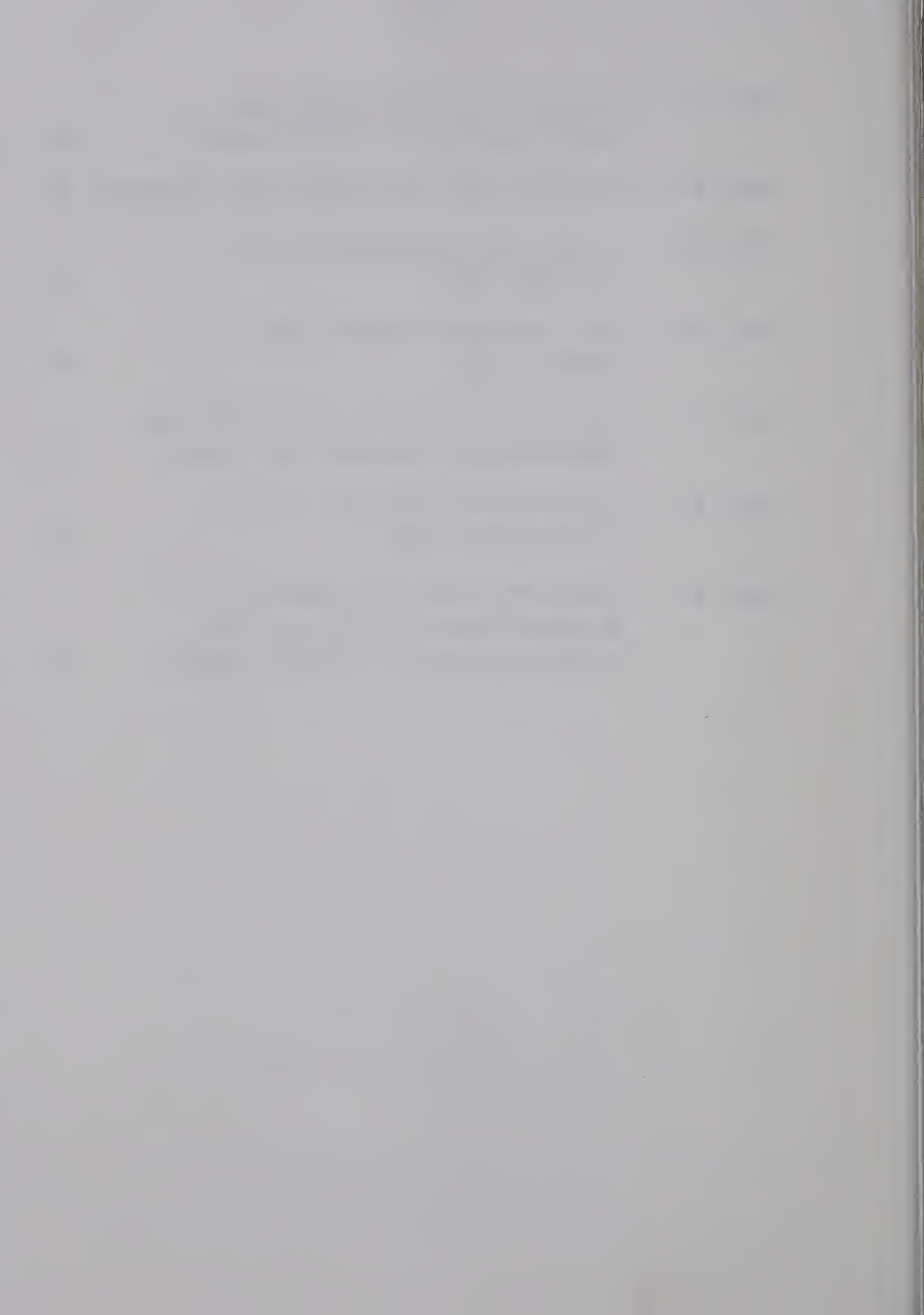


TABLE 5-1	Calculated ages for zircon and apatite samples (in million years)	37
TABLE 5-2	Estimated ages for apatite-rock isochrons	51
TABLE 5-3	A table for determining t_m in a two-stage model	61
TABLE 5-4	Whole rock and feldspar-rock isochron ages	61
TABLE 5-5	The present radiogenic $^{206}\text{Pb}/^{238}\text{U}$ and $^{207}\text{Pb}/^{235}\text{U}$ for the whole rock system	74
TABLE 5-6	Observed and calculated u values for two-stage model	78
TABLE 5-7	Initial Pb ratios corrected for in situ U-decay to 1850 m.y. ago in whole rock and K-feldspar samples	86



CHAPTER 1 INTRODUCTION

OBJECTIVES

The present study is carried out as a small part of a long-range project on the geochronological investigation of the N.E. Alberta sector of the Western Canadian Shield. Geological information on the area is detailed enough at the present time to allow a reasonably reliable correlation with geochronological information.

In this study granitic rocks from the Charles Lake area, N.E. Alberta are the main target of investigation. The writer has attempted to derive, through the investigation, evidence concerning the geological history of these rocks. Specific objectives of the present study can be outlined as follows:

- (1) To obtain a better understanding of the behaviour of U-Th-Pb systems in rocks and minerals in response to post-depositional metamorphic events, especially open system conditions;
- (2) To find indications of the source and development of common lead from a correlation of Pb isotopic compositions of whole rock and K-feldspar;
- (3) To provide new data of sufficient quality to further the understanding of various whole rock Pb development models.

However, it must be emphasized that the present attempt to obtain some information on the geochronological

history of the rocks is not the primary objective since the limited choice of samples in the present study necessarily restricts the interpretation of the history of the different rock types.

PREVIOUS WORK

The geological mapping of the N.E. Alberta sector of the Precambrian Shield can be dated back to as early as 1896 (Tyrrell, 1896). Since then several geologists have worked intermittently in this area. An organised reconnaissance was made in 1960 by the Geological Survey of Canada (Riley, 1960). Since 1961, an extensive and detailed mapping project has been conducted by the Research Council of Alberta under the direction of Dr. J.D. Godfrey (Godfrey, 1961, 1963; Godfrey and Peikert, 1963, 1964; Watanabe, 1961, 1966; Godfrey, 1966). Geological maps on the scale of 2 inches to a mile have been published together with the reports by Godfrey and his associates.

Geochronological investigation of the region was initiated by the K-Ar study of the Andrew Lake area by Godfrey and Baadsgaard (1962). In 1967, a more extensive and detailed geochronological study on the Andrew Lake area was conducted by Baadsgaard and Godfrey (1967). Since then, under the direction of Dr. Baadsgaard, an extensive geochronological study covering various portions of the region has been carried out in the Department of Geology, University of Alberta. A fairly large amount of data has

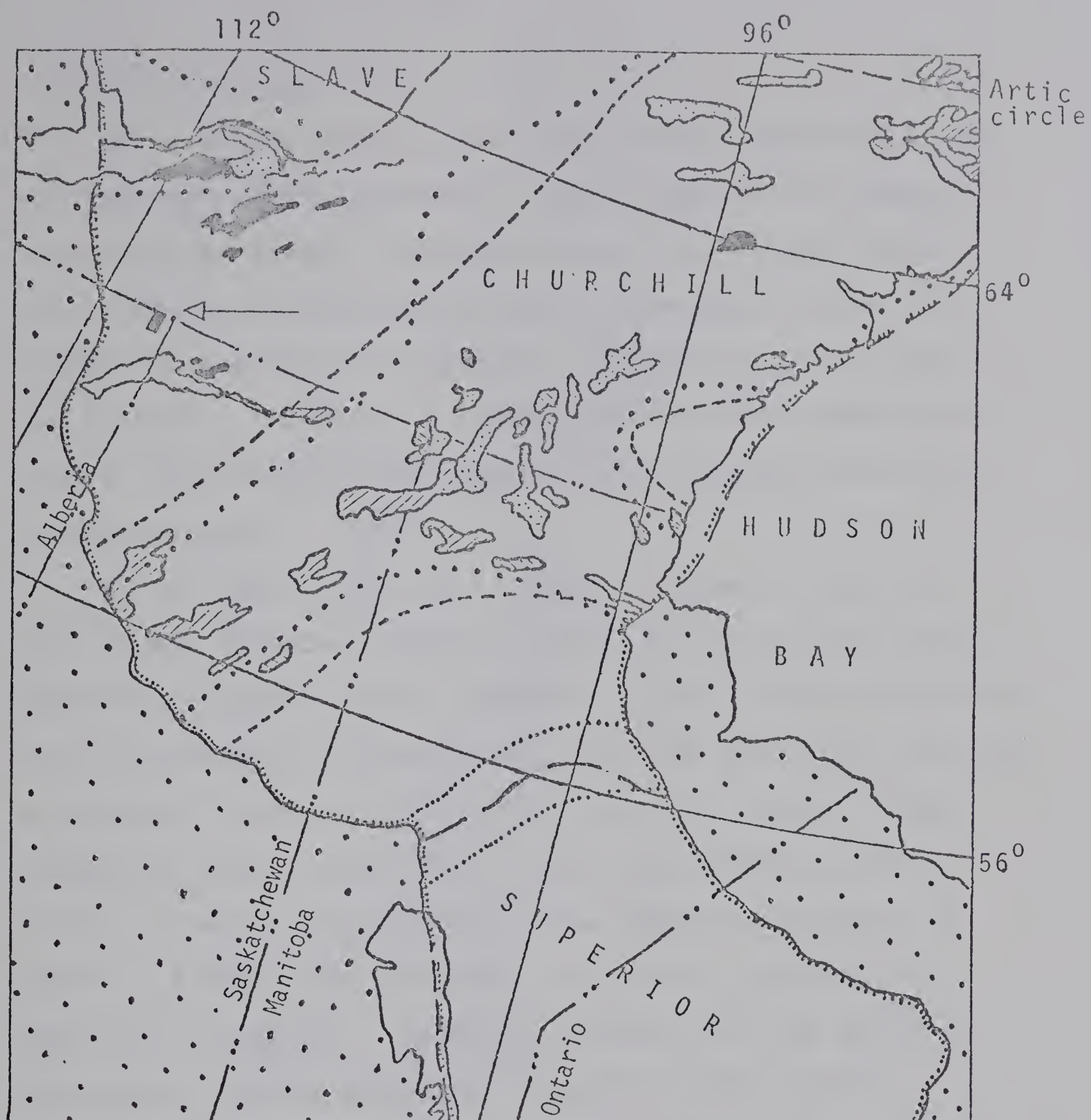
been accumulated so far. Some of the data will be used in the present study for comparison and correlation.

CHAPTER 2 GENERAL GEOLOGY

INTRODUCTION

The present study area (the Charles Lake area) forms a part of the N.E. Alberta Shield area, which is located at the border junction of Alberta, Saskatchewan and the N.W. Territories and north of Lake Athabasca. The location of the Charles Lake area is shown in Figure 2-1.

As can be seen from Figure 2-1, the N.E. Alberta Shield area is located in the northwestern fringe of the Churchill Province and south of the Slave Province. The area is characterized by a northerly trend and steeply inclined attitude of all major geological features such as the foliation and gneissosity, the metasedimentary and amphibolitic bands, the mylonite zones, and the elongated outlines of granitic rocks (Godfrey, 1966). The oldest rocks are the basement igneous and metamorphic complex consisting of granite gneisses and granites. The metasedimentary and amphibolitic bands which occur in the gneissic complex are products of possibly several orogenic cycles and derived from various materials including the gneissic materials. Subsequent tectonic movements such as plastic deformation and cataclastic deformation resulted in the imposition of northerly strike and steep dip to most rock bodies, and in the formation of four major mylonite bands in the area (Godfrey, 1966). Some young granites have intruded most other rock types in the area and they form



- [Dots] Paleozoic sediments
- [Small block with diagonal line] Late or post-tectonic sedimentary basins
- [Diagonal hatching] Granitic rock intruded during phases of Hudsonian Orogeny
- [Horizontal hatching] Gneisses formed during phases of Hudsonian Orogeny
- [Grid dots] Aphebian miogeosynclinal sediments
- [Dotted line] Possible boundary of geosynclines
- [Dash-dot line] Possible boundary of Hudsonian Orogeny
- [Dash-dot-dot line] Boundary of Canadian Shield
- [Wavy line] Boundary of structural province
- [Wavy line] Fault

FIGURE 2-1 Location of the Charles Lake area in the Western Canadian Shield (see arrow). (Map after J.C. McGlynn, in "Geology & Economic Minerals of Canada", p.86)



granodioritic complexes.

The oldest basement rocks are probably Archean in age, and they have been affected to varying degrees by phases of the Hudsonian Orogeny during which northerly fault zones with brecciation and mylonitization developed in the area. Before the deposition of Aphebian sediments, all of what is now Churchill Province is thought to have been underlain by Archean supracrustal and granitic rocks deformed during the Kenoran Orogeny.

As is shown in Fig. 2-1, the N.E. Alberta sector of the Western Canadian Shield is located in one of the three Hudsonian orogenic zones (Stockwell, 1970) in which Aphebian rocks are folded, metamorphosed, and some have been intruded by granitic rocks and converted to granite gneiss. These orogens coincide approximately with the Aphebian geosynclines. The main expression of the Hudsonian Orogeny in the N.E. Alberta and bordering area may be faulting and Hudsonian intrusions. Aphebian sediments in the area are represented by the Athabasca Formation south of Lake Athabasca and the Martin Formation at N.W. Saskatchewan near Uranium City (Stockwell, 1970).

The general geological feature of the Charles Lake area is characterized by a northerly trend and steeply inclined mylonite zone developed in an older gneissic-granitic complex and along a major N-S trend fault zone (Allan fault zone, see Fig. 2-2). Some granitic bodies occur as remnants along this zone have been considered as

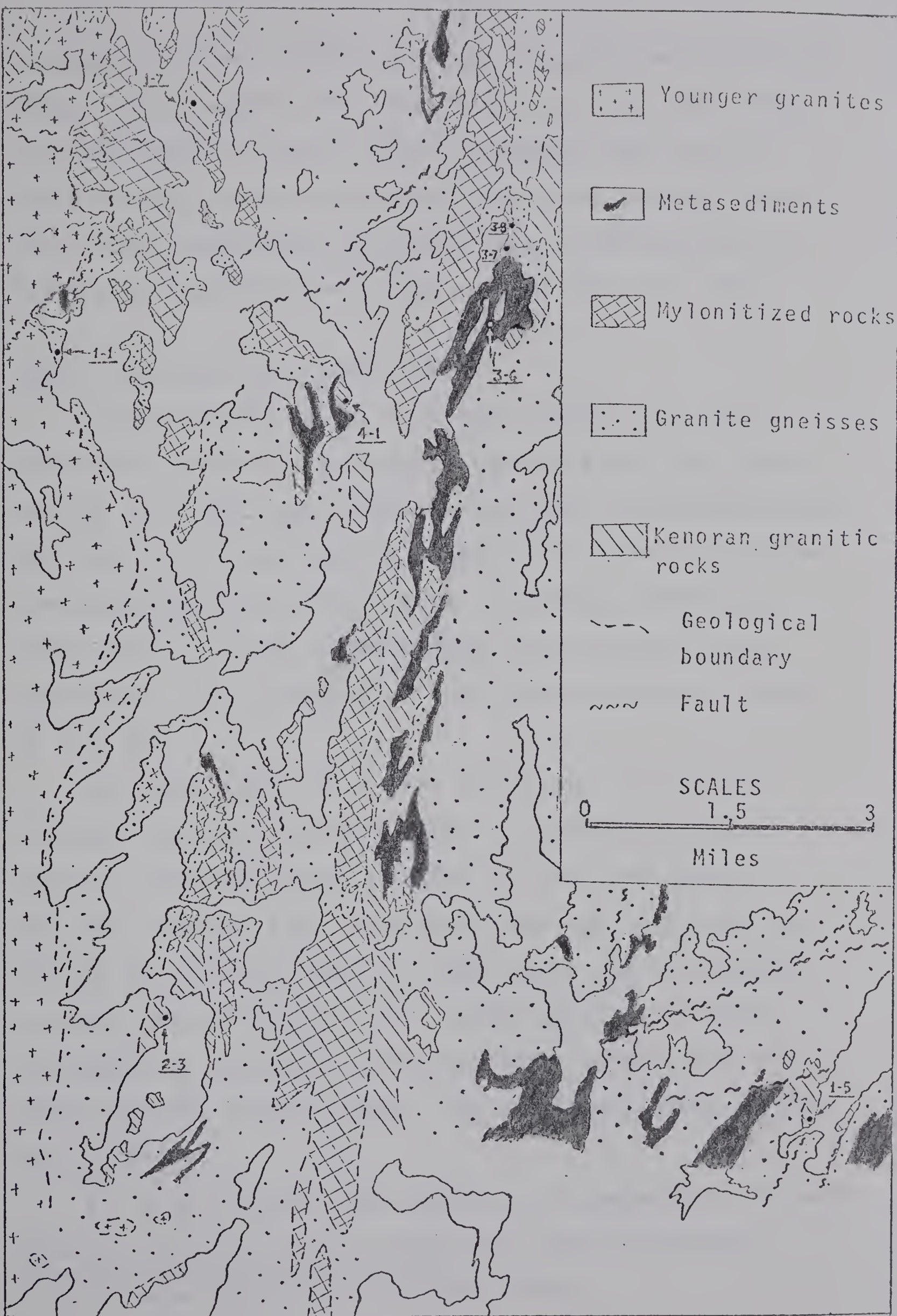


FIGURE 2-2 Geological map of the Charles Lake area (with
rock sample locations)

younger intrusives formed after the basement gneiss (Godfrey, 1966). Rock samples from these bodies are the main target of investigation in this study. Along the west side of Charles Lake, younger intrusives (Arch Lake granite, Raisin granite and Leucocratic granite*) form a continuously N-S trending granodiorite-monzonite complex (see Fig. 2-2).

SAMPLE LOCATION AND DESCRIPTIONS

In the present study, five rock samples (and their associated minerals K-feldspar, zircon and apatite) representing four major rock types — Foliated hornblende granite (JG 68-1-7), Biotite granite F (JG 68-4-1), Grey hornblende granite (JG 68-2-3), and Biotite "q" granite (JG 68-1-5, JG 68-3-8)* — were selected from the collection of Dr. Baadsgaard. The locations of these rock samples are shown in Fig. 2-2.

The rocks chosen have been considered up to now as "younger" than the basement gneiss, as mentioned above. However, geochronological studies on these rock types in the area indicate a possibly much older age. In order to clarify the possible dates of these rocks and to establish a better understanding of the basement materials, these rock types of granodiorite and monzonite composition were chosen for the present study. The geochronological studies are as follows:

(1) A Rb-Sr whole rock dating on six pegmatites intruded in these granites of the Charles Lake area indicates a

* Field terms according to Godfrey (1966).

Kenoran age of 2550 m.y. (Dr. Baadsgaard, personal communication).

(2) A granitic rock (Quartz monzonite, Sample 151-11) yields a U-Pb zircon diffusion date of 2250 m.y. together with basement gneiss samples, indicating a possible older Archean igneous intrusion (Baadsgaard and Godfrey, 1967).

(3) K-Ar dates on 20 rocks from a northern basement complex (granodiorite-diorite series) in the Tazin Lake region, N.W. Saskatchewan give a mean age of 2370 + 40 m.y., with some dates up to 2450 m.y. This related area is considered as geologically similar to the N.E. Alberta Shield area. (Koster and Baadsgaard, 1970).

A brief outline of the field occurrence and petrography of these five rock samples is given below, while their thin section descriptions are given in Appendix A.

(1) Foliated hornblende granite (Sample no. JG 68-1-7, abbreviated as sample 1-7)

The rock sample is located at the western part of a peninsula at the Charles Lake North area, about 400 feet west of a contact with granite gneiss. Homogeneous outcrop with hornblende clots streaked into the foliation; coarse grain phase. In the field, this rock generally forms an elongated body which encloses small lenses of biotite granite gneiss. It probably represents a granite syntectonically intruded concordant with the northerly structural trend of the enclosing rocks (Watanabe, 1966).

(2) Biotite granite F (Sample no. JG 68-4-1, abbreviated

as sample 4-1)

Biotite granite F occurs closely with its cataclastic derivative (Recrystallized mylonite P) in the field, and they are typically enclosed together in a sheath of garnetiferous quartzitic metasedimentary rocks. A major belt of Biotite granite F and its associated rocks occur along the Selwyn-Charles-Alexander Lake area. The rock sample is taken from biotite-rich phase, foliated to granoblastic, with large subhedral feldspar porphyroblasts (50 mm. to 1 cm. long) enclosed in a rather fine to medium-grained granular matrix of quartz, feldspar and biotite. The sample site is located about 500 to 600 feet east of a contact with quartzitic metasedimentary rocks.

(3) Grey hornblende granite (Sample No. JG 68-2-3, abbreviated as sample 2-3)

Grey hornblende granite is commonly associated with hornblende cataclasite in the field, the contact of which is transitional. The field occurrence of this rock is restricted in the Charles Lake South area. It is probably interlensed with hornblende granite gneiss. The rock sample is light grey with foliated to uniform texture, fine to medium-grained and composed of dark clots of mafic minerals in a slightly foliated quartzo-feldspathic matrix, in which large porphyroclasts of feldspars are occasionally present.

(4) Biotite "q" granite (Sample No. JG 68-1-5, and Sample No. JG 68-3-8)

Biotite "q" granite is present as narrow layers, lenses

and small masses in the region east to southeast to Charles Lake. It is a megacrystic phase of the young biotite granites and contains about equal amounts of quartz, K-feldspar and plagioclase, with lesser amount of biotite and some muscovite. Continuous layers several feet thick are commonly interlayered with granite gneiss, indicating that Biotite "q" granite was intruded in a mobile and liquid state (Watanabe, 1966).

Sample 1-5

The rock sample is collected from an outcrop about 600 feet east of a contact with hornblende granite gneiss. It shows some variations in composition and texture, and some streaky mafic phases (amphibolitic) in the outcrop look transitional to granite gneiss in one 6 foot wide band. The sample site is at the south end of a N-S trend mylonite belt and several faults occur in the vicinity.

Sample 3-8

The rock sample is from a typical Biotite "q" granite outcrop about 100 feet west of a contact with a band of metasedimentary rocks. The two rocks sheared at the contact. Several hundred feet to the west of the sample site there exist numerous quartz veins, a minor scarp and a lake, suggesting the presence of a fault zone.

Besides the above described rock samples, there are three rock samples which have been analysed for Pb in the earlier phase of the present work; their Pb data will be used in the interpretation for comparison whenever necessary.

They are Biotite "q" granite (Sample no. JG 68-3-7), Biotite granite gneiss (Sample no. JG 68-1-1) and Leucocratic granite (?) (JG 68-3-6). Their locations are also shown in Fig. 2-2. Sample descriptions of these rocks are given in Appendix B.

Since zircon separates from the previous five rocks are utilized in U-Th-Pb concordia study, observation on their crystal morphology has also been made; a brief description of the five zircon separates is given in Appendix C.

CHAPTER 3 METHODS

INTRODUCTION

The analytical work has led to the determination of the following isotopic compositions in various samples:

- (1) Pb isotopic compositions of 5 whole rock samples (plus 3 additional reference samples), 5 zircons, 5 apatites, and 5 K-feldspars;
- (2) U and Th isotopic compositions of 5 whole rocks and 5 zircons;
- (3) U isotopic compositions of 5 apatites.

All reagents used in the analytical work were purified and maintained throughout the whole period. Reagent preparation and reagent Pb blank determination are similar to those described by O'Nions (1969). All glassware used in the present work is cleaned in hot concentrated HNO_3 , rinsed in triple distilled "pure" water and wrapped in "parafilm" as necessary. Only triple distilled water is used in the preparation of reagents and for the extraction of Pb. Two sets of reagents were used for the Pb extraction. The first set was prepared by the writer and used in the earlier phase of the work (Winter, 1970); the second set was prepared by Dr. Baadsgaard (Spring, 1971).

SAMPLE PREPARATION

(1) Whole rock samples

All whole rock samples for isotopic analysis were

broken from larger block samples and put through a steel jaw crusher. The smaller splits were then ground in a stainless steel mill to about -100 mesh powder. Each rock powder sample was then collected. About 2 to 3 grams of sample was dissolved in a "bomb-sealed" Teflon cup with 10 ml. HF and 2 ml. concentrated HNO_3 and was heated in an electric oven at 120°C for 12 hours. The heated sample was dissolved in 5 ml. concentrated HNO_3 and evaporated to dryness, this was repeated twice, after which it was dissolved in 20 ml. 1.5N HCl and then was centrifuged. The supernatant liquid was added to a 20 cm. Dowex 1-x8 anion-exchange resin column supplied in the Cl^- form. After eluting with 40 ml. of 1.5N HCl through the column, Pb was stripped from the column by eluting with 40 ml. "pure" water and the eluent was collected in a clean beaker and sealed with "parafilm".

(2) Mineral separates

All mineral samples used in the present study are from a collection of mineral separates originally obtained by using standard techniques of magnetic and heavy liquid separation. Some purification or pre-treatment of the mineral samples were made by the writer.

A) Zircon ----- Zircon sample was acid-washed by treatment with warm 8N HNO_3 (at 60°C) for one hour, and then washed with distilled water. About 100 – 500 mg. of zircon sample was fused in a platinum crucible with purified sodium tetraborate ("Borax", 10 times as much as zircon in weight) at about 1000°C for 4 hours. The fused sample was carefully transferred to a clean beaker, and dissolved by

constant stirring (thus silica remained in solution). The solution was diluted to volume and stored in volumetric flask sealed with "parafilm".

B) Apatite ----- Apatite samples were purified by magnetic separation ($\alpha = 10^0$, $I = 1.5$ Amps.), tetrabromomethane sink and methylene iodide float procedures. The purified sample was dissolved in warm concentrated triple distilled HNO_3 by constant stirring (very small amounts of insoluble silica remained). The aqueous solution was filtered, diluted to volume and stored in volumetric flask sealed with "parafilm".

C) K-feldspar ----- originally separated feldspar sample was further purified with heavy liquid sink-float procedure by adjusting tetrabromomethane with acetone to allow visible sinking and floating fractions in each sample (estimating the K-feldspar and plagioclase proportions with the knowledge from thin-section observation). The floating fraction (K-feldspar) was cleaned, dried and collected. The procedure to obtain sample solution from K-feldspar is identical to that for whole rock sample.

EXTRACTION OF LEAD, URANIUM AND THORIUM

The extraction procedure of Pb from whole rock (same for zircon, apatite and K-feldspar) is similar to that described by O'Nions (1969). A brief outline of the extraction procedure of Pb is given in Appendix D. The extraction

procedure of Pb for the "spiked" aliquot (for the determination of the Pb concentration) is similar except for adding isotope dilutant (^{207}Pb - ^{204}Pb double spike for whole rock, ^{208}Pb spike for zircon and apatite) prior to the first dithizone extraction.

All Pb spikes used in the present study were prepared and maintained by Dr. Baadsgaard. The calibrations of these spikes was made against the National Bureau of Standard "equal-atom" Pb standard.

Sample solution of whole rock for U-Th analysis was prepared by fusion of one gram rock powder with 4 gram Borax and dissolution with 6N HCl. Another procedure involving HF decomposition of the rock sample was also made to obtain sample solution. Both sample solutions were analysed for U and Th. The extraction procedure of U and Th is given in Appendix E.

MASS SPECTROMETER MEASUREMENTS

Pb isotopic composition was measured on a 12 inch radius curvature, 90° sector, single focussing mass spectrometer equipped with vibrating-reed amplifier, digital volmeter, tape-recorder and facilities for switching between preset magnet positions. Normal operating conditions were 4.5 KV accelerating voltage and a 10^{10} ohm leak resistor on a Keithley amplifier. Pb emission started after the decay of potassium and varied at different filament currents from one run to another. Normally Pb emission began at

around 1.7 Amps. Output signals for rock lead and feldspar lead isotope spectra were recorded on magnetic tape and Pb isotopic compositions were calculated by a computer program written by Dr. G.L. Cumming of the Department of Physics. For measurements of zircon lead, peak switching between preset magnet current positions at masses 206, 207 and 208 was used. The alternating signals of two masses were measured by a digital volmeter and printed out on paper tape. Pb isotopic ratios of apatite were measured from chart-scans. The 206, 207, 208 masses were resolved in the runs, and little tail correction was necessary. Mass discrimination corrections were made for measured rock lead ratios using the double spike method of Compston and Oversby (1969).

U and Th were measured on the same 12 inch radius mass spectrometer as described above for lead. A sample loading procedure similar to that described by O'Nions (1969) was adopted. U and Th were loaded on an outgassed single Tantalum filament with the addition of H_3BO_3 solution (which formed a B_2O_3 bead), and the filament was glowed in air prior to mass spectrometer measurement. U emission as UO_2^+ started at about 2.9 Amps. filament current at an accelerating voltage of about 4.6 KV and a magnet field current of about 6.5 to 6.8 Amps. The UO_2^+ emission was measured using a 10^{12} ohm leak resistor, and peak switching between preset magnet position for masses 235 and 238 was made whenever strong and stable peaks were available. Otherwise chart-scans were made. After UO_2^+ emission decreased, the magnet field current was changed to around 6.2 to 6.4 Amps. in order to detect the

growth of UO^+ . Then the filament current was increased to about 3.2 Amps. and the magnet field current was also changed to about 6.15 Amps. to check the presence of ThO^+ . Th was measured digitally by peak switching between masses 230 and 232 whenever possible, otherwise data were measured from the chart-scan output on poorer runs.

CHAPTER 4 RESULTS

INTRODUCTION

Analytical results are presented in this Chapter. Also presented are the compositions of U, Th and Pb isotope dilutants (spikes) used and reagent Pb blank calibration. Earlier and poorer results obtained for rock leads will not be presented except those of rock samples 1-1, 3-6 and 3-7.

The rock lead results are calculated and internally corrected by a computer program (by Dr. Cumming) designed to calculate a mean value for each set of ratios. U and Th values are calculated from the weighted mean average of two or more sets of ratios from the chart-scans or peak-switching digital outputs.

Measurement of a Broken Hill # 1 standard reference lead made by the writer during May 1971 are listed in Table 4-1. Some mass discrimination corrections are thus necessary and these are applied in results reported later. Measurement precision of the $^{207}\text{Pb}/^{206}\text{Pb}$ and $^{208}\text{Pb}/^{206}\text{Pb}$ ratios was about 0.15% and the $^{206}\text{Pb}/^{204}\text{Pb}$ about 0.13% (ranging from 0.05 to 0.2%) for rock leads. In the case of apatite where common lead corrections were somewhat higher, the $^{206}\text{Pb}/^{204}\text{Pb}$ ratios yield a standard deviation of about 1%. No calibration analysis of the ^{235}U and ^{230}Th isotope dilutants was made during the course of this study, but a reproducibility of 0.3% and 0.8% for the $^{238}\text{U}/^{235}\text{U}$ and $^{232}\text{Th}/^{230}\text{Th}$ ratios,

respectively, is estimated for zircons, and about 1.7% is estimated for apatites. A reproducibility of about 1.6% for $^{238}\text{U}/^{235}\text{U}$ and about 1% for $^{232}\text{Th}/^{230}\text{Th}$ is estimated for whole rocks. The reproducibilities were estimated from the mean standard deviations (95% confidence limits) of the measured ratios in zircons, apatites and whole rocks. Assigned errors in the measured U-Pb ratios in whole rock and zircon samples are therefore estimated to be about 4-5 % and 2% respectively. (These errors are due largely to the uncertainties in the measured U and Th isotopic ratios). In the case of apatite in which common lead correction is larger, approximately 5% error has been assigned for U-Pb ratios. Assigned errors in Th-Pb ratios in whole rock and zircon samples are estimated to be about the same range as that of U-Pb ratios.

SPIKES

The compositions of spikes used in Pb isotopic analysis of whole rock, zircon, apatite and K-feldspar are shown in Table 4-2 together with the compositions of the standard stock solutions for various spikes. In the present study, double-spike $^{207}\text{Pb}-^{204}\text{Pb}$ (DS-3) was used in the analyses of rock leads, and spike ^{208}Pb (#3) was used in the lead analyses of zircon and apatite. All spikes were prepared and calibrated by Dr. Baadsgaard during the course of this study.

The compositions of U and Th spikes for whole rock, zircon and apatite are also shown in Table 4-2. Double

(mixed) spikes of U and Th were used (except apatite in which only U spike was used). Two sets of special U-Th mixed spikes were prepared for U-Th analyses of two sets of whole rock samples which were treated by different procedures (Borax fusion and HF decomposition) before the ion exchange procedure. Mixed spikes of U-set 1 and Th-set 2, spikes of U-set 2 were used for analyses of zircon and apatite samples respectively.

REAGENT BLANKS

Owing to the importance of blank corrections in the case of rock lead analysis, several blank analyses for the overall reagents used (referred to as "total blank") were made before, in between and after analyses for the determination of both the isotopic composition and the concentration. Besides, several lead blank analyses on individual reagents (major reagents used such as HF and HCl) were also made accompanying the rock lead analyses. The results of these total and individual blank analyses are shown in Table 4-3 together with some other published results on reagent Pb blanks calibrated for rock lead analyses by various analysts.

The present chemical procedures for rock lead isotopic analysis, though somewhat lengthy and requiring caution and patience, are considered by the writer to be less dangerous and less possible to contaminate the samples. However, the relatively large amount of laboratory contaminant lead found

in the present study is considered to be mainly due to atmospheric dust. Catanzaro and Gast (1960) have shown that this factor is controllable if certain precautions are taken. The total blank represents about 1.5% of the rock lead for ratio determinations and 0.4% of the rock lead in (spiked) concentration determinations. The proportions of total lead blanks for both ratio and concentration determinations of zircon lead and apatite lead are also estimated and shown in Table 4-4. Further efforts to reduce the laboratory contamination limits should and can be made, among which filtered-air-laboratory and better purified reagents are essential.

No efforts were made to detect the blanks of U and Th, but it is assumed to be the same as those estimated by O'Nions (1969) since a similar technique for U-Th extraction was employed. O'Nions' estimate gives no blank for Th, and approximately 0.005 μg per sample for U.

ANALYTICAL RESULTS

The measured results of U, Th and Pb isotopic abundances for all samples analysed are listed in Table 4-4 together with approximate Pb contamination limits and $^{206}\text{Pb}/^{204}\text{Pb}$ measurement uncertainties. The Pb contamination limits are based upon the estimated total reagent Pb blank of 0.4895 μg for whole rock, 0.3896 μg for zircon (Dr. Baadsgaard, personal communication) and 0.0974 μg for apatite (loc. cit.). The measured and corrected (for mass discrimination) Pb isotopic compositions for whole rock samples are presented in Table 4-5.

Mean standard deviations are also presented with the measured ratios. In Table 4-6, measured ratios of U and Th isotopes with mean standard deviations, the correspondingly calculated ratios of U-Pb, Th-Pb for whole rock * and apatite samples, and the ratios of Pb/U and Pb/Th for zircon and apatite samples are listed. The derived U-Pb, Th-Pb and Pb-Pb ages for zircon and apatite samples will be given in Chapter 5 in which interpretation is made. The measured (unspiked and spiked) Pb isotopic compositions with mean standard deviations for these samples are presented in Table 4-7. Finally, the measured Pb isotopic compositions for K-feldspar samples are shown in Table 4-8 together with Pb contamination limits and $^{206}\text{Pb}/^{204}\text{Pb}$ measurement errors.

* The $^{238}\text{U}/^{204}\text{Pb}$, $^{235}\text{U}/^{204}\text{Pb}$ and $^{232}\text{Th}/^{204}\text{Pb}$ ratios for whole rock samples are calculated with the aid of an A.P.L. computer program (MDCOM) written by Dr. Baadsgaard.

TABLE 4-1 Interlaboratory comparison of isotopic composition
of Broken Hill Standard Lead #1.

Analysis	$\frac{206\text{Pb}}{204\text{Pb}}$	$\frac{207\text{Pb}}{204\text{Pb}}$	$\frac{208\text{Pb}}{204\text{Pb}}$	$\frac{207\text{Pb}}{206\text{Pb}}$	$\frac{208\text{Pb}}{206\text{Pb}}$
Present (1V)	15.9607 $\pm .0290$	15.3378 $\pm .0270$	35.5024 $\pm .0630$	0.9610 $\pm .0016$	2.2244 $\pm .0040$
	15.9002 $\pm .0351$	15.2973 $\pm .0330$	35.4261 $\pm .0747$	0.9621 $\pm .0018$	2.2280 $\pm .0049$
Work* (10V)	16.0034 $\pm .0237$	15.4071 $\pm .0223$	35.6913 $\pm .0505$	0.9627 $\pm .0012$	2.2302 $\pm .0033$
Average	15.9548 $\pm .0424$	15.3441 $\pm .0455$	35.5933 $\pm .0383$	0.9621 $\pm .0005$	2.2275 $\pm .0024$
Ulrych, Denver (1967)	16.0050	15.3970	35.6640	0.9620	2.2283
Stacey et al (1969)	16.0070 $\pm .0100$	15.3971	35.6732	0.9619 $\pm .0005$	2.2286 $\pm .0013$
Ozard (1970)	16.0048	15.4008	35.7070	0.9623	2.2310

* Single run at different output intensities.

TABLE 4-2 Composition of U, Th and Pb spikes and standards

Spikes	Concentration (μg)				Remark
	208Pb	207Pb	206Pb	204Pb	
Spike 208Pb #3	20.863	0.0104	0.0456	-	For zircon & apatite
Standard #3					0.8954 gm. of stock sol'n #3
Spike 207Pb-204Pb DS-3	0.10024	71.8167	0.05216	4.38572	For whole rock
Std. stock 207Pb(3)	-	3047.64	-	-	
Std. stock 204Pb(3)	-	-	-	186.223	
	238U	235U	232Th	230Th	
U-set (1)	0.026	20.130	-	-	For zircon
U-set (2)	0.0266	20.4252	-	-	and
Th-set (2)	-	-	1.066	12.217	apatite
Special U-Th spikes (whole rock)					
Set (1)					
1-5	0.0078	6.020	0.620	7.102	For Borax fusion rock samples
1-7	0.0090	6.916	0.712	8.159	
2-3	0.0081	6.184	0.637	7.296	
3-8	0.0121	9.260	0.953	10.924	
4-1	0.0068	5.225	0.538	6.164	
Set (2)					
1-5	0.0075	5.7294	0.5980	6.8540	For HF decomposition rock samples
1-7	0.0013	8.7066	0.9088	10.4155	
2-3	0.0091	7.0254	0.7333	8.4043	
3-8	0.0071	5.4205	0.5658	6.4844	
4-1	0.0084	6.4456	0.6728	7.7107	

TABLE 4-3 Interlaboratory comparison of reagent lead blanks

Analysis	Method	Amounts (μg)
(Present work)		
Total blank (Apr.30, 1971)	Chemistry	0.4895 (1 : 19.41 : 16.40 : 42.71)
HCl blank (Apr.24, 1971)	"	0.2376 (1 : 17.80 : 15.04 : 38.98)
HF blank (Apr.25, 1971)	"	0.1095 (1 : 18.72 : 15.82 : 33.88)
Catanzaro & Gast (1960)	"	0.37
Wampler & Kulp (1964)	"	0.2
Zartman (1965)	"	0.3 – 0.4
Tatsumoto (1966)	"	0.08
O'Nions (1969)	"	0.979
Tatsumoto (1970)	"	0.015 – 0.032
Silver (1970)	"	0.04 – 0.12
Hamilton (1966)	Volatilezation	0.15
Sinha (1969)	"	0.212 – 0.320
Cumming et al (1970)	"	0.5
Ozard & Russell (1971)	"	0.16

TABLE 4-4 U, Th and Pb concentrations in whole rock, zircon and apatite samples

Sample No.	Concentration (ppm)				Contam. Pb(%)*		206Pb/204Pb meas. error(%)	
	238U	Th	206Pb	Total Pb	IR	ID	IR	ID
WR 1-5	1.744	56.21		24.626	1.63	0.50	0.18	0.10
WR 1-7	0.440	14.59		14.394	2.04	0.43	0.13	0.08
WR 2-3	0.603	10.27		28.179	1.63	0.44	0.23	0.05
WR 3-8	5.374	61.32		31.335	1.22	0.34	0.044	0.10
WR 4-1	3.655	42.80		29.016	1.22	0.24	0.063	0.10
WR 2-3V	-	-		19.214	1.63	-	0.083	0.083
WR 3-8V	-	-		15.947	1.22	-	0.060	0.060
WR 4-1V	-	-		19.263	1.22	-	0.059	0.071
ZR 1-5	421.10	220.60	119.98	-	0.61	0.22	1.88	2.81
ZR 1-7	230.29	114.79	72.44	-	0.57	0.14	0.87	1.87
ZR 2-3	697.36	221.09	162.79	-	0.34	0.11	1.04	1.34
ZR 3-8	373.89	190.98	98.76	-	0.58	0.29	0.97	0.57
ZR 4-1	1567.18	512.14	314.98	-	0.22	0.11	1.73	0.70
AP 1-5	24.02	-	6.570	22.321	0.18	0.077	0.87	1.097
AP 1-7	4.74	-	0.657	5.961	0.31	0.104	0.77	5.84?
AP 2-3	13.21	-	3.082	9.749	0.15	0.079	0.99	0.90
AP 3-8	28.86	-	8.118	22.987	0.26	0.150	0.78	0.99
AP 4-1	43.70	-	10.522	20.428	0.07	0.039	1.41	0.81

* Contamination % of Pb for whole rock is based on a total blank of 0.4895 µg; that of zircon: 0.3896 µg; and that for apatite: $0.3896 \times 1/4 = 0.0974 \mu\text{g}$.

Note: WR: whole rock; ZR: zircon; AP: apatite; IR: Pb isotope ratio analysis; ID: Pb concentration analysis.

TABLE 4-5 Measured and corrected lead isotope compositions for whole rock samples

Sample No.	206Pb/204Pb	207Pb/204Pb	208Pb/204Pb
WR 1-1	16.815	15.927	38.988
	16.783	15.884	38.844
WR 1-5	16.902 \pm .030	15.424 \pm .027	45.143 \pm .081
	16.824	15.397	45.233
WR 1-7	14.901 \pm .020	14.835 \pm .020	41.175 \pm .057
	14.717	14.775	41.130
WR 2-3	15.829 \pm .036	15.233 \pm .034	35.951 \pm .082
	15.732	15.204	35.759
WR 3-6	15.760 \pm .029	15.360 \pm .029	35.350 \pm .066
	15.730	15.319	35.219
WR 3-7	20.699 \pm .054	15.769 \pm .041	49.796 \pm .132
	20.660	15.727	49.612
WR 3-8	18.286 \pm .008	15.461 \pm .007	42.197 \pm .020
	18.245	15.430	42.194
WR 4-1	19.038 \pm .012	15.720 \pm .010	38.098 \pm .024
	19.025	15.700	17.953
WR 2-3V	15.636 \pm .013	15.121 \pm .013	35.597 \pm .031
	15.574	15.038	35.332
WR 3-8V	18.410 \pm .011	15.430 \pm .009	42.039 \pm .026
	18.354	15.361	41.797
WR 4-1V	18.742 \pm .011	15.597 \pm .099	38.161 \pm .022
	18.740	15.595	38.153

Note: Second-row values are corrected for mass discrimination;
 those for samples 1-1, 3-6 and 3-7 are corrected results
 by MTS computer program.

TABLE 4-6 Measured and calculated ratios of U and Th isotopes; U-Pb, Th-Pb for whole rock, zircon and apatite samples.

Sample No.	238U/235U	232Th/230Th	238U/204Pb	235U/204Pb	232Th/204Pb	$\frac{206\text{Pb}}{238\text{U}}$	$\frac{207\text{Pb}}{235\text{U}}$	$\frac{208\text{Pb}}{232\text{Th}}$
WR 1-5	0.302 \pm .003	8.24 \pm .17	4.17	0.0303	137.982	-	-	-
WR 1-7	0.0642 \pm .0008	1.862 \pm .007	1.908	0.0138	64.879	-	-	-
WR 2-3	0.098 \pm .003	1.30 \pm .01	1.263	0.0092	19.087	-	-	-
WR 3-8	0.574 \pm .002	4.47 \pm .03	11.48	0.0850	105.471 (125.775)	-	-	-
WR 4-1	0.559 \pm .015	5.6	8.08	0.0590	97.239 (82.439)	-	-	-
ZR 1-5	0.9064 \pm .0031	0.8754 \pm .0027	-	-	-	0.3292	5.578	0.8584
ZR 1-7	0.5237 \pm .0005	0.5182 \pm .0002	-	-	-	0.3634	6.447	0.1085
ZR 2-3	0.9240 \pm .0010	0.5730 \pm .0020	-	-	-	0.2697	4.694	0.0678
ZR 3-8	0.6845 \pm .0063	0.6660 \pm .0230	-	-	-	0.3052	4.820	0.0940
ZR 4-1	1.3840 \pm .0020	0.8409 \pm .0003	-	-	-	0.2322	3.444	0.0720
AP 1-5	0.1248 \pm .0036	-	206.802	1.5003	-	0.3190	4.7591	-
AP 1-7	0.0287 \pm .0005	-	74.104	0.5376	-	0.2223	3.3011	-
AP 2-3	0.0974 \pm .0009	-	129.067	0.9364	-	0.2785	3.8049	-
AP 3-8	0.2797 \pm .0059	-	185.361	1.3448	-	0.3289	5.1787	-
AP 4-1	0.3805 \pm .0033	-	309.115	2.2426	-	0.2765	4.5643	-

Note: 232Th/204Pb ratios in parenthesis for WR 3-8 and WR 4-1 are calculated from alternative HF decomposition sample determination.

TABLE 4-7 Measured (unspiked and spiked) lead isotopic compositions for zircon and apatite samples.

Unspiked	206Pb/204Pb	207Pb/204Pb	208Pb/204Pb
ZR 1-5	1225 ± 23	164 ± 3.08	204.9 ± 3.85
ZR 1-7	805 ± 7	116.9 ± 1	155.7 ± 1.35
ZR 2-3	579 ± 6	86 ± 0.9	82.6 ± 0.86
ZR 3-8	2156 ± 21	260.5 ± 2.5	381.3 ± 3.70
ZR 4-1	636 ± 11	82.2 ± 1.39	100.2 ± 1.73
<hr/>			
Spiked			
ZR 1-5	1173 ± 33	159.1 ± 4.5	2446.7 ± 68.8
ZR 1-7	695 ± 13	103 ± 1.9	4255.5 ± 79.6
ZR 2-3	523 ± 7	80.5 ± 1.08	1488.7 ± 19.9
ZR 3-8	1571 ± 8	195 ± 1	2883.1 ± 14.7
ZR 4-1	428 ± 3	57.94 ± 0.41	671.8 ± 4.7
<hr/>			
Unspiked			
AP 1-5	80.50 ± .70	22.29 ± .19	121.64 ± 1.06
AP 1-7	29.85 ± .23	16.60 ± .13	81.47 ± .63
AP 2-3	50.73 ± .50	18.72 ± .19	41.58 ± .41
AP 3-8	75.53 ± .59	22.09 ± .17	77.46 ± .60
AP 4-1	100.86 ± 1.42	25.60 ± .36	41.95 ± .59
<hr/>			
Spiked			
AP 1-5	81.33 ± .89	22.41 ± .25	597.26 ± 6.55
AP 1-7	27.23 ± 1.59	13.84 ± .81	653.98 ± 38.18
AP 2-3	54.48 ± .49	20.02 ± .18	874.10 ± 7.83
AP 3-8	85.90 ± .85	23.45 ± .23	306.46 ± 3.03
AP 4-1	91.87 ± .74	24.25 ± .20	855.40 ± 6.89

TABLE 4-8 Measured lead isotopic compositions, contamination Pb % and $^{207}\text{Pb}/^{204}\text{Pb}$ measurement errors for K-feldspar samples.

Sample No.	$\frac{206\text{Pb}}{204\text{Pb}}$	$\frac{207\text{Pb}}{204\text{Pb}}$	$\frac{208\text{Pb}}{204\text{Pb}}$	Contam. Pb % *	$^{206}\text{Pb}/^{204}\text{Pb}$ meas. error %
KF 1-5	$15.276 \pm .013$	$15.230 \pm .013$	$37.274 \pm .031$	1.63	0.082
	15.248	15.188	37.137		
	(15.246)	(15.207)	(37.213)		
KF 1-7	$13.592 \pm .099$	$14.851 \pm .099$	$34.338 \pm .237$	1.75	0.730
	13.583	14.831	34.266		
	(13.595)	(14.866)	(34.386)		
KF 2-3	$15.113 \pm .046$	$15.189 \pm .057$	$34.893 \pm .157$	1.63	0.087
	15.086	15.158	34.789		
	(15.114)	(15.200)	(34.918)		
KF 3-8	$14.836 \pm .010$	$15.160 \pm .010$	$35.017 \pm .023$	0.77	0.065
	14.808	15.118	34.888		
KF 4-1	$15.883 \pm .010$	$15.425 \pm .009$	$35.489 \pm .022$	0.77	0.060
	15.853	15.383	35.357		
	(15.877)	(15.419)	(35.505)		

* Approximate contaminant Pb is estimated on the basis of a total blank of $0.4895 \mu\text{g}$, similar to that of whole rock samples.

Note: The values presented in the second-row for each sample are ratios corrected for standard errors by computer program; the values in parenthesis are within run results of lower voltage on electrometer.

CHAPTER 5 INTERPRETATION

INTRODUCTION

As has been mentioned in Chapter 2, a Rb-Sr whole rock dating on 6 pegmatites intruded in rocks similar to the present rock samples indicates a Kenoran age of 2550 m.y. (Rocks 2-3, 3-8 and 4-1 definitely are cut by the concordant pegmatites). Again, K-Ar dates on biotite of different rock types including the present rock types indicate a metamorphic event at about 1800 m.y. ago. (Baadsgaard and Godfrey, 1967). Since the pegmatites all plot on a Rb-Sr isochron giving $^{87}\text{Sr}/^{86}\text{Sr} = 0.703$, it is assumed that these rocks are "normally" derived from a common well-mixed source (i.e. from mantle or homogeneous lower crust) and the different rocks are produced by a variety of differentiation from this common source (Baadsgaard, personal communication). Therefore a basic assumption is that these rocks are Archean rocks which involved in subsequent Aphebian (Hudsonian) diastrophic events (metamorphism and intrusion).

One of the main objectives of this study is thus to provide some understanding of the behaviour of the U-Th-Pb and Pb-Pb systems in the mineral phases and whole rock with regard to different diastrophic events, and to the provenance of the source rocks.

The interpretation of the data is carried out in several ways which can be catagorically classified as follows:

(1) U-Th-Pb systematics in zircon and apatite (concordia interpretation);

- (2) Apatite-rock isochron and apatite Pb isotope interpretation;
- (3) K-feldspar Pb isotope and feldspar-rock isochron interpretation;
- (4) Whole rock modified concordia interpretation;
- (5) Whole rock Pb isotope interpretation.

The resultant ages and possible indications from the above interpretations are discussed in this Chapter. Various comparisons with results of other works from related areas are made in the next Chapter.

Statistical assessments that are well-suited to the Rb-Sr system are also suitable for evaluating the slope and position of U-Th-Pb isochrons. However, the requisite error factors, obtained from replicate runs, have not yet been determined. An estimate of the limits of measurement errors is possible and this has been briefly given in Chapter 4.

Rock Pb data both measured and corrected (for mass discrimination) are presented in the rock-feldspar isochron and Pb isotope interpretations. Rock Pb data of 3 samples determined by volatilization method by Mr. F. Tsong of the Department of Physics are also presented in the interpretations for comparison.

U-Th-Pb SYSTEMATICS IN ZIRCON AND APATITE

(1) Introduction

U-Th-Pb dating using concordia plots for U-Pb and Th-Pb systems in U-Th minerals such as zircon, etc. has been extensively used and greatly developed in the past 15 years. Many studies have been made on possible Pb loss mechanisms, age discordance patterns and other evaluations from the isotope analyses of zircon and other U-Th minerals.

In the present study, zircon separates from the five rock samples have been analysed for U-Th-Pb systems. Also under consideration in the systems are five apatite samples.

One main objective of this study is to find a possible Pb loss mechanism and to compare the behaviour of the different systems in response to the several geological events in these minerals. Only single-phase U-Th-Pb systems are considered for these minerals in the present study.

There are four dates or values for "t" obtainable from U-Th-Pb systems in a given U-Th mineral (presumably remained closed system) since a time t until present; three of these t values can be obtained from the following equations*:

$$t_{206} = 6.49 \times 10^9 \ln (1 + 1.155 \times 206\text{Pb}/238\text{U})$$

$$t_{207} = 1.03 \times 10^9 \ln (1 + 1.135 \times 207\text{Pb}/235\text{U})$$

$$t_{208} = 20.0 \times 10^9 \ln (1 + 1.115 \times 208\text{Pb}/232\text{Th})$$

* After Dr. Baadsgaard, personal communication.

A fourth date may be obtained from the ratio of radiogenic $^{207}\text{Pb}/^{206}\text{Pb}$.

Zircon often yields four t values which are discordant and thus deviates from the ideal closed system behaviour. One of the most commonly observed discordance patterns is that $t_{206} < t_{207} < t_{207/206}$; this is normally explained by a model of daughter (Pb) loss mechanism (Rankama, 1954; Baadsgaard, 1965).

The problem of the cause of the discordance in U-Pb dates drew many workers' attention to the various possible geological or geochemical mechanisms. Many U-minerals also exhibit the same discordance pattern and regularities shown by zircon.

There have been three hypotheses proposed to account for the behaviour of U-Pb system in zircon:

- (1) Episodic loss of radiogenic Pb (Wetherill, 1956; Catanzaro and Kulp, 1964) — including diffusion loss of Pb during thermal event, and ground water leaching.
- (2) Continuous diffusion loss of radiogenic Pb — this includes a constant D/a^2 model [$D(t)=D_0$, Tilton, 1960] and a time-dependent, integrated radiation damage model [$D(t)=D_1 T$, Wasserburg, 1963]. In this connection, Wetherill (1963) has also considered various models such as pure diffusion Pb loss with and without pulse of metamorphism, combined Pb and U loss with and without pulse of metamorphism, in terms of Tilton's model.
- (3) Fractionation of Pb isotopes plus recent removal —

the proposed mechanism is that members of the ^{238}U and ^{235}U decay series are made more available to leaching due to recoil following alpha emission (Ahrens, 1955; Russell and Ahrens, 1957).

It has been successfully shown that in some cases it is very hard to distinguish between episodic Pb loss and Pb loss by one of the proposed continuous diffusion models, in addition to the combined complexity of some small U loss.

An attempt to interpret the discordance patterns and the U-Th-Pb behaviour in zircon, apatite and other U-Th minerals is made in terms of possible mechanism or mechanisms as proposed by various models, among which are the episodic and continuous diffusion Pb loss models. These models are considered on the basis of non-fractionating diffusion loss from a single-phase system.

(2) Interpretation

Isotopic data of Pb/Pb , Pb/U and Pb/Th ratios for the five zircons and five apatites are presented in Table 4-8 and Table 4-9 in Chapter 4. Their calculated $^{206}\text{Pb}/^{238}\text{U}$, $^{207}\text{Pb}/^{235}\text{U}$ and $^{208}\text{Pb}/^{232}\text{Th}$ ages are listed in Table 5-1.

Results of Pb/U ratios from zircon and apatite analyses are plotted on a $^{206}\text{Pb}/^{238}\text{U}$ versus $^{207}\text{Pb}/^{235}\text{U}$ diagram in Figure 5-1. A measurement error of $\pm 2\%$ in Pb/U ratios is assumed for zircon data. A slightly larger error is considered for apatite in which the common lead correction is larger.

TABLE 5-1 Calculated ages for zircon and apatite samples (in million years)

Sample No.	Calculated ages (m.y.)			
	206Pb-238U (t_{206})	207Pb-235U (t_{207})	208Pb-232Th (t_{208})	207Pb-206Pb ($t_{207/206}$)
Zircon 1-5	1851	1938	1650	2030
Zircon 1-7	2017	2065	2064	2115
Zircon 2-3	1554	1789	1315	2080
Zircon 3-8	1733	1812	1801	1905
Zircon 4-1	1359	1534	1394	1787
Apatite 1-5	1801	1801	-	1799
Apatite 1-7	1306	1500	-	1790
Apatite 2-3	1598	1615	-	1634
Apatite 3-8	1850	1873	-	1898
Apatite 4-1	1588	1765	-	1984

Note: The ages for zircon samples are calculated with the aid of an A.P.L. computer program UPBCOMP L; the ages for apatite samples are calculated directly from equations.

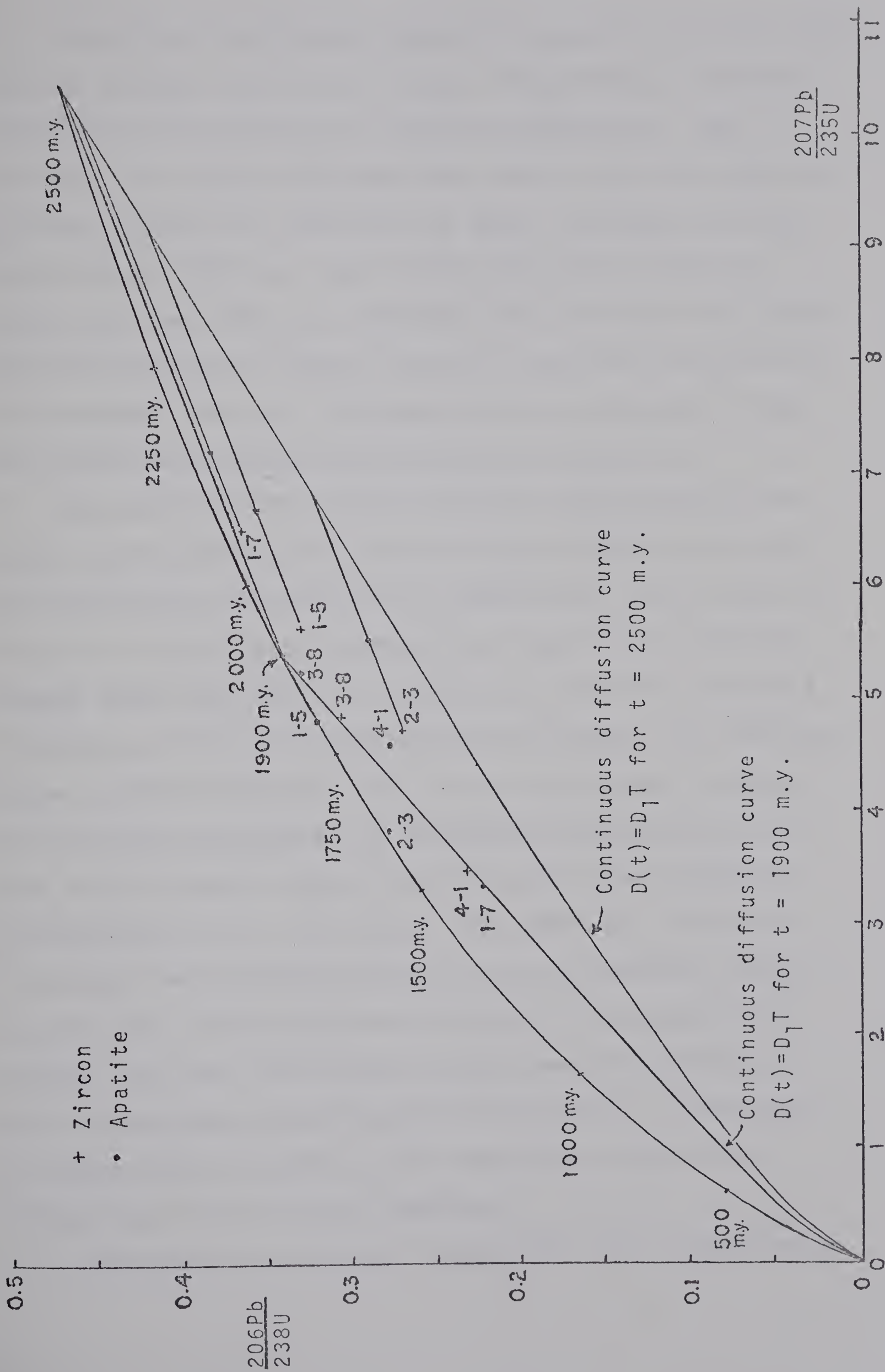


FIGURE 5-1 Concordia plot of zircon and apatite samples.

The five zircon points appear to be quite scattered and do not indicate any overall linear relationship. Therefore they must have experienced different evolutions. One straight line with a minimum slope can be drawn for the two zircons 3-8 and 4-1, which has an upper intercept with the concordia at 1905 m.y. and a lower intercept at 360 m.y. Since the lower 360 m.y. intercept does not appear to represent any geological event, the only significant implication is the upper 1905 m.y. intercept, which corresponds to an intrusion-metamorphism event during the Hudsonian.

An alternative but more reasonable interpretation for these scattered data of zircon is thus a combined episodic and continuous diffusion Pb loss mechanism. As is shown in Fig. 5-1, two diffusion curves for a continuous radiation damage model [$D(t)=D_1 T$] of a 1900 m.y. old U-Pb system and a 2500 m.y. old U-Pb system have been plotted. The 1900 m.y. curve is that calculated for zircons of "younger" granites in the Andrew Lake Area (cf. Baadsgaard and Godfrey, 1967) and is the probable age of the last major event affecting the episodic Pb loss in zircon. The 2500 m.y. curve was chosen on the ground that this may be the maximum original age for all zircons presumably formed in the source rock system. (A line with maximum slope drawn from 1900 m.y. point on the concordia through zircon point 1-7 intersects at about 2500 m.y. point on the concordia, indicating a maximum age for all zircon samples.)

The combined continuous and episodic Pb loss mechanism

would explain the results as follows:

At least three of the zircons (1-7, 1-5, 2-3) were originally formed or reset at some time 2500 m.y. ago; the 1900 m.y. thermal event caused episodic loss of varying amounts of Pb. Zircon 1-7 may have been affected almost solely by the 1900 m.y. episode and has undergone no or negligible continuous diffusion loss of Pb before and after the 1900 m.y. event. Zircon 1-5 and zircon 2-3 systematically lost Pb by continuous diffusion until 1900 m.y. event when an episodic Pb loss occurred. An estimate of the amounts of episodic Pb loss for zircons 1-5, 1-7 and 2-3 shows that zircon 1-5 has been subjected to the greatest intensity of episodic diffusion loss (84%), zircon 1-7 to a lesser intensity (77%) and zircon 2-3 to a even lesser intensity (65%). However, the difference in the intensity of episodic loss of these zircon samples is not very sizable. After the 1900 m.y. thermal event, zircons 1-5 and 2-3 continued to lose Pb by continuous diffusion. The diffusion coefficient D_1/a^2 for each zircon sample is governed by the $D(t)=D_1 T$ model where diffusion parameter $k = D_1/a$, and $D_1=\text{constant}$. (cf. Wasserburg, 1963).

The zircon samples 3-8 and 4-1 plot on the 1900 m.y. diffusion curve, within experimental error. The interpretation for these two samples seems equivocal. They can be considered as "younger" zircons which were formed at the 1900 m.y. event, and lost their leads subsequently by continuous diffusion. An equally reasonable mechanism is

that they were 2500 m.y. old zircons and lost Pb by continuous diffusion until 1900 m.y. ago when they lost most of their leads by episodic diffusion, and continued to lose Pb by continuous diffusion subsequently. The only problem in the latter interpretation is that zircon 3-8, while having a smaller k value (thus smaller diffusion coefficient D_1/a^2) than zircon 2-3, could have suffered much greater amount of Pb loss during the 1900 m.y. event. Here we have to assume that zircon 2-3 had been subjected to incomplete loss of Pb during the episode, and subsequently lost Pb by continuous diffusion up to the present time. (cf. Baadsgaard, 1965, p.19). However, this assumption is directly related to a change in the intensity of episodic diffusion loss, and the latter is in turn attributable to a partial recrystallization including a metamorphic recrystallization of the zircon.

As has been pointed out by Baadsgaard (1965), a combination of continuous diffusion and episodic loss may make the final composition of the Pb plot almost anywhere within the area bounded by two diffusion curves and the episodic line connecting 2500 m.y. and 1900 m.y. points on the concordia. Furthermore, a "mixture" of 1900 m.y. and 2500 m.y. zircons undergoing diffusion loss of Pb will also plot within the bounded area in Fig. 5-1, and cannot be distinguished from a combined diffusion-episodic Pb loss history for a single zircon without other information.

Zircons 3-8 and 4-1 are, from crystal morphological observation (see Appendix C), somewhat different from other

three zircons in that they are less euhedral and have quite abundant malformed crystals, greater variability in elongation ratio and crystal size, and larger amounts of subhedral to rounded (detrital?) grains. No clear evidence of overgrowth is observable in all the zircons. In thin section, rock samples 3-8 and 4-1 show some alteration phenomena such as chloritized biotite, crushed quartz, sericitized plagioclase and sometimes eroded plagioclase. (Although rock samples 1-5 and 1-7 also show similar alteration phenomena, but to a much lesser degree.) Again from field occurrence, rock samples 3-8 and 4-1 are from outcrops close to a fault contact or sheared zone with metasedimentary rocks.

Therefore it might be reasonable to say that zircons 3-8 and 4-1, if not completely reset or formed during metamorphism, might have been subjected to some deformation and minor reconstitution as a result of the 1900 m.y. event. They could have been admixtures of magmatic, older zircons and authigenic zircons, and subjected to partial recrystallization during metamorphism.

Calculated ages of t_{208} for Th-Pb system in zircons are also reported in Table 5-1. The generally observed discordance between U-Pb and Th-Pb systems can be seen in the ages of zircons 1-5, 2-3, 3-8 and 4-1. The t_{208} age of zircon 1-7 are concordant with other three U-Pb and Pb-Pb ages.

In a $^{208}\text{Pb}/^{232}\text{Th}$ versus $^{207}\text{Pb}/^{235}\text{U}$ plot for zircons (not shown), all the data points are quite scattered and uninterpretable. Even though two linear arrays can be drawn

for two groups of data points with upper intercepts at the concordia of ages 2070 m.y. and 1820 m.y. respectively, these data points do not show similar arrays in the $^{206}\text{Pb}/^{238}\text{U}$ versus $^{207}\text{Pb}/^{235}\text{U}$ diagram. Besides, the extrapolated lines for the 2070 m.y. and 1820 m.y. array lie to the right of the origin, in contrast to the requirement in $^{235}\text{U}-^{238}\text{U}$ system that all points subjected to non-fractionating Pb loss must lie in an accessible region (Wasserburg, 1963). Therefore, for a single-phase system in Th-U-Pb system, the above observed linear arrays cannot be explained only in terms of a non-fractionating diffusion loss mechanism (which is assumed for the present interpretation of U-Pb system and Th-U-Pb system).

It is felt that a consideration of the degree of metamictization affecting various zircon fractions (multiphase U-Th-Pb systems), i.e. a consideration of diffusion Pb loss with fractionation for multiphase systems is necessary before a thorough understanding and a reliable conclusion can be obtained about the complex mechanisms and effects operative within various zircon fractions.

The U-Pb ratios of five apatite samples are presumably subjected to a larger measurement error than those of zircons. The common lead corrections for apatite samples were made by using the Pb isotopic ratios of their associated K-feldspars. The five apatite analyses are also plotted in Figure 5-1, and their calculated ages are given in Table 5-1.

It can be readily seen that apatite 1-5 fits very well on the concordia with an age of 1800 m.y. The calculated ages t_{206} , t_{207} and $t_{207/206}$ for this apatite are also concordant. Apatites 2-3 and 3-8 plot slightly below the concordia, and their calculated age pattern is also slightly discordant, showing $t_{207/206} > t_{207} > t_{206}$. Apatite 2-3 gives an age of about 1610 ± 20 m.y.; whether this is indicative of a post-Hudsonian disturbance and whether gain or loss of parent or daughter occurred subsequent to the Hudsonian event is not clear at the moment, however, more can be said about this when we have further evidence from apatite Pb isotope and apatite-rock U-Pb isochron interpretations. Apatite 3-8 plots below the concordia but on the 1900 m.y. diffusion curve, but its calculated ages are reasonably concordant with a mean age of 1874 ± 25 m.y. This apatite is thus considered to be a thoroughly reset mineral at the Hudsonian event. Apatite 1-7 plots far below the concordia but also on the 1900 m.y. diffusion curve, its calculated age pattern is $t_{207/206} > t_{207} > t_{206}$, thus showing a Pb loss mechanism. This apatite was also possibly reset at about 1800 — 1900 m.y. ago. Apatite 4-1 plots significantly below the concordia and within the combined diffusion-episodic bounded area, its calculated ages display a discordance pattern of $t_{207/206} > t_{207} > t_{206}$, again inferring a Pb loss effect.

In all cases, apatite samples display a very complicated situation in the U-Pb system where three apatite samples (1-7, 3-8 and 4-1) fall within the combined diffusion-episodic

bounded area (thus indicating that they have been affected by the last major episodic loss of Pb); one apatite (1-5) falls on the concordia indicating that its last resetting or emplacement was about 1800 m.y. ago; one apatite (2-3) falls slightly below the concordia giving an unexpectedly younger age of 1610 m.y. Therefore it is felt that more evidence from the U-Pb isochron and Pb isotope interpretations of these apatite samples should be considered before any conclusions are made.

APATITE-ROCK ISOCHRON & APATITE Pb ISOTOPE INTERPRETATION

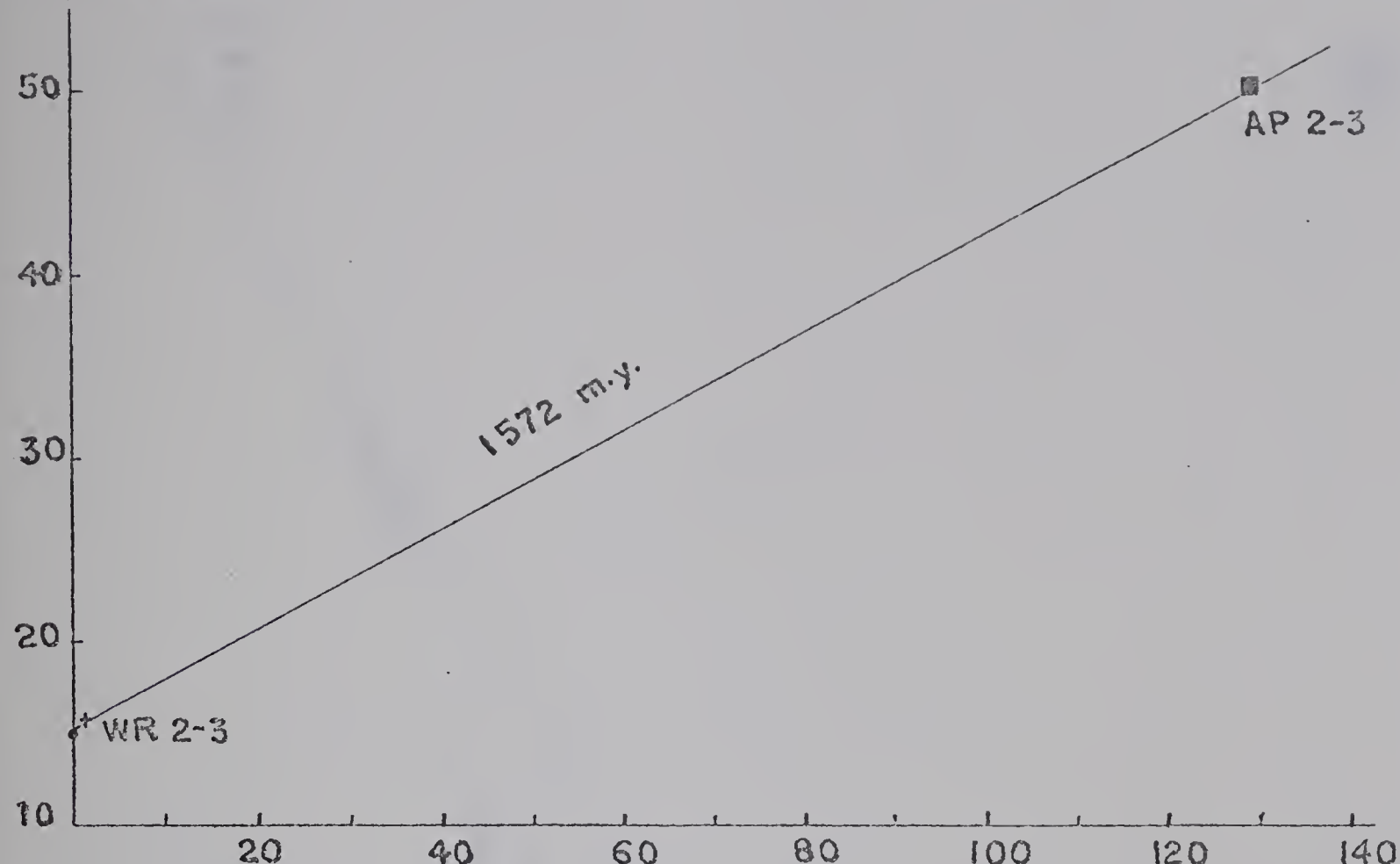
(1) Apatite-rock (U-Pb) isochron interpretation

Age information for apatite samples can be obtained by a U-Pb isochron interpretation of apatite and rock samples. The data are plotted on $^{206}\text{Pb}/^{204}\text{Pb}$ versus $^{238}\text{U}/^{204}\text{Pb}$ and $^{207}\text{Pb}/^{204}\text{Pb}$ versus $^{235}\text{U}/^{204}\text{Pb}$ diagrams, as shown in Figures 5-2 and 5-3. An isochron line is drawn for each pair of apatite-rock data points in both diagrams, and the slope age of each isochron line estimated. The estimated ages for these ten isochrons are listed in Table 5-2. In both U-Pb systems, all isochron ages are consistent with the calculated ages given in Table 5-1.

Sample pairs 1-5, 2-3 and 3-8 have concordant isochron ages of 1802 ± 23 m.y., 1603 ± 31 m.y. and 1858 ± 31 m.y. in both systems respectively. The results for apatite-rock isochrons 1-5 and 3-8 are indicative of the time of the Hudsonian event 1800 — 1900 m.y. ago. Apatite-rock sample pair 4-1 gives somewhat discordant ages, yet having a $^{207}\text{Pb}-^{235}\text{U}$ isochron age of 1765 m.y., which is consistent with the calculated $^{207}\text{Pb}-^{235}\text{U}$ age of 1765 m.y. for this apatite (see Table 5-1). Only sample pair 1-7 gives highly discordant and younger isochron ages, with 1265 m.y. in $^{206}\text{Pb}-^{238}\text{U}$ system, and 1495 m.y. in $^{207}\text{Pb}-^{235}\text{U}$ system.

It must be mentioned that the slope of each isochron in Figures 5-2 and 5-3 is largely controlled by the Pb isotopic compositions of apatite samples, in which a slight variation

$206\text{Pb}/204\text{Pb}$



■ Apatite

+ Whole rock

• K-feldspar

AP 1-5

1779 m.y.

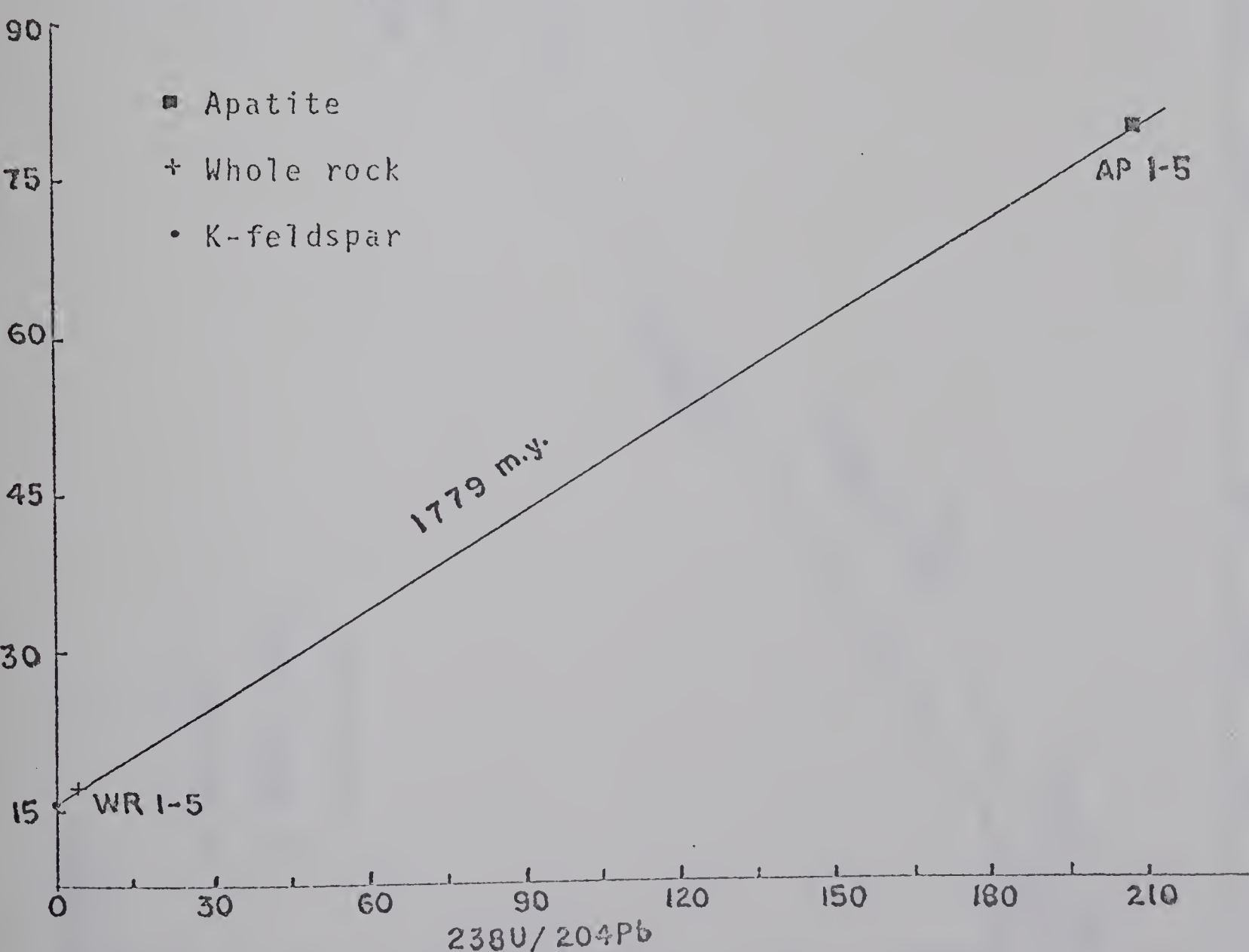


FIGURE 5-2a $206\text{Pb}/204\text{Pb}$ versus $238\text{U}/204\text{Pb}$ for apatite-rock pairs 1-5 and 2-3.

206Pb/204Pb

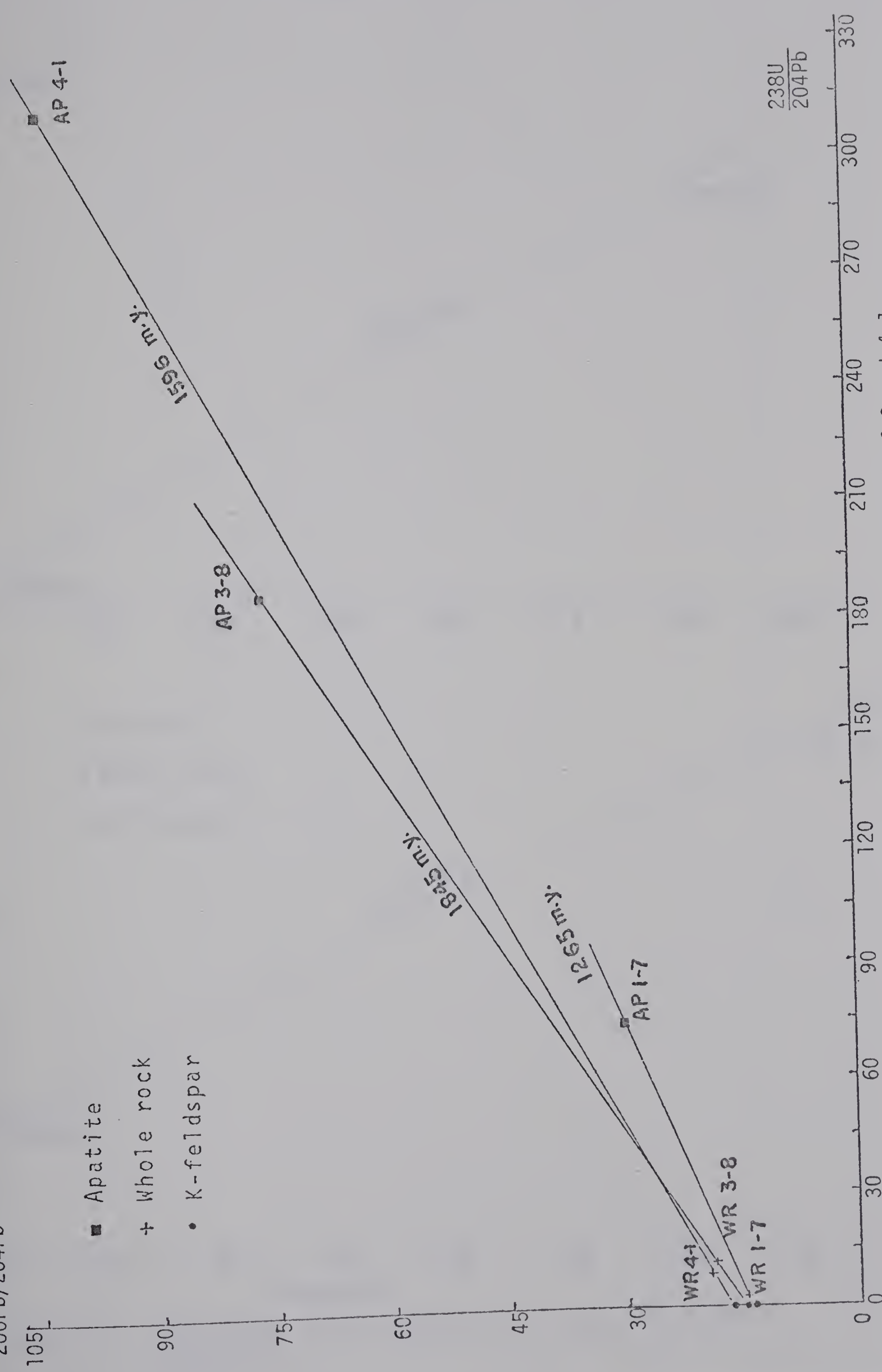


FIGURE 5-2b 206Pb/204Pb versus 238U/204Pb for apatite-rock pairs 1-7, 3-8 and 4-1.

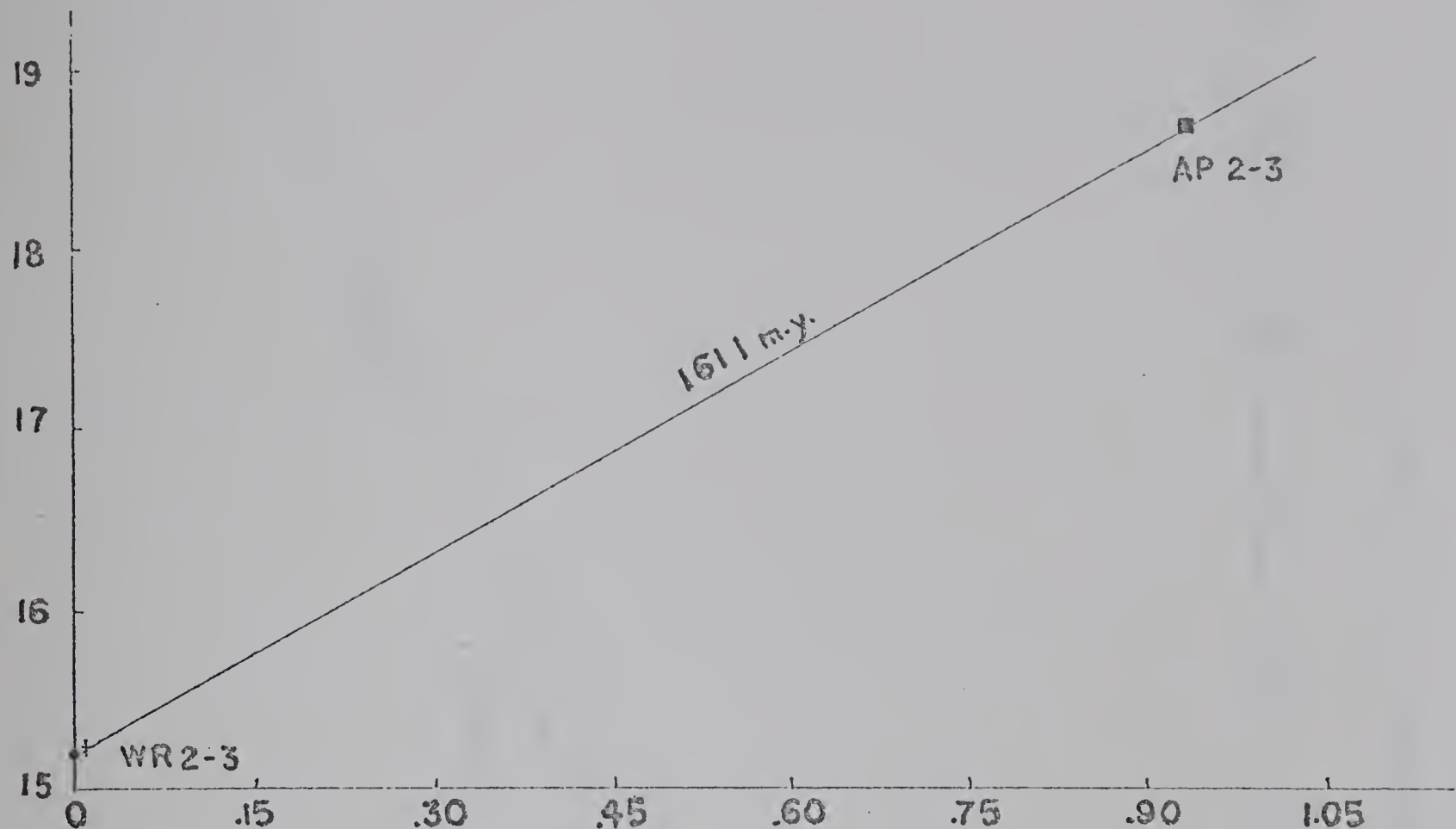
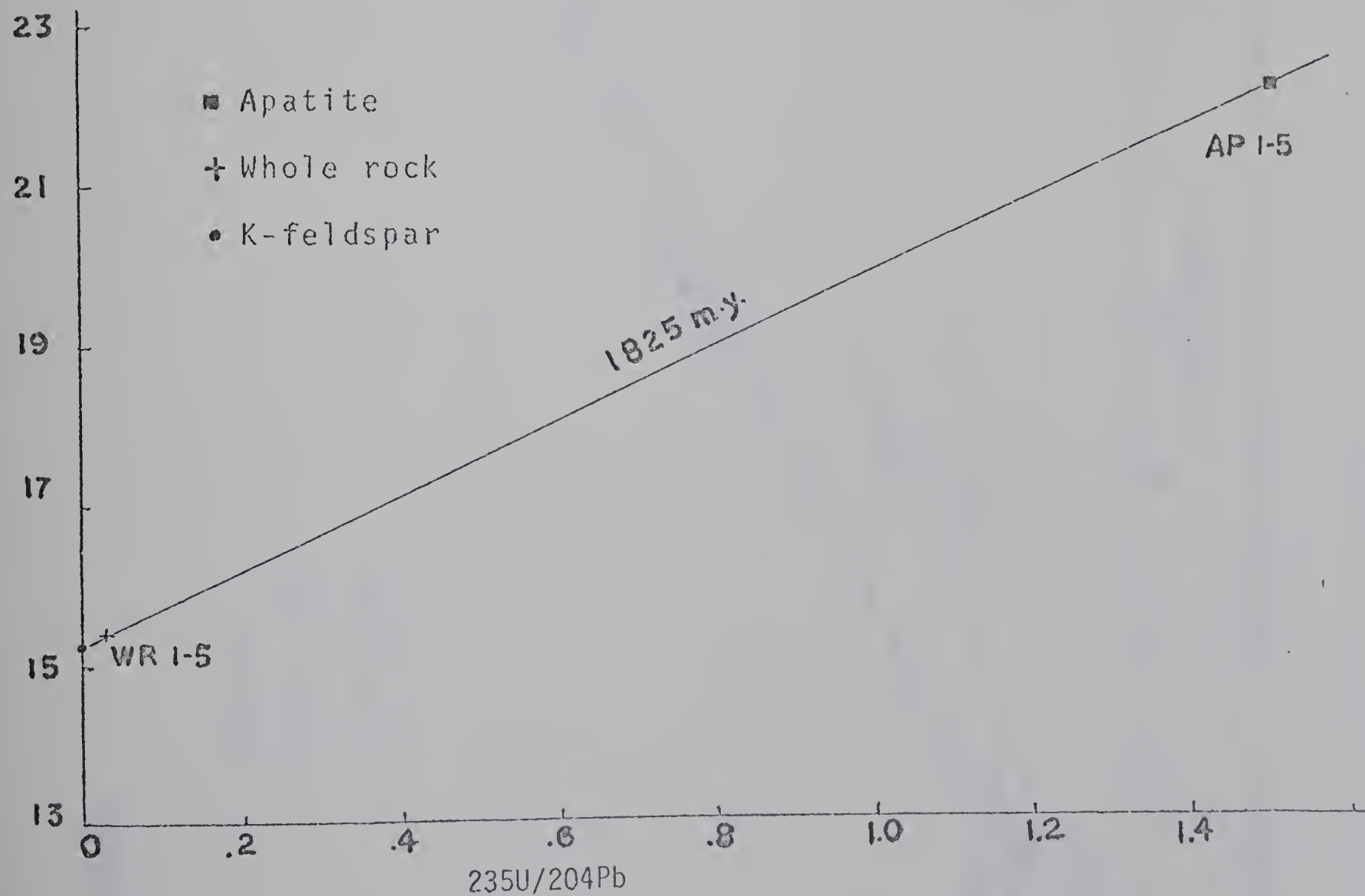
$^{207}\text{Pb}/^{204}\text{Pb}$  $^{207}\text{Pb}/^{204}\text{Pb}$ 

FIGURE 5-3a $^{207}\text{Pb}/^{204}\text{Pb}$ versus $^{235}\text{U}/^{204}\text{Pb}$ for apatite-rock pairs 1-5 and 2-3.

$^{207}\text{Pb} / ^{204}\text{Pb}$

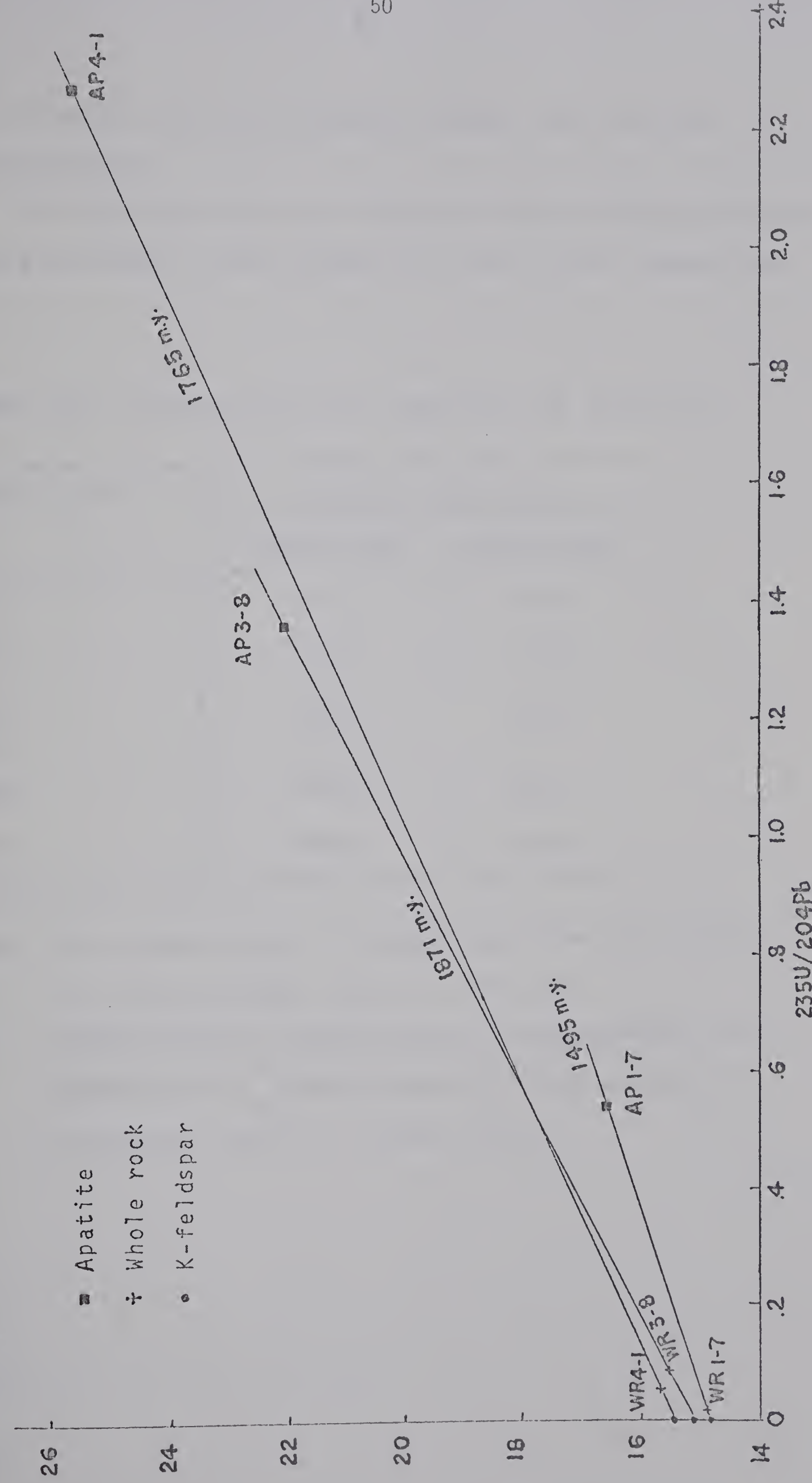


FIGURE 5-3 b $^{207}\text{Pb}/^{204}\text{Pb}$ versus $235\text{U}/^{204}\text{Pb}$ for apatite-rock pairs 1-7, 3-8 and 4-1.

in Pb ratios would considerably affect the resultant isochron age.

Pb isotopic ratios of the associated K-feldspar samples are also shown in both Figures 5-2 and 5-3 for comparison.

TABLE 5-2 Estimated ages for apatite-rock isochrons

Sample pair	Isochron age (m.y.)	
	206Pb-238U	207Pb-235U
1-5	1779	1825
1-7	1265	1495
2-3	1572	1611
3-8	1845	1871
4-1	1596	1765

Note: The isochron age t is calculated from the equation

$$t = (1/\lambda) \ln(1+R)$$
, where R refers to

$$[(206\text{Pb}/204\text{Pb})_p - (206\text{Pb}/204\text{Pb})_i]/(238\text{U}/204\text{Pb})_p$$
 or

$$[(207\text{Pb}/204\text{Pb})_p - (207\text{Pb}/204\text{Pb})_i]/(235\text{U}/204\text{Pb})_p$$
 ;
 p : present ratio, i : initial ratio.

(2) Apatite Pb isotope interpretation

Measured Pb isotopic ratios of five apatite samples are plotted on a conventional $^{207}\text{Pb}/^{204}\text{Pb}$ versus $^{206}\text{Pb}/^{204}\text{Pb}$ diagram (Figure 5-4) together with isotopic ratios of K-feldspar and whole rock leads. The analytical uncertainty is estimated to be 2% for $^{207}\text{Pb}/^{204}\text{Pb}$ ratios, and 1% for $^{206}\text{Pb}/^{204}\text{Pb}$ ratios in apatite samples. An isochron line fits most data points (except rock and feldspar leads 1-7 which fall below the isochron line) within analytical errors. This isochron is compared to an age of 1905 ± 40 m.y. with a slope of $0.1147 \pm .0020$. Apatites 1-5, 1-7 and 3-8 fit reasonably well to the line, indicating that their lead development has been quite "stable" with regard to subsequent disturbances. Apatites 1-5 and 3-8 are concordant in both Pb-Pb and U-Pb systems, indicating that these apatites have been "stable" in terms of U or Pb migration since their formation during the major Hudsonian event, and that their ages derived from U-Pb and Pb-Pb systems are real and representative. However, apatite 1-7, which has the highest common Pb correction, behaves quite differently in the U-Pb system. Apparent ages estimated from U-Pb system (concordia and apatite-rock isochron) are significantly discordant and younger ($t_{206} = 1300$ m.y. and $t_{207} = 1500$ m.y.) for this apatite, yet it has a $t_{207/206}$ age of 1790 m.y. Since it plots on a 1900 m.y. diffusion curve in the concordia interpretation, this apatite was probably formed at the Hudsonian time and subsequently subjected to either U

addition or continuous diffusion Pb loss effect. Apatite 2-3 falls below the Pb-Pb isochron, implying a younger emplacement age; judging from ages derived from concordia and U-Pb isochron interpretations, this apatite is thus considered to be thoroughly reset at a post-Hudsonian time (1600 m.y. ago) in which open system effects in Pb and U systems occurred. On the other hand, apatite 4-1 plots above the isochron, giving a $t_{207/206}$ age of 1984 m.y. Considering the estimated ages from the concordia and U-Pb isochron interpretations ($t_{206}=1590$ m.y., $t_{207}=1765$ m.y.), it is possible that some U addition or diffusion Pb loss had affected this apatite and consequently it is updated in the U-Pb system.

It is obvious from Fig. 5-4 that the resultant slope is controlled by the compositions of apatite leads. The simplest explanation for the scattering of apatite, feldspar and rock Pb points about the isochron line is that an incomplete homogenization (or variable mixing) of leads in apatite and feldspar phases could have taken place as a result of internal and partial phase contamination in the whole rock system.

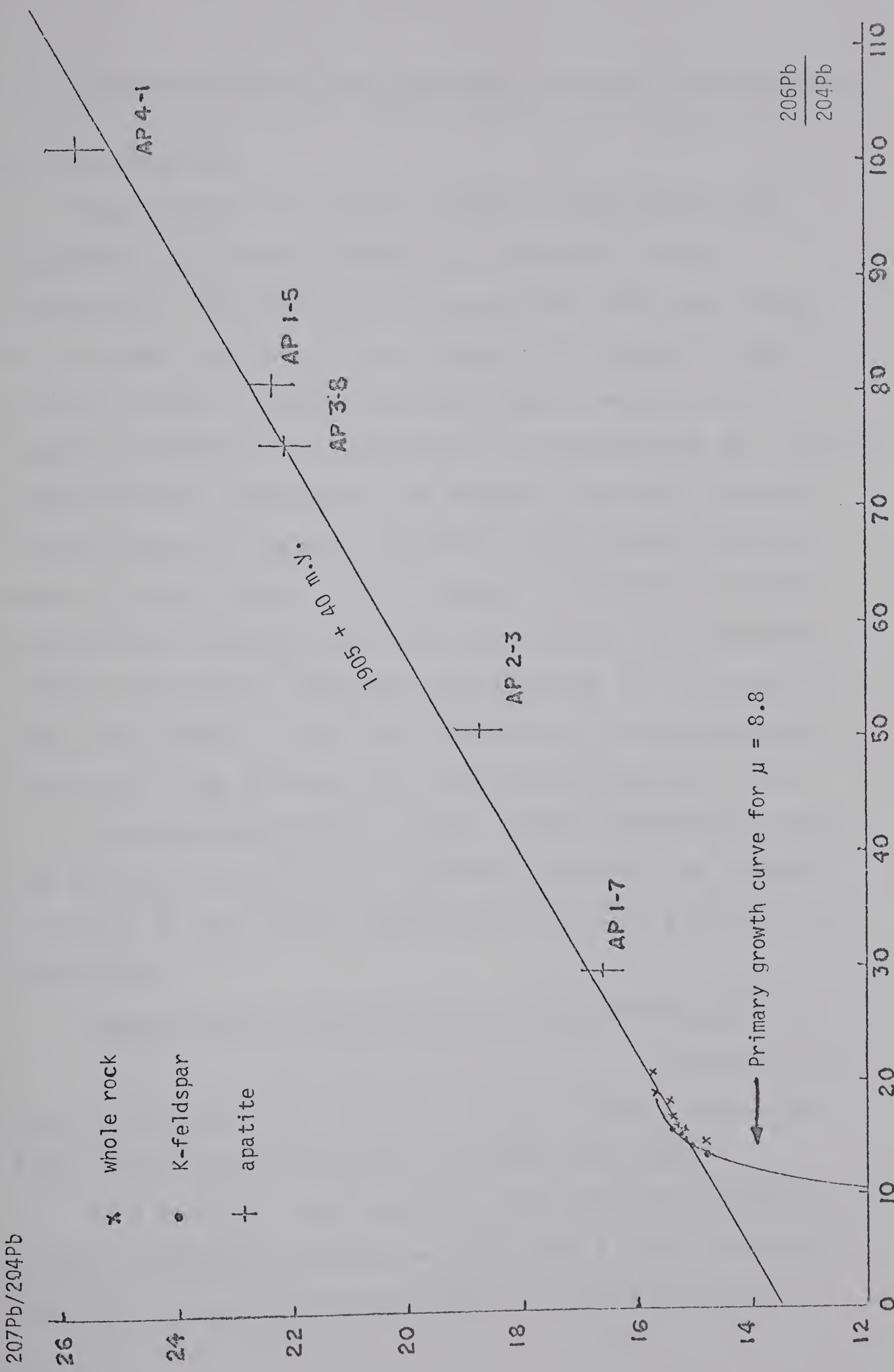


FIGURE 5-4 $^{207}\text{Pb}/^{204}\text{Pb}$ versus $^{206}\text{Pb}/^{204}\text{Pb}$ for whole rock, K-feldspar and apatite samples.

K-FELDSPAR Pb ISOTOPE & FELDSPAR-ROCK ISOCHRON INTERPRETATION

(1) Introduction

Many analyses on the Pb isotopic compositions and abundances in natural minerals are available in the literature. The majority of the analyses have been those of ore leads, and to a lesser extent, of feldspar leads in plutonic rocks. However, as knowledge of whole rock Pb isotopic composition is important in interpreting the isotopic composition of the lead in ore deposits (as well as other crustal deposits) several studies on rock leads have been made in recent years. In an attempt to clarify the understanding of available rock lead data, Ulrych and Reynolds (1966) have made an important contribution to the study of whole rock leads. They have presented an interpretation analogous to Rb-Sr whole rock studies (Nicolaysen, 1961). For a rock starting from a common initial $^{206}\text{Pb}/^{204}\text{Pb}$ ratio, and for which the rock has remained closed to the transfer of Pb and U, the present $^{206}\text{Pb}/^{204}\text{Pb}$ ratio is given by the expression:

$$(206\text{Pb}/204\text{Pb})_p = (206\text{Pb}/204\text{Pb})_{it} + (238\text{U}/204\text{Pb})_p (e^{\lambda t} - 1) \quad \dots\dots (\text{Equation 5-1})$$

where p: present day ratio, it: initial ratio t years ago. Equivalent expressions exist for ^{207}Pb and ^{208}Pb .

If a suite of rocks satisfies the assumption then a linear relationship results with a slope R, which depends only on t; t can be obtained from: $t = (1/\lambda) \ln(1+R)$.

In their model they proposed a consideration of two-stage whole rock history for a first stage "common Pb environment" and a second stage "radiogenic Pb environment". The first stage can be likened to the history of some common leads and may correspond to MORE THAN ONE U-Pb system. The second stage is the one in which the U-Pb system presently observed is responsible for the last enrichment of the radiogenic Pb component through the decay of U and Th. This consideration has the advantage that independent age information may be obtained from an interpretation of initial Pb ratios of each stage. Therefore the initial ratios $(206\text{Pb}/204\text{Pb})_{it}$ and $(207\text{Pb}/204\text{Pb})_{it}$ represent the ratios of the common lead incorporated into the whole rock at the time of crystallization t ; in some cases these may be identified with a single stage Pb. The initial ratios $(206\text{Pb}/204\text{Pb})_{it_m}$ and $(207\text{Pb}/204\text{Pb})_{it_m}$ represent the result of mixing, t_m years ago, of a single stage Pb with radiogenic Pb which has developed in different U-Pb environment between the two times t and t_m .

(2) K-feldspar Pb isotope interpretation

It is well known that Pb isotopic composition in K-feldspar usually represents the common Pb component of a closed rock system. Therefore it is important to check the feldspar leads in order to seek some information regarding the first stage common Pb environment.

Observed Pb isotopic ratios of K-feldspars from the

five rock samples are plotted in Figure 5-5. A best fit straight line is drawn through the five data points. The slope R of a linear relationship between the ratios $^{206}\text{Pb}/^{204}\text{Pb}$ and $^{207}\text{Pb}/^{204}\text{Pb}$ for common leads is given by:

$$R = \frac{e^{\lambda t} - e^{\lambda t_m}}{\alpha(e^{\lambda t} - e^{\lambda t_m})} \quad \dots \dots \quad (\text{Equation 5-2})$$

where $\alpha = (238\text{U}/235\text{U})_p$, $\lambda = 0.9722 \times 10^{-9}/\text{yr}$, $\lambda = 0.1537 \times 10^{-9}/\text{yr}$, t: time of rock crystallization. t_m : time of metamorphism or mineralization.

The leads governed by the linear relationship have developed in different U-to-Pb environments from initial $^{206}\text{Pb}/^{204}\text{Pb}$ and $^{207}\text{Pb}/^{204}\text{Pb}$ ratios x and y in a closed system between the times t and t_m . At time t_m mixing occurred and the Pb isotopic ratios have remained unchanged to the present. The ratios x and y and the time t may be identified with the initial whole rock Pb isotopic ratios $(^{206}\text{Pb}/^{204}\text{Pb})_{it}$ and $(^{207}\text{Pb}/^{204}\text{Pb})_{it}$ and the single-stage model age which corresponds to these ratios. The single-stage model age (Holmes-Houterman model) for the whole rock is calculated to be 2475 m.y. The least radiogenic K-feldspar is sample KF 1-7 *, which has $^{206}\text{Pb}/^{204}\text{Pb} = 13.60$, $^{207}\text{Pb}/^{204}\text{Pb} = 14.85$, and $^{208}\text{Pb}/^{204}\text{Pb} = 34.32$. The single-stage model age for this K-feldspar is calculated to be

* It should be noted that the measured $^{206}\text{Pb}/^{204}\text{Pb}$ and $^{207}\text{Pb}/^{204}\text{Pb}$ ratios of KF 1-7 are subject to a quite large analytical uncertainty ($\pm .099$); $^{207}\text{Pb}/^{204}\text{Pb}$ ratio of KF 1-7 is unexpectedly greater than that of WR 1-7.

2720 m.y. In this case, the initial whole rock Pb ratios are not identified with the Pb ratios of the least radiogenic K-feldspar, even without correction for in situ U decay. A discussion of this problem will be given in the "whole rock Pb isotope interpretation" section.

The slope of the best fit straight line (Fig. 5-5) is $0.269 \pm .009$; now, if we take a t value of 2500 m.y. (as given by Rb-Sr dates on pegmatites) as the time when initial common leads incorporated into the whole rock system, and solve for Equation 5-2, a metamorphic age t_m of 1775 ± 100 m.y.* is then obtained from Table 5-3. Thus the simplest explanation is that the feldspars were affected by metamorphism of 1800 m.y. in which partial mobilization of radiogenic Pb had caused variable extent of radiogenic addition to a more typical 2700 m.y. old feldspar Pb (1-7) which appears to be least affected by the metamorphism. Feldspar 1-7 could have developed in a low U and Th environment (like lower crust) or derived directly from the contamination of a mantle-derived magma with the lower crustal materials. It is also possible that it derived from the melting of pre-existing older crustal terrain in the area. On the other hand, feldspar 4-1 appears to have

* $^{207}\text{Pb}/^{204}\text{Pb}$ ratio of KF 1-7 is considered to be in error because it is higher than that of WR 1-7. If a lower ratio is considered, the slope age t_m would be older than 1775 m.y. Also the two intercepts of the slope on the growth curve would be different (lower intercept older than 2500 m.y.).

$207\text{Pb}/204\text{Pb}$

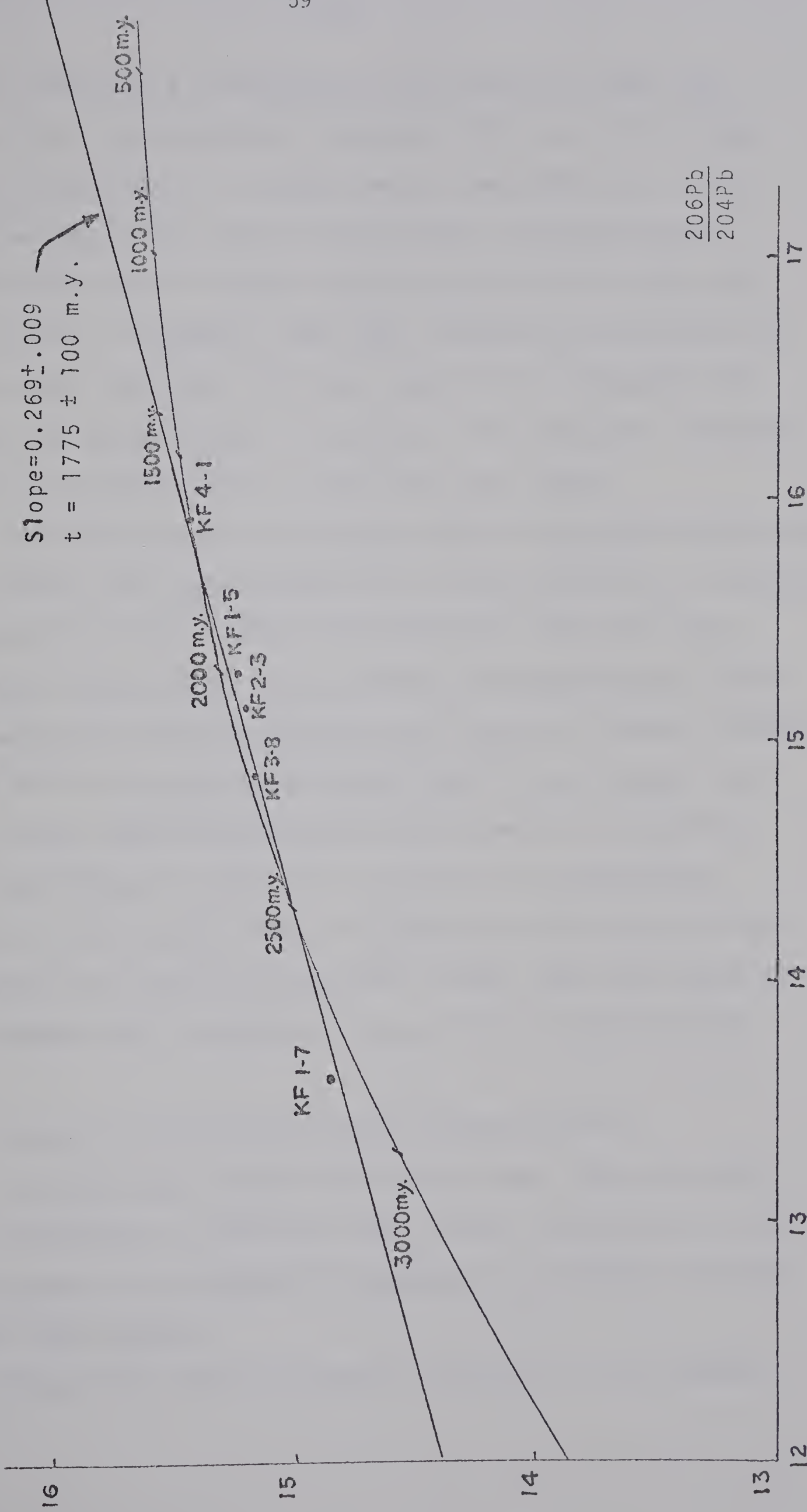


FIGURE 5-5 $207\text{Pb}/204\text{Pb}$ versus $206\text{Pb}/204\text{Pb}$ for K-feldspar samples; primary growth curve is for $\mu = 8.8$.

greater addition of radiogenic and younger Pb than the other three "intermediate" feldspars (KF 1-5, KF 2-3 and KF 3-8), and yields a younger model age (1600 m.y.) than the true age of the rock it associates; considering the higher U/Pb and Pb isotopic ratios in the whole rock and apatite 4-1, it appears that this feldspar was involved in a two-stage evolution with the addition of radiogenic Pb during the second stage. The three "intermediate" feldspars appear to be admixtures of the above two types.

The variation in Pb isotopic compositions and model ages may reflect the real variability in the evolution of feldspar leads prior to their final incorporation into the rocks. Therefore, as pointed out by Zartman and Wasserburg (1969), the danger of overinterpreting model ages of igneous feldspar leads should be cautioned and avoided in the present case.

If the above speculation holds, then it is possible that the feldspar leads are a product of a multistage history in the crust; this is consistent with the previous assumption by Ulrych and Reynolds (1966) that the common Pb environment may correspond to more than one U-Pb system.

(3) Feldspar-rock (U-Pb) isochron interpretation

We would now examine the U-Pb systems in whole rocks and K-feldspars in order to seek further information on the development of radiogenic Pb components and parent isotopes in the rock system.

Figures 5-6 and 5-7 show the variation of the ratios

TABLE 5-3 A table for determining t_m in a 2-stage model

$$R = \frac{e^{\lambda t} - e^{\lambda t_m}}{\alpha(e^{\lambda t} - e^{\lambda t_m})} \quad t = \text{constant} = 2500 \text{ m.y.}$$

t_m (m.y.)	R	t_m (m.y.)	R
1000	0.2092	1600	0.2533
1100	0.2156	1700	0.2622
1200	0.2223	1800	0.2716
1300	0.2295	1900	0.2810
1400	0.2370	2000	0.2921
1500	0.2490		

TABLE 5-4 Whole rock & feldspar-rock isochron ages

Assemblage	isochron ages (m.y.)		
	206Pb-238U	207Pb-235U	208Pb-232Th
(Whole rock)			
1-5, 2-3, 4-1	2513	2461	-
(3-8, 1-7)	2224	2363	-
(Feldspar-rock)			
1-5	1926	1898	1089
1-7	3901	negative	1941
2-3	2530(1822*)	1818	1059
3-8	1694(1814*)	1557	1209
4-1	2096(1948*)	1859	486

* Age obtained by comparison with rock point from volatilization analysis.

$^{206}\text{Pb}/^{204}\text{Pb}$ and $^{207}\text{Pb}/^{204}\text{Pb}$ with $^{238}\text{U}/^{204}\text{Pb}$ and $^{235}\text{U}/^{204}\text{Pb}$, respectively, in five rock samples and their associated K-feldspars. The fit of points to a single straight line in these two figures is not possible, and because the standard deviation of the age based on the fit of the data points to a single line is greater than the standard deviation based on the precision of the data, the model can only be considered to be an approximation to the history of the samples.

The age of the whole rock system can be determined from the slope of isochron lines through whole rock points. In Figure 5-6, one best fit isochron line for three rock points 1-5, 2-3 and 4-1 give an age of 2513 m.y., with an initial intercept $^{206}\text{Pb}/^{204}\text{Pb}$ ratio of 15.06. Rock points 1-7 and 3-8 do not plot together with the above three rock points on a single line, and this may indicate that these two rocks have different initial Pb ratios (common lead) at the time of crystallization. No reasonable rock isochron line can be drawn for these two points, however, if a line is allowed to be imposed on rock point 3-8 (volatilization value) and rock point 1-7, an age of 2224 m.y. with an initial $^{206}\text{Pb}/^{204}\text{Pb}$ ratio 14.00 is obtained.

In Figure 5-7, three rock points 1-5, 2-3 and 4-1 fit very well on a single isochron line having $t = 2461$ m.y. and an initial ratio $^{207}\text{Pb}/^{204}\text{Pb} = 15.133$. Again, rock points 3-8 and 1-7 deviate quite significantly from this single line, indicating that they could have had a different

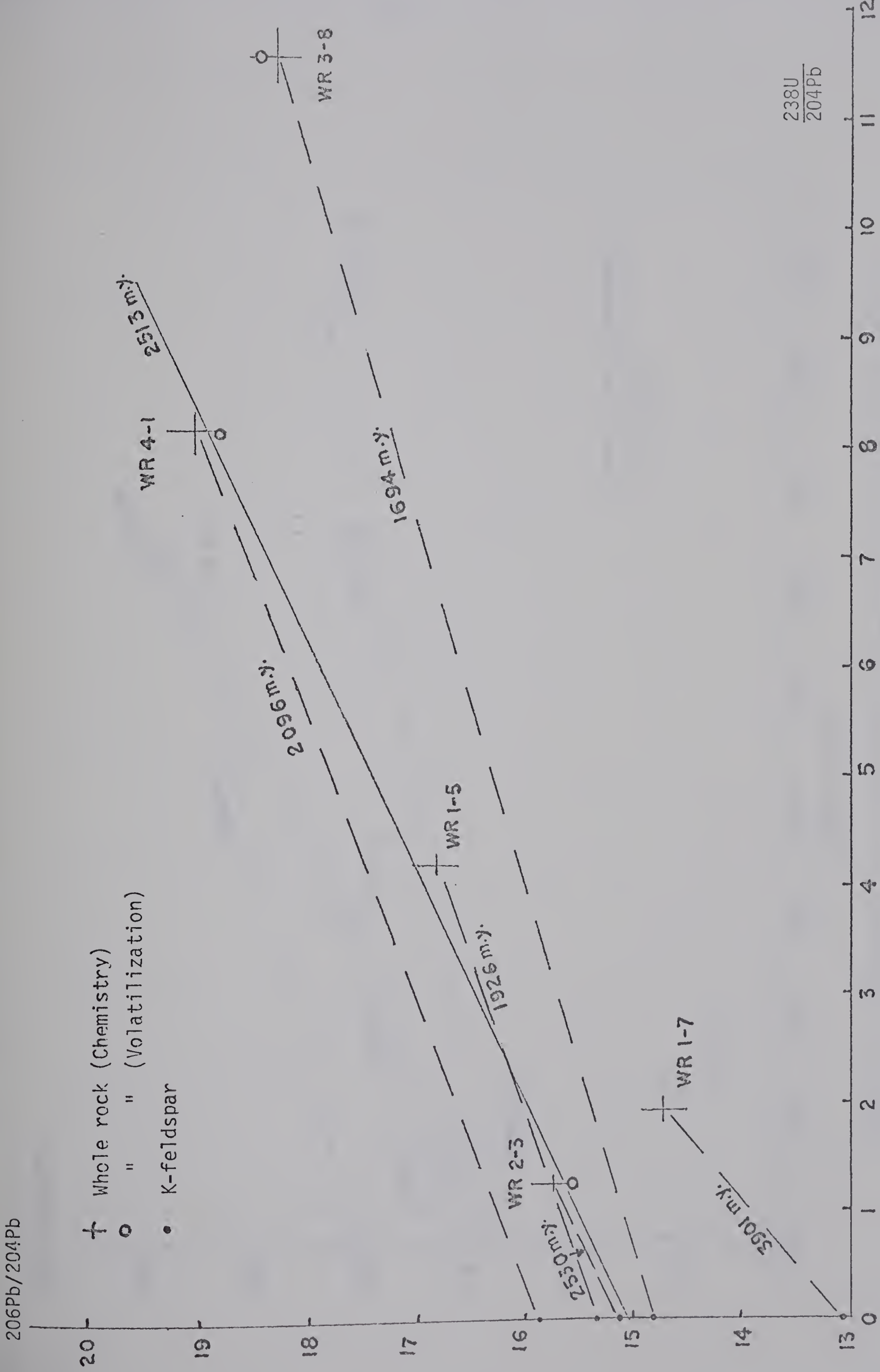


FIGURE 5-6 206Pb/204Pb versus 238U/204Pb for whole rock and K-feldspar samples.

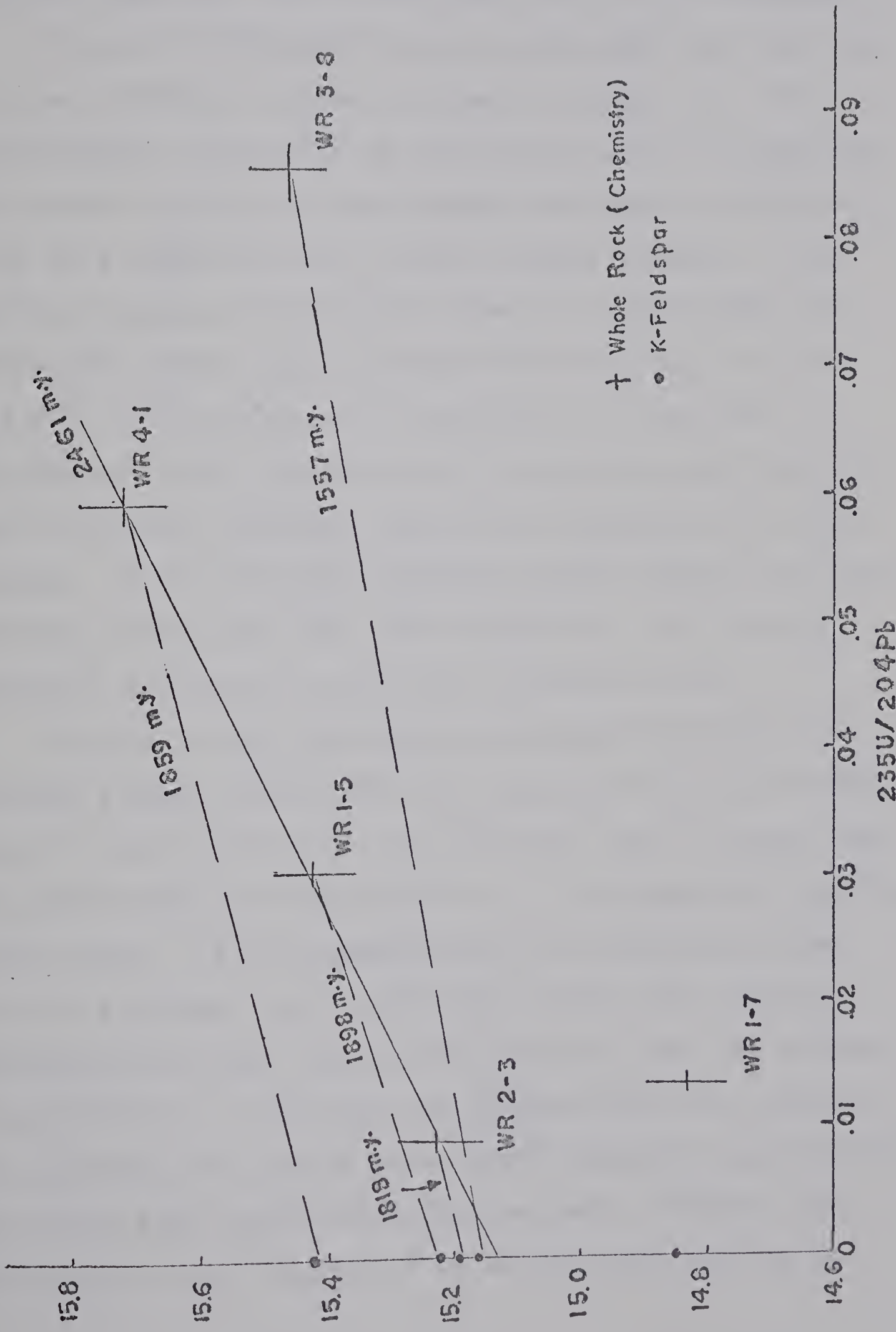


FIGURE 5-7 207Pb/204Pb versus 235U/204Pb for whole rock and K-feldspar samples.

common Pb component. If a line is allowed to be drawn through these two points, an age of 2363 m.y. with an initial intercept ratio $207\text{Pb}/204\text{Pb}$ of 14.70 is obtained.

A plot of $208\text{Pb}/204\text{Pb}$ versus $232\text{Th}/204\text{Pb}$ for the same rock and feldspar samples is shown in Figure 5-8. The experimental uncertainty for the Th-Pb ratios is about 5%. The greater scatter of data leaves considerable uncertainties in a regression of a single, common isochron. No similar grouping for isochron line as in $206\text{Pb}-238\text{U}$ and $207\text{Pb}-235\text{U}$ systems can be drawn for rock points 1-5, 2-3 and 4-1, or in the case of rock points 1-7 and 3-8. Therefore further consideration of any meaningful isochron age or initial intercept ratio is not attempted for Th-Pb system. It is felt that the Th-Pb system commonly displays different behaviour from U-Pb systems not only in U-Th minerals, but also in whole rock systems as well.

The whole rock isochron age estimated from the U-Pb systems average around 2487 m.y. (considering only isochron ages for rock points 1-5, 2-3 and 4-1), this is lower than the Rb-Sr whole rock age (2550 m.y.) for pegmatites cutting these rocks. If the pegmatite date can be used as some sort of a primary age for the rock system, the simplest explanation of this "aberration" would be that the Archean rocks (2550 m.y. old) have not remained entirely closed to the transfer of U and Th after their formation, and probably have been open during the Hudsonian event. Whether they were open to the transfer of Pb or not would have to be

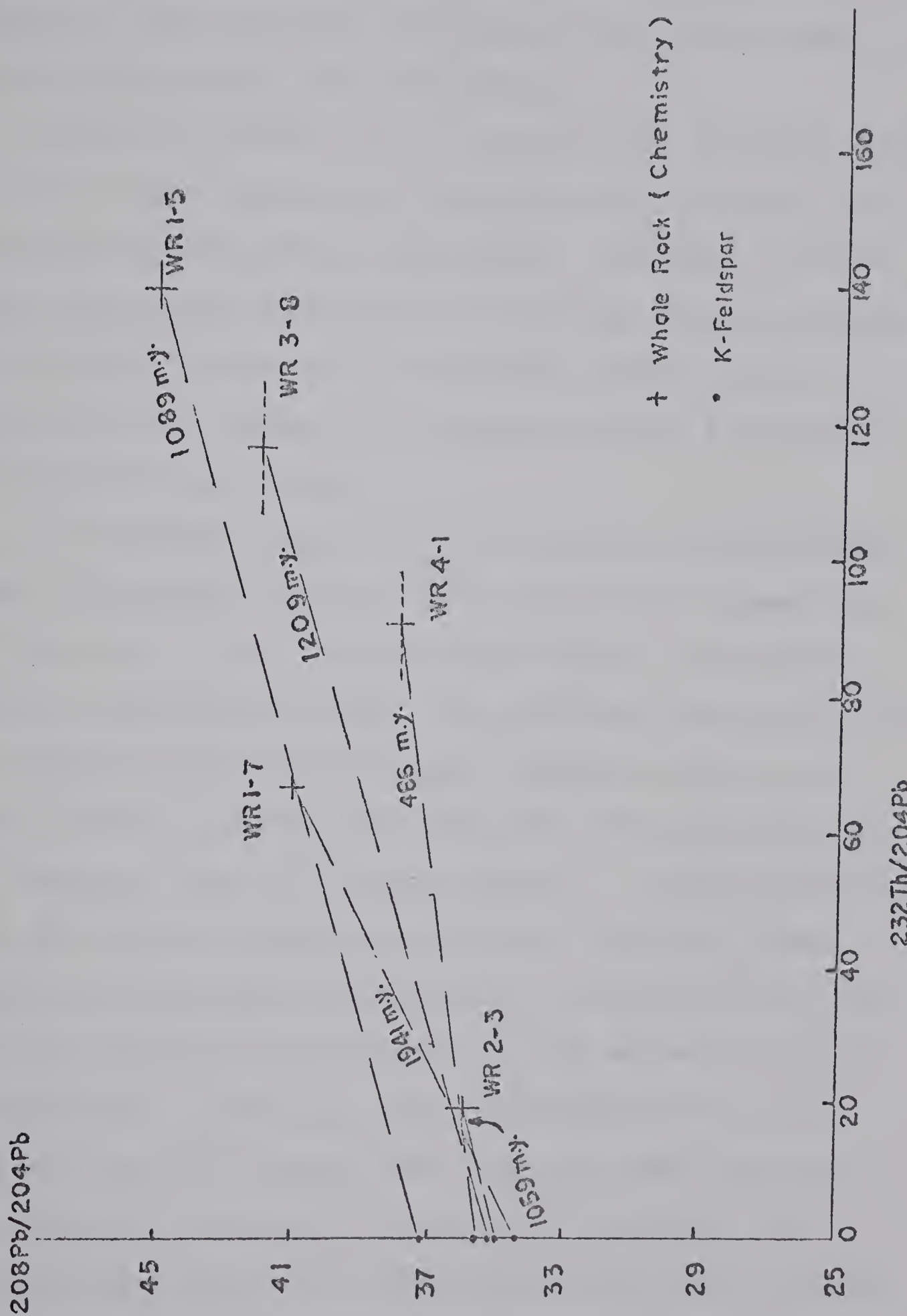


FIGURE 5-8 208Pb/204Pb versus 232Th/204Pb for whole rock and K-feldspar samples.

checked in the light of rock lead isotope interpretation. The different behaviour of rock samples 3-8 and 1-7 seems to indicate that either they have different initial lead ratios or they have been subjected to an intense open system effect after their formation.

Again in Figures 5-6, 5-7 and 5-8, Pb isotopic compositions of the associated K-feldspars are compared with the corresponding whole rock points. The ages as determined from these feldspar-rock isochrons should represent a metamorphic event which caused the remobilization or remixing of the leads in K-feldspars within a presumably closed whole rock system.

The estimated ages from the isochrons in the ^{206}Pb - ^{238}U , ^{207}Pb - ^{235}U and ^{208}Pb - ^{232}Th systems are summarized in Table 5-4. Also listed are the whole rock isochron ages for different systems. As mentioned previously, the Pb isotopic ratios of K-feldspar samples reveal a two-stage history in which the Hudsonian event had affected the feldspar leads in varying degrees. If the assumption that the event had caused remixing of feldspar leads within a closed whole rock system is acceptable, all the mineral isochron ages should also give metamorphic ages around 1800 — 1900 m.y. ago. From Table 5-4, it is obvious that all isochron ages are discordant and most ages (except isochron 1-5 in both U-Pb systems, and isochrons 2-3 and 4-1 in ^{207}Pb - ^{235}U system) deviate significantly from the metamorphic age range.

The variations in the U-Pb and Th-Pb systems of these isochrons are considered to be mainly due to open system behaviour of whole rocks in terms of U transfer (gain or loss) during or after the Hudsonian event. The extremely wild age relationship of the feldspar-rock pair 1-7 in both systems can be explained by the open system effect of U and Pb transfer in the rock system, and by the fact that K-feldspar 1-7 was least or almost not affected by the last 1800—1900 m.y. event. Also, since the analytical measurements of the U and Th isotopes in rock samples are poor and may be subject to larger errors than has been expected, this may also contribute to the variations. Another essential factor is the lack of satisfactorily precise determination of rock leads for this type of isochron interpretation since the isochron slope is largely controlled by rock Pb isotopic ratios; a slight uncertainty will result in significantly variable estimation of isochron age, as can be seen from the different isochron age values estimated for the present Pb analyses and the volatilization analyses (see Table 5-4). A less important but worth reminding point is that U and Th isotope analysis in K-feldspar samples was not made because the present study assumes that all K-feldspar samples are free of U and Th. However, this might be a bias since small amounts of U and Th are usually present in K-feldspar, and the isochron lines for all feldspar-rock pairs would have been different if this is taken

into account.

The above attempt to interpret the feldspar and rock leads in terms of a second stage (metamorphic) mineral isochron model has cast some light on the difficulty and great caution required in this type of interpretation.

WHOLE ROCK MODIFIED CONCORDIA INTERPRETATION

(1) Introduction

A concordia plot involving the U-Pb ratios $^{206}\text{Pb}/^{238}\text{U}$ and $^{207}\text{Pb}/^{235}\text{U}$ has been one of the basic tools of U-Pb geochronology, and many studies have shown that it is useful in the quantitative interpretation of the Pb/U isotopic ratios in U-minerals (such as zircon) which have experienced a single metamorphic event resulting in the loss or gain of the parent or daughter element.

The first attempt to apply such a plot to the interpretation of rock leads was made by Gerling and Shukolyukov (1962). This attempt was unsuccessful because it did not make suitable correction for primeval non-radiogenic Pb. Ulrych (1967), in a study of oceanic basalts and continental granites, has demonstrated that suitable correction for primeval Pb of the observed isotopic ratios provides an excellent graphical description of the relationship of the common and radiogenic Pb contained in a U/Pb system (i.e. a two-stage history). Russell, et al (1968) have extended the modified procedure to the evaluation of $^{238}\text{U}/^{204}\text{Pb}$ ratio for the first stage of the two-stage model assumed.

The present investigation makes use of the procedures modified by Ulrych (1967) and Russell, et al (1968). A brief presentation of the procedures is given below.

Assuming a two-stage history for leads in the rocks

under consideration, the $^{238}\text{U}/^{204}\text{Pb}$ ratios will be different in the two stages of development. Assign μ_1 and μ_2 for the present $^{238}\text{U}/^{204}\text{Pb}$ values characteristic of the first and second stages respectively, x and y for $^{206}\text{Pb}/^{204}\text{Pb}$ and $^{207}\text{Pb}/^{204}\text{Pb}$ ratios at present, and a_0 and b_0 * for $^{206}\text{Pb}/^{204}\text{Pb}$ and $^{207}\text{Pb}/^{204}\text{Pb}$ at time t_0 (primeval leads) respectively, then

$$\begin{aligned} x &= a_0 + \mu_1(e^{\lambda t_0} - e^{\lambda t_1}) + \mu_2(e^{\lambda t_1} - 1) \\ y &= b_0 + (\mu_1/137.8)(e^{\lambda t_0} - e^{\lambda t_1}) + (\mu_2/137.8)(e^{\lambda t_1} - 1) \end{aligned} \quad \dots \quad (\text{Equations 5-3})$$

rearrangement of these equations gives the expression for the present radiogenic $^{206}\text{Pb}/^{238}\text{U}$ and $^{207}\text{Pb}/^{235}\text{U}$ (assigned as α and β respectively), then

$$\begin{aligned} \alpha &= \frac{x-a_0}{\mu_2} = \frac{\mu_1}{\mu_2}(e^{\lambda t_0} - e^{\lambda t_1}) + (e^{\lambda t_1} - 1) \\ \beta &= \frac{(y-b_0) \cdot 137.8}{\mu_2} = \frac{\mu_1}{\mu_2}(e^{\lambda t_0} - e^{\lambda t_1}) + (e^{\lambda t_1} - 1) \end{aligned} \quad \dots \quad (\text{Equations 5-4})$$

If we assume that t_0 is a unique time for all terrestrial rocks, and that t_1 is also a unique time for any particular suite of rocks being studied, Equations 5-4 are only valid if a two-stage model adequately approximates the history of the lead. In these equations, the only parameter that varies is μ_1/μ_2 . Therefore the equations represent, in parametric form, the equations of a straight

* a_0 and b_0 values of Patterson (1956) are used. ($a_0 = 9.50$, $b_0 = 10.36$).

line of slope

$$R = (e^{\lambda t_0} - e^{\lambda t_1})/(e^{\lambda t_0} - e^{\lambda t_1})$$

If this straight line is plotted and a concordia curve superimposed on it, the line will be found to intersect the curve at two points; the significance of these two points can be seen as follows:

In Equations 5-4,

(A) if $\mu_1 = 0$: $\alpha/\beta = (e^{\lambda t_1} - 1)/(e^{\lambda t_1} - 1)$; it will clearly define a point on the concordia at the time corresponding to t_1 , which is the lower intersection with concordia.

(B) if $\mu_1/\mu_2 = 1$: $\alpha/\beta = (e^{\lambda t_0} - 1)/(e^{\lambda t_0} - 1)$; it will give a point on the concordia at the time t_0 . Therefore the second (and upper) intersection with the concordia must correspond to the time t_0 .

It is also clear from Equations 5-4 that the values α and β are linearly related to the quantities μ_1/μ_2 . Since the ratio μ_1/μ_2 is zero at the younger intercept and unity at the older intercept, we may write the following two equations to give μ_1 in terms of μ_2 :

$$\mu_1 = \mu_2(\alpha - \alpha_1)/(\alpha_0 - \alpha_1)$$

$$\mu_1' = \mu_2(\beta - \beta_1)/(\beta_0 - \beta_1) \dots \text{.}(Equations\ 5-5)$$

where (α_0, β_0) are the coordinates of the older intersection and (α_1, β_1) are the coordinates of the younger intersection. But, if the U and Pb abundances of the samples are known and if it is assumed that these represent the second stage, μ_2 is known and therefore μ_1 can be

calculated. In most practical cases, the values for μ_1 depend critically on the Pb isotopic ratios but are rather insensitive to the value of μ_2 . Values calculated for μ_1 are strongly dependent on the value obtained for t_0 since in Equations 5-5 the calculated μ_1 depends on the coordinates of the older intercept with the concordia which intercept also fixes the time t_0 .

(2) Interpretation

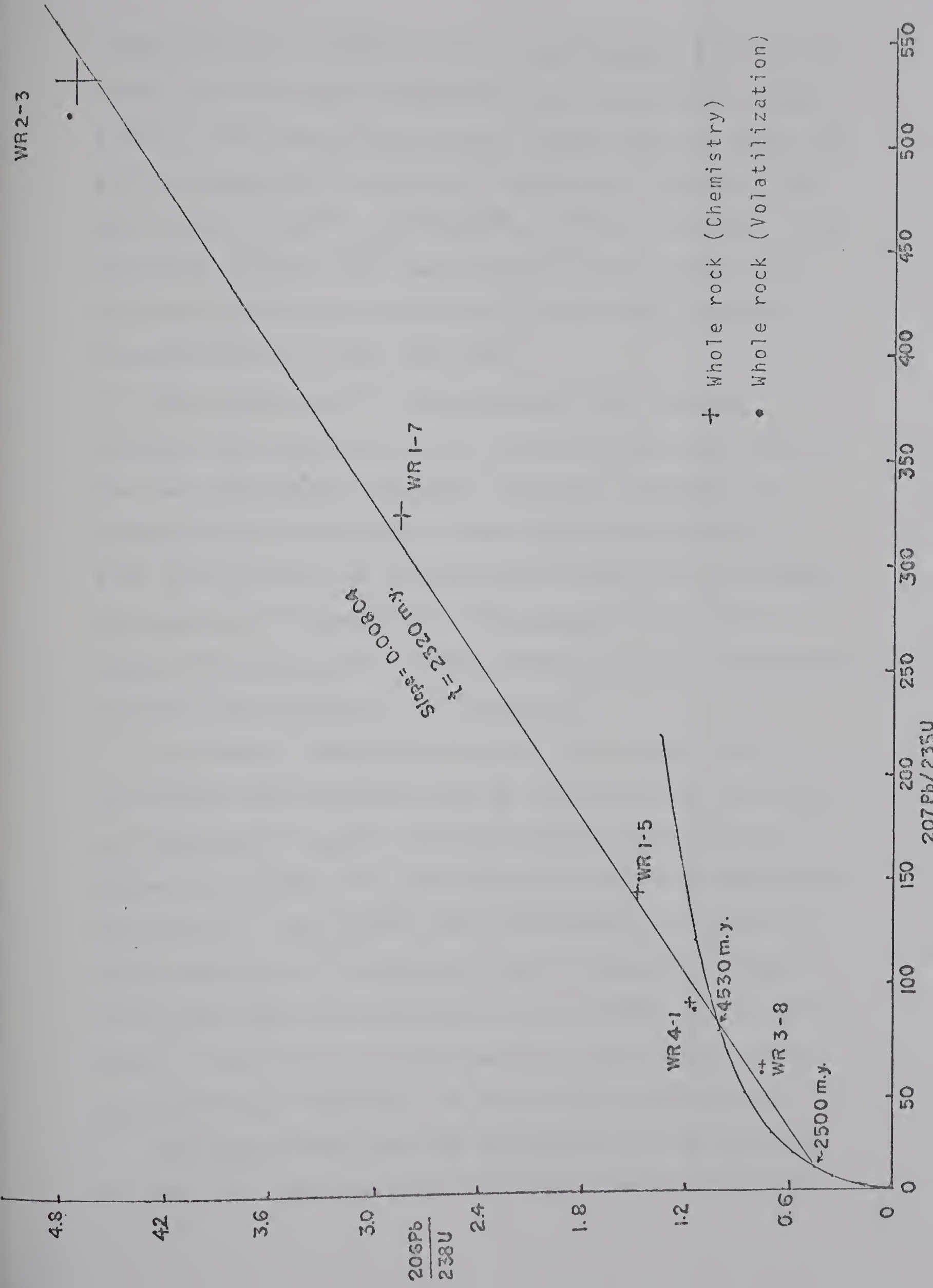
In the present investigation, the modified $206\text{Pb}/238\text{U}$ and $207\text{Pb}/235\text{U}$ ratios for five whole rocks were calculated from Equations 5-4 and the results are given in Table 5-5. Three rock Pb data by volatilization analysis were also used in calculating these ratios.

According to the modified model, a linear relationship should result if the assumptions of the model are justified for the suite of rocks. The $206\text{Pb}/238\text{U}$ versus $207\text{Pb}/235\text{U}$ plot for the rock samples are shown in Figure 5-9, and a best fit line for all the data points is drawn. The time value for the upper intercept of the line with the concordia is interpreted as the age of the earth, and the lower intercept time value as the time of commencement of the last stage, i.e., the time of formation of the U-Pb system which is the immediate source of the rock leads analysed. The inferred age of the earth for these rocks is 4530 ± 50 m.y., which is in good agreement with the age of 4550 ± 70 m.y., obtained by Murthy and Patterson

TABLE 5-5 The present radiogenic $^{206}\text{Pb}/^{238}\text{U}$ and $^{207}\text{Pb}/^{235}\text{U}$ for the whole rock system.

Sample No.	$^{206}\text{Pb}/^{238}\text{U}$	$^{207}\text{Pb}/^{235}\text{U}$
1-5	1.475	143.90
1-7	2.838	324.28
2-3	4.705	529.51
	4.743*	513.04*
3-8	0.767	60.72
	0.774*	59.25*
4-1	1.174	90.66
	1.144*	88.76*

* Values calculated from the average rock lead data by volatilization analysis. The maximum measurement error is assigned to be about 5%.



(1962), the age of 4530 ± 30 m.y. obtained by Ostic et al (1963), and the age of 4530 ± 40 m.y. obtained by Ulrych (1967). The inferred age of the second stage is 2500 ± 50 m.y., as compared to the age of 2320 m.y. estimated from the slope $R = (e^{\lambda t_0} - e^{\lambda t_1})/(e^{\lambda t_0} - e^{\lambda t_1}) = 0.00804$. The agreement between this lower intercept time (2500 m.y.) and the age obtained in the whole rock U-Pb isochron interpretation is also very good.

The scattering of the data about the line may indicate that the whole rock U-Pb system does not satisfy the two-stage model very well and that a violation of closed system conditions in some rocks had occurred. Also it may be due to a multistage history for the common Pb component, in contrary to the assumption that the common Pb developed in a closed system and was incorporated into the rock system at its formation.

μ_1 ratios ($^{238}\text{U}/^{204}\text{Pb}$ for the first stage) were calculated from Equations 5-5 by using the two intercepts on the concordia curve, and the results are listed in Table 5-6 together with the presently observed $^{238}\text{U}/^{204}\text{Pb}$ (μ_2) ratios. The results are normalized to a single t_0 value (4550 m.y.) in order to have a standard of comparison with other data (Russell, et al, 1968; Ostic, et al, 1967). The μ_1 and μ'_1 values would be only about 1-1.5% greater if $t_0 = 4530$ m.y. is used in the calculation.

As can be seen from the variability of the μ_1 value in Table 5-6, the deviation from the "normal" uniformity

as observed by Russell, et al (1968) for well-established two-stage model data is probably due to the fact that the two-stage model is inadequate for these rock samples. In addition, μ_1 values in rock samples 1-5, 2-3 and 4-1 are much higher than the values obtained for a common Pb environment of ore deposits and two-stage crustal rocks (8.94 and 8.70 respectively). This can be explained by:

(A) The rock leads are products of a multistage history in the crustal system where higher U/Pb ratio exists;

(B) The higher μ_1 ratios are due to errors in measurement resulting from fractionation processes.

Ulrych et al (1967) have shown in a study of least radiogenic terrestrial leads that even after eliminating mass fractionation the common leads they studied have in fact not developed in the postulated primary system (i.e. deviated from single-stage growth curve) and have been multistage products in the crust.

The lower μ_1 values of samples 1-7 and 3-8 are more difficult to reconcile. However, the simplest speculation is that these rocks have somewhat different initial common leads incorporated in them, and that they have been open after crystallization and have involved some loss of the parent isotopes.

Despite the deviations, the overall average μ_1 value for the rock samples agrees quite well with the average μ_1 value for crustal rocks by Russell et al (1968). (see Table 5-6)

TABLE 5-6 Observed and calculated μ values for
two-stage model.

Rock sample	μ_2	μ_1 from 206Pb-238U	μ_1 from 207Pb-235U	Average μ_1
1-5	4.17	9.541	8.967	9.254+.287
1-7	1.908	7.588	8.024	7.806+.218
2-3	1.263	9.840	8.910	9.375+.465
3-8	11.48	6.602	8.093	7.348+.745
4-1	8.08	10.353	8.988	9.670+.682
Average	-	8.785	8.596	8.690+.940
Average μ_1 value of 41 rock samples*				8.700+.120
Average μ_1 value of 48 conformable ores**				8.940+.130

* Russell et al., 1968.

** Ostic et al., 1967.

Note: μ_1 and μ_2 are the values of 238U/204Pb for the first and second stages, respectively, extrapolated to the present.

If the average μ_1 value can represent the primary or common Pb environment of the whole rock system, it will provide further supporting evidence for the argument of Russell et al (1968) that there was an approximate homogeneity in U/Pb ratio of the ultimate source region of oceanic basalts and continental rocks. Russell et al (1968) believe that this source has apparently existed for as long as the earth existed.

It should be mentioned that the modified concordia method has been proven suitable to either younger volcanic rocks or continental igneous rocks (including granitic rocks) which are clearly of two-stage history and are essentially without fractionation of U and Pb (or of which the time of fractionation of U and Pb is essentially zero). In regard to the only two published examples of continental granite and pegmatite (i.e. granitic rocks of Llano Uplift, Texas; and pegmatites of Balmat, New York), Gast (1969) has pointed out that:

(A) their observed μ values apply to a clearly recognized second stage, i.e. the crustal history of pegmatites and granites;

(B) their Pb isotopic compositions fell on the geochron (zero isochron line) when they were formed, indicating that the time of U and Pb fractionation is essentially zero;

(C) the lines generated by observed U/Pb ratios and Pb isotopic compositions on a concordia diagram can only

have meaning insofar as they result from a positive correlation between observed μ values and Pb isotopic composition variations.

The present results do satisfy the fact that the observed μ values correspond to the crustal history of the rocks, which appear to have more than two-stage development in their history as is in the case of Llano rocks. However, the present data do not meet the remaining criteria mentioned above.

The two-stage interpretation in the modified concordia method is based on the assumption that even in a three-stage system μ_3 is equal to μ_2 , as suggested by Ulrych (1969). Both Gast (1969) and Tatsumoto (1969) have also assumed that there may be several events involving changes in the history of a rock system, and that the event postulated in a two-stage model is the average of the two or more fractionations that have taken place (in other words, μ_1 and μ_2 may be averages of a few fractionations).

Therefore it is reasonable that there might be some variations in μ_1 .

WHOLE ROCK Pb ISOTOPE INTERPRETATION

(1) Introduction

Studies on Pb isotopic compositions of crustal rocks, especially granitic rocks, in whole rock system have been made by many workers (Farquharson, 1968; Rosholt and Bartel, 1969; Ozard, 1970; Reynolds, 1971). All these studies have cast some light on the behaviour of rock leads which have complex crustal history and involved multistage development.

Theoretical consideration of simplified multistage models has been made by Kanasewich (1962), Kanasewich and Slawson (1964) and Ulrych (1964) on anomalous ore leads, mainly Ivigtut, Greenland. Application of these kinds of models to the crustal rocks was not made because of the difficulty in the precise determination of rock lead isotopes and also because of various other problems involving indeterminate constants, etc.

In the present interpretation of the rock Pb results, a three-stage development model is applied. This model is analogous to the simplified three-stage model suggested by Kanasewich and Slawson (1964) but with some modification. A modified approach by Ulrych (1964) is taken into account.

In order to find a secondary anomalous Pb line for the second stage, Pb isotopic compositions of associated K-feldspars are checked against their ability to represent the "crude" initial Pb ratios of each rock unit at the close of the last stage (i.e. at approximately 1850 m.y.).

ago as determined by K-Ar dating on biotite of all rock types, etc.). Next extrapolated initial Pb ratios from U-Pb plots and best calculated estimates of initial Pb ratios for all samples are briefly examined. The three-stage interpretation is attempted, and some limiting ages of t_1 , t_2 and t_3 are derived.

Some observations from this interpretation are mentioned thereafter, with special attention made to the possibility of Pb remobilization subsequent to the second stage.

(2) Principle

It has been shown that (Kanasewich, 1962; Kanasewich and Slawson, 1964; Ulrych, 1964) the isotopic development of the presently observed Pb isotopic ratios x , y and z with primeval Pb ratios a_0 , b_0 and c_0 from the initial time t_0 can be represented by the following equations:

$$\begin{aligned} x &= a_0 + \mu_1(e^{\lambda t_0} - e^{\lambda t_1}) + \mu_2(e^{\lambda t_1} - e^{\lambda t_2}) + \mu_3(e^{\lambda t_2} - e^{\lambda t_3}) + \dots \\ y &= b_0 + v_1(e^{\lambda t_0} - e^{\lambda t_1}) + v_2(e^{\lambda t_1} - e^{\lambda t_2}) + v_3(e^{\lambda t_2} - e^{\lambda t_3}) + \dots \\ z &= c_0 + w_1(e^{\lambda t_0} - e^{\lambda t_1}) + w_2(e^{\lambda t_1} - e^{\lambda t_2}) + w_3(e^{\lambda t_2} - e^{\lambda t_3}) + \dots \end{aligned}$$

. . . . (Equations 5-6)

where μ_i , v_i and w_i refer to $^{238}\text{U}/^{204}\text{Pb}$, $^{235}\text{U}/^{204}\text{Pb}$ and $^{232}\text{Th}/^{204}\text{Pb}$ for each stage respectively.

A modified three-stage model may be written as follows by setting all the μ 's except μ_1 and μ_3 to be equal to zero:

$$x = a_0 + \mu_1(e^{\lambda t_0} - e^{\lambda t_1}) + \mu_3(e^{\lambda t_2} - e^{\lambda t_3})$$

. . . . (Equation 5-7)

similar expression exists for y and z . Here $\mu_2 = 0$ has been imposed; in other words, from time t_1 (the time of ordinary Pb separation from radioactivity in the deep source and incorporation into the upper crust) to time t_2 (U and Th incorporation in the crustal rock system), the Pb isotope abundances of the ordinary Pb were not altered.

The $^{206}\text{Pb}/^{204}\text{Pb}$ ratio for an ordinary or single-stage Pb (x_1) is defined by the first two terms in Equation 5-7. Thus Equations 5-6 can be expressed in terms of ordinary Pb ratios (x_1, y_1, z_1) as:

$$x = x_1 + \mu_3(e^{\lambda t_2} - e^{\lambda t_3}) \dots \dots \dots \text{(Equation 5-8a)}$$

$$y = y_1 + v_3(e^{\lambda t_2} - e^{\lambda t_3}) \dots \dots \dots \text{(Equation 5-8b)}$$

$$z = z_1 + w_3(e^{\lambda t_2} - e^{\lambda t_3}) \dots \dots \dots \text{(Equation 5-8c)}$$

On a graph of $^{207}\text{Pb}/^{204}\text{Pb}$ versus $^{206}\text{Pb}/^{204}\text{Pb}$, Equations 5-8a and 5-8b represent a straight line passing through the ordinary Pb ratios (x_1, y_1). The slope of this anomalous Pb line is

$$R = \frac{y - y_1}{x - x_1} = \frac{e^{\lambda t_2} - e^{\lambda t_3}}{\alpha(e^{\lambda t_2} - e^{\lambda t_3})} \dots \dots \dots \text{(Equation 5-9)}$$

Here, a modified approach is preferred. Instead of following the procedure of Kanasewich and Slawson (1964) by assigning values for t_2 and t_3 (from other independent methods) in order to determine x_1, y_1 and t_1 , the approach is taken to find "limiting age values" (Russell and Farquhar, 1960) for t_2 and t_3 from Equation 5-9 and for t_1 from the first two terms in Equation 5-7.

(3) Interpretation

Many attempts to search for possible genetic relationships among Pb isotopic compositions of intrusive rocks and their associated K-feldspars or ores have been made. Among these, various works by Catanzaro and Gast (1960), Doe (1962), Doe and Hart (1963), Doe et al (1965), Zartman (1965), Zartman and Wasserburg (1969) have provided a better understanding of Pb isotopic patterns of K-feldspars in different geological environments. It has been shown that in unmetamorphosed (or weakly metamorphosed) rocks, with small or insignificant correction for in situ radioactive decay, the K-feldspars contain leads whose isotopic compositions approximate those of the initial ratios of the rock system. Yet some feldspar leads may display remobilization caused by either open system disturbance or internal redistribution. However, in most cases, with careful correction for in situ generated radiogenic Pb * both in K-feldspars and rocks, it is possible to clarify the following problems:

* Zartman and Wasserburg (1969) have pointed out that K-feldspar samples with large corrections of dubious values were caused by analytical uncertainties, sample behaviour during the leaching step, and movement of U, Th and Pb throughout the post-crystallization history of K-feldspar. They excluded the samples from isotopic composition correction study if they required more than 2% radiogenic correction.

(A) whether initial homogeneity existed between whole rock and K-feldspar prior to the last geological event;

(B) whether a closed system in the whole rock has been maintained;

(C) whether the feldspar leads are compatible or anomalous compared with the primary, single-stage growth curve of ordinary leads, and what implications can be derived.

In situ radiogenic Pb corrections to 1850 m.y. ago were made for the five whole rock-feldspar pairs. The corrections for the whole rock system are made by calculating the initial $^{206}\text{Pb}/^{204}\text{Pb}$ and $^{207}\text{Pb}/^{204}\text{Pb}$ ratios at 1850 m.y. ago for each rock sample, using the following equations:

$$\left(\frac{206\text{Pb}}{204\text{Pb}}\right)_{it} = \left(\frac{206\text{Pb}}{204\text{Pb}}\right)_p - \left(\frac{238\text{U}}{204\text{Pb}}\right)_p (e^{\lambda t} - 1)$$

$$\left(\frac{207\text{Pb}}{204\text{Pb}}\right)_{it} = \left(\frac{207\text{Pb}}{204\text{Pb}}\right)_p - \left(\frac{235\text{U}}{204\text{Pb}}\right)_p (e^{\lambda t} - 1)$$

. (Equations 5-10)

where $t = 1850$ m.y., and $p =$ present.

The corrections for the K-feldspars (except sample 1-7 in which no correction was made) are made by the best visual estimation of the intercepts at $^{206}\text{Pb}/^{204}\text{Pb}$ and $^{207}\text{Pb}/^{204}\text{Pb}$ axes by imposing isochron lines of slope equal to $(e^{\lambda \cdot 1850 \text{ m.y.}} - 1)$ through the rock-feldspar points in Figures 5-6 and 5-7. The results of these corrections are listed in Table 5-7.

No demonstrable differences in K-feldspar Pb isotopic compositions were found after the correction (about 1% or

TABLE 5-7 Initial Pb ratios corrected for in situ
U-decay to 1850 m.y. ago in whole rock
and K-feldspar samples.

	1-5	1-7	2-3	3-8	4-1
$(x)_p$ (WR)	16.850	14.809	15.570*	18.400*	18.750*
$(x)_i$ (WR)	15.209	14.184	15.146	14.620	16.090
$(x)_p$ (KF)	15.250	13.600	15.110	14.840	15.880
$(x)_i$ (KF)	15.250	13.600	15.110	14.810	15.880
$t_{\text{intercept}}$ (m.y.)	1810	>3600	1880	1760	1960
$(y)_p$ (WR)	15.390	14.805	15.230	15.570	15.700
$(y)_i$ (WR)	15.237	14.798	15.184	15.141	15.402
$(y)_p$ (KF)	15.230	14.850	15.200	15.160	15.420
$(y)_i$ (KF)	15.230	14.850	15.185	15.145	15.415
$t_{\text{intercept}}$ (m.y.)	1890	∞	1850	1840	1770

* Data obtained from volatilization analysis, being used
in U-Pb isochron plots.

Note: $(x)_p$ = $^{206}\text{Pb}/^{204}\text{Pb}$ at present; $(x)_i$ = $^{206}\text{Pb}/^{204}\text{Pb}$
at 1850 m.y. ago. Similar symbol for $^{207}\text{Pb}/^{204}\text{Pb}=(y)$.

$t_{\text{intercept}}$ refers to the time when initial homogeneity
occurred. $^{206}\text{Pb}/^{204}\text{Pb}$ and $^{207}\text{Pb}/^{204}\text{Pb}$ ratios for
whole rocks are averages of measured and corrected
results. WR: whole rock; KF: K-feldspar.

less), and it is also clear that except for sample 1-7, the correction results for the whole rocks (i.e. the calculated initial ratios for the whole rock system) give isotopic compositions almost indistinguishable from those of the feldspars. This implies that in the four pairs of whole rock-feldspar samples (1-5, 2-3, 3-8, 4-1), the corrected ratios become equal at about 1760 to 1960 m.y. ago. This is shown in Figures 5-10a and 5-10b. Only in sample pair 1-7 does there appear to be an extreme discrepancy between the whole rock and K-feldspar Pb isotopic compositions at 1850 m.y. ago. Theoretically, either different initial ratios between the whole rock and the K-feldspar at the time of the last event or subsequent open system conditions could account for this phenomenon. The apparently good agreement of the corrected initial ratios in sample pairs 1-5 and 2-3 suggests that these rocks did remain closed systems and had initial Pb homogeneity at approximately 1850 m.y. ago. The slight deviations in sample pairs 3-8 and 4-1 could be the results of slight open system effects; or alternatively, slight initial isotopic variations. Nevertheless, the initial Pb isotopic compositions calculated for the time of last event show good agreement and it is seen that the effect of any post-Hudsonian disturbance was quite small in these samples.

The Pb isotopic compositions of the rock samples and their associated K-feldspars are compared in x-y and x-z

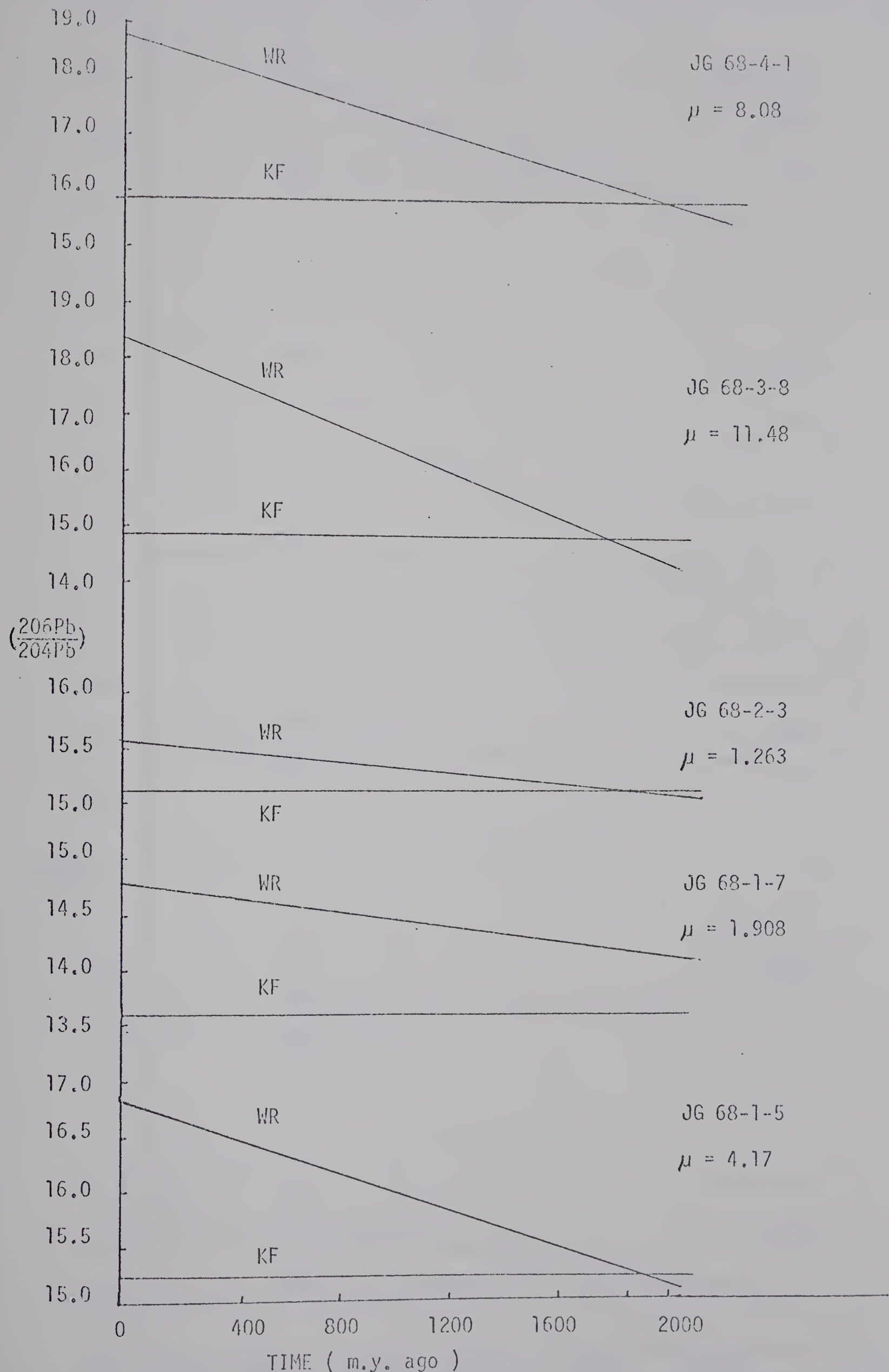


FIGURE 5-10a $206\text{Pb}/204\text{Pb}$ vs. time in m.y. ago for whole rock & K-feldspar samples.

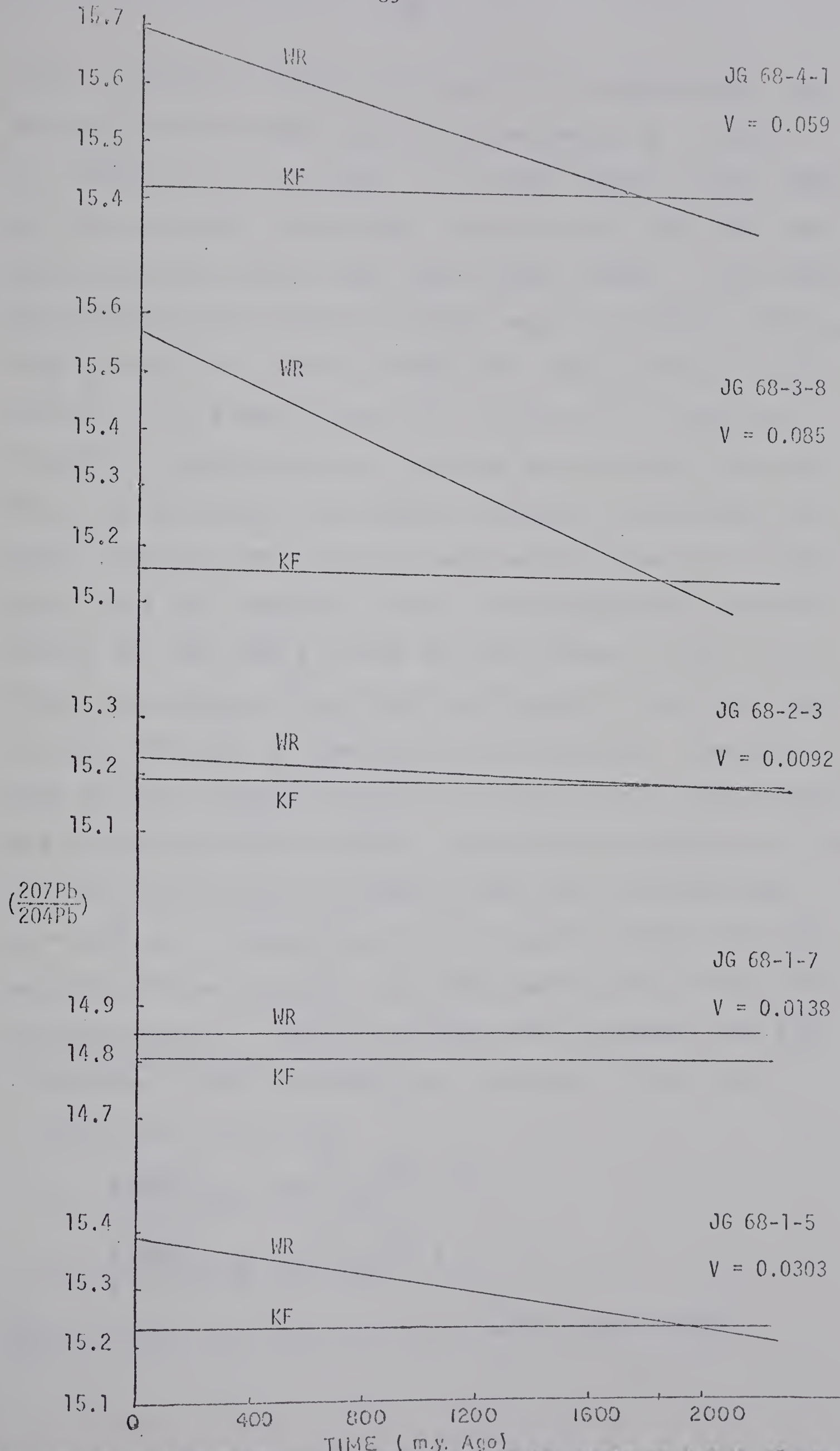


FIGURE E-105. $^{207}\text{Pb}/^{204}\text{Pb}$ vs. time in m.y. ago for whole rock & K-feldspar samples.

plots as shown in Figures 5-11 and 5-12 respectively. An absolute ore-Pb growth curve with parameters $\mu = 8.79$, $t_0 = 4580$ m.y., $a = 18.322$, $b = 15.622$ (Cooper et al, 1969) has been used for comparison. In Fig. 5-11, the rock lead data points do display two crude linear trends. The inferred age, based on the Russell-Farquhar model, is 2450 ± 100 m.y. with a slope of $0.15556 \pm .00010$ for sample suite 1-5, 2-3 and 4-1. For sample suite 1-7, 3-8 and 3-7, a slope of $0.16615 \pm .00010$ yields an inferred age of 2550 ± 100 m.y. These two different but somewhat parallel rock lead lines might indicate that the rock leads are mixtures of a radiogenic lead with anomalous leads. The estimated initial Pb ratios for two sample suites are also shown in Fig. 5-11. These are obtained from visual estimation of the intercepts in the U-Pb plots of the whole rock isochrons. However, they are poor estimates because of possible Pb remobilization and analytical uncertainties. Thus a best estimation of the initial ratios was calculated on the basis of Pb-Pb age $t_1 = 2500$ m.y. (average age of two sample suites) and the centroid of the data for two rock sample suites in the U-Pb isochron plots*. These calculated best estimates are also

* Equations used in solving best estimates of initial Pb ratios (x_{it} , y_{it}) are:

$$t_1 = \frac{2.3026}{1.54 \cdot 10^{-10}} \log\left(\frac{\bar{x} - x_{it}}{\mu} + 1\right)$$

$$t_1 = \frac{2.3026}{9.72 \cdot 10^{-10}} \log\left(\frac{\bar{y} - y_{it}}{\mu/\alpha} + 1\right)$$

where \bar{x} and \bar{y} are the centroid of each sample suite.

207Pb/204Pb

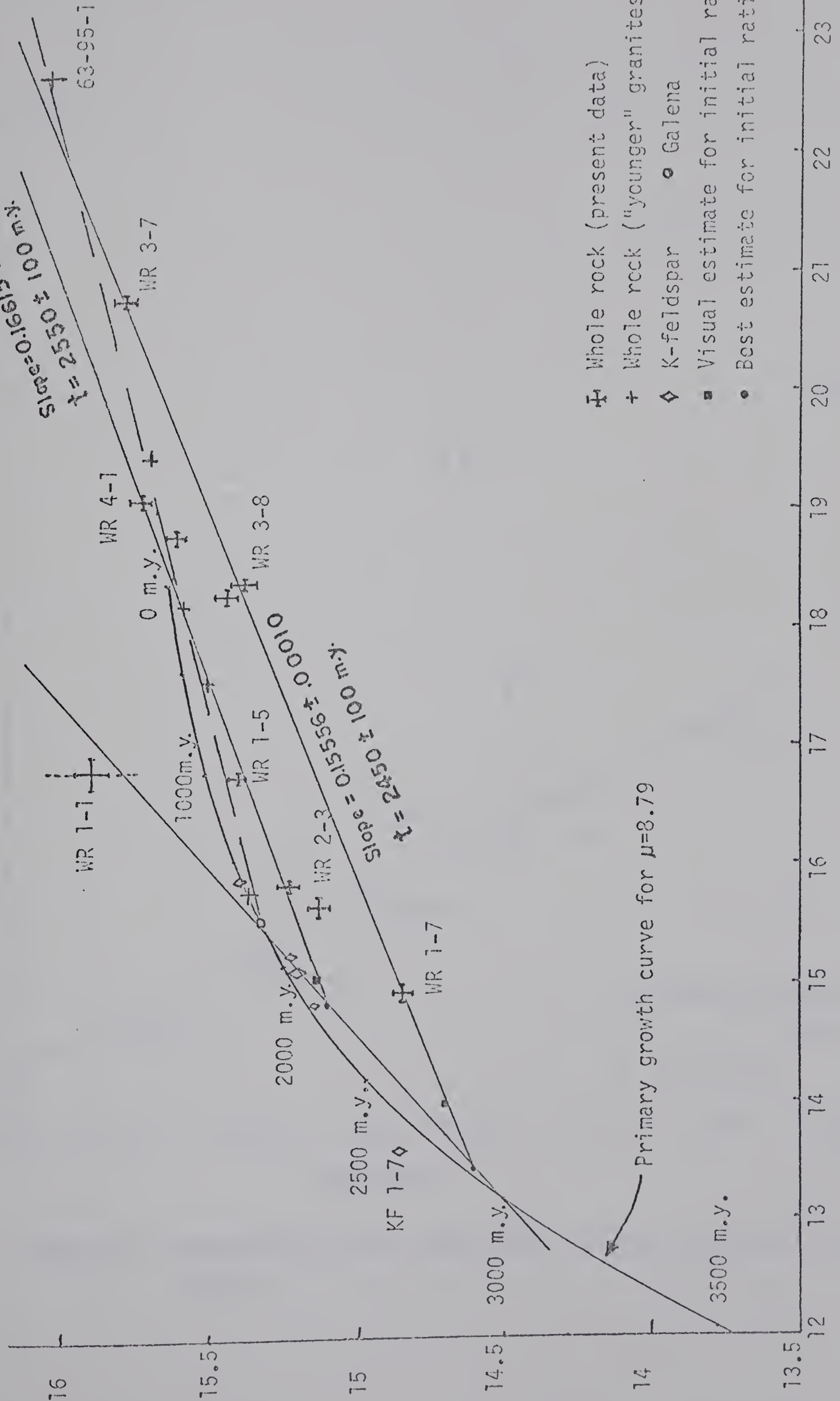


FIGURE 5-11 207Pb/204Pb versus 206Pb/204Pb for whole rock and K-feldspar samples.

208Pb/204Pb

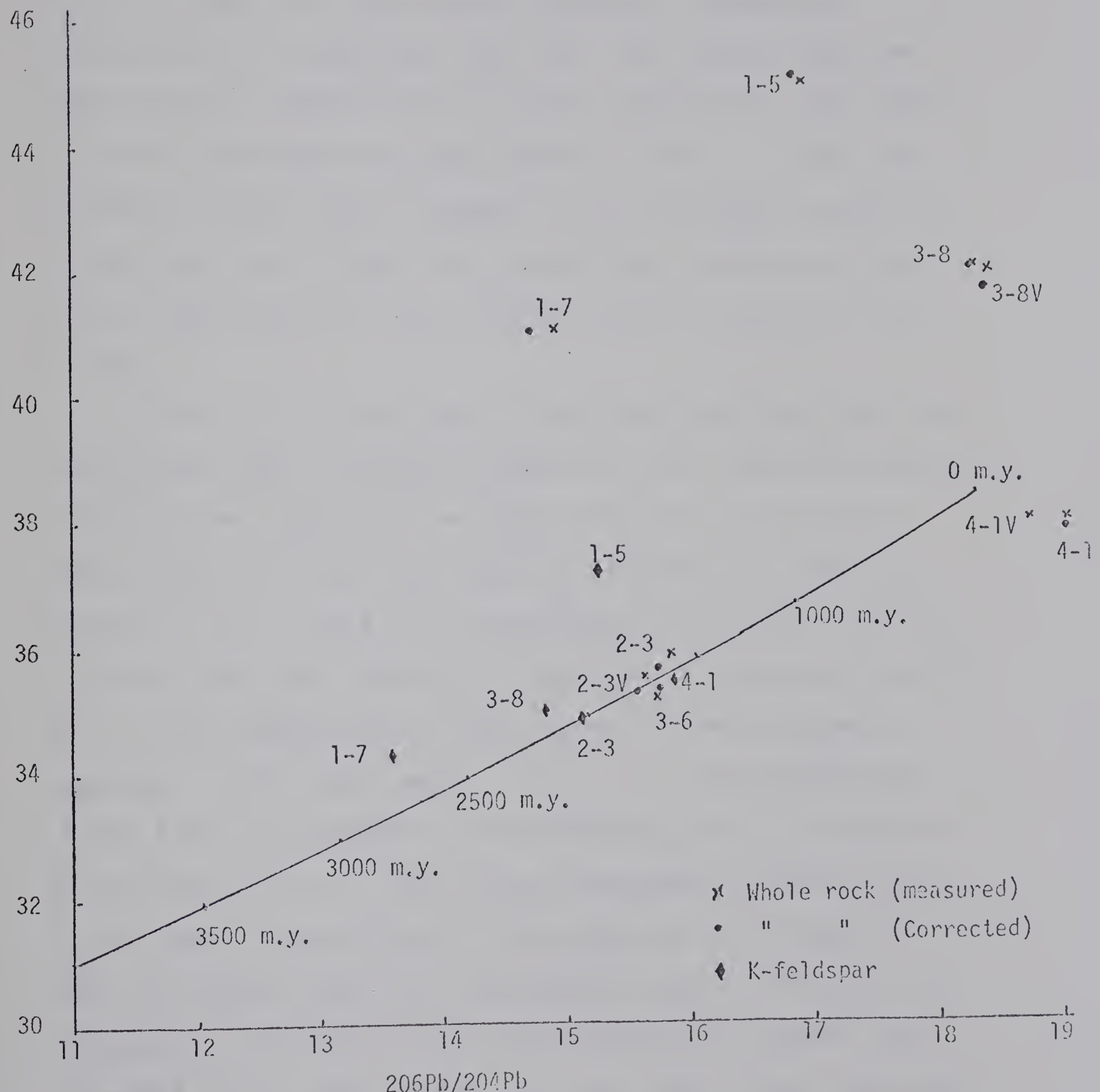


FIGURE 5-12 208Pb/204Pb versus 206Pb/204Pb for whole rock and K-feldspar samples.

shown in Fig. 5-11.

Also shown for comparison are some rock leads of "younger" granites (Sample Nos. 63-95-1, 63-99-5, 63-616-2, 63-101-1) and a galena lead of a younger metasediment (Orthquartzite, Sample No. 58-1-3). The former data are from personal communication with Dr. Baadsgaard, the latter is taken from Baadsgaard and Godfrey (1967). A line can be drawn through these "younger" rock and galena leads and a rock lead point (Sample No. JG 68-3-6), giving an inferred age of approximately 1730 ± 20 m.y. with a slope of 0.104 $\pm .001$.

In Fig. 5-11, the slope of the two rock lead lines for the present data is given by Equation 5-9, from which possible limiting time values can be found (Russell and Farquhar, 1960, p.64). If the rock lead was disturbed or emplaced recently, $t_3 = 0$, and t_2 is calculated to be 2500 ± 50 m.y. for both rock lead lines (cf. slope age obtained previously), this is the maximum age of the source of the radiogenic component of the rock leads. If $t_2 = t_3$, the maximum age of the final emplacement of the anomalous Pb is calculated to be 1860 ± 70 m.y.. This value represents an upper limit to the time of separation of the radiogenic Pb component from its source rocks (i.e. metamorphic age). Also we can calculate a limiting age for the formation of common lead component in the rock system (i.e. the time of the formation of the second stage) from the first two terms of Equations 5-7. This time is calculated to be 2460 ± 10 m.y. and 2920 ± 20 m.y. for sample suite 4-1, 1-5, 2-3 and sample

suite 1-7, 3-8, 3-7 respectively. In this case, however, as has been pointed out by Ulrych (1964), the simplified three-stage model proposed by Kanasewich and Slawson (1964) would require two common lead formations, at 2460 m.y. and 2920 m.y. ago. Since all sample locations are separated from each other within less than 10 miles, the differing time of common lead formation and the mixing of rock leads would have to be very localized. A possibility of this kind seems quite remote. Thus the alternative interpretation would have to consider the information derived from the anomalous Pb line along initial ratios (both visual estimates from U-Pb isochron plots and calculated best estimates) and K-feldspar leads.

We have shown that K-feldspar leads in four rock samples except 1-7 do closely resemble the corrected ratios in rock leads prior to the third stage or at the close of the second stage. And from the estimates of the initial Pb ratios of various rock types within the area, we have some idea about the common lead composition at 2500 m.y. ago, i.e., at the start of or prior to the second stage. If these ratios can be correlated to some known older basement material such as the Biotite Granite Gneiss, then this kind of anomalous Pb line will give us some idea about the second stage.

Since K-feldspar leads have been interpreted previously to have a metamorphic age of 1775 m.y. and a primary age of 2487 m.y. or older, they therefore reflect the anomalous

leads in a span of the second stage. In Fig. 5-11, three feldspar leads (except 1-7 and 4-1) are compared with two best estimates of the initial Pb ratios of two rock sample suites, and with a rock lead (Sample No. JG 68-1-1, Biotite granite gneiss). They all fit quite well on an anomalous Pb line. The greatest estimate of the time of formation of the second stage based on this anomalous Pb line is about 3000 m.y. However, this is apparently an overestimation because the slope of the whole rock sample suite 1-7, 3-8, 3-7 has been reduced by the lead remobilization or initial isotopic variation (as has been shown for sample 1-7, and to a slighter extent, probably sample 3-8).

The anomalous Pb line has an upper intercept with the growth curve indicating a lower time value of the second stage around 1800 m.y. ago. It is interesting to note that this anomalous Pb line also fit quite well with the "younger" galena 58-1-3, which can be regarded as a common lead component of the "younger" rocks.

(4) Discussion

The oldest radiometric age obtained so far in the region is 2550 m.y., as given by Rb-Sr dating on pegmatites that intruded into the present rock types. At present it is not known whether there is any crustal material older than 3000 m.y. existing in this region, but if the incorporation of the common lead into the crust in this region occurred as recently as possible, then the formation of the crust and

of the common lead into crustal system may have taken place around 2550 m.y. ago or before. It is worth mentioning that the possibility of the existence of a 3000 m.y. old crustal material in this region cannot be ruled out, for the "outliers" of the Superior Province (and possibly the Slave Province?) extend to this region and "may constitute portions of an originally continuous Archean complex now partly obscured and transected by later fold-belts but preserving its broad-scale structural trends." (Dearnley, 1966).

A piece of evidence which supports the existence of a crust in this region around or prior to 2550 m.y. is given by the fact that the calculated best estimates of 2500 m.y. old initial common lead ratios fall below the growth curve, thus this may reflect a crustal history for these common lead components prior to the start of the second stage during which most of the initial components were derived.

It may be concluded that all rock samples under study were probably partially derived from rocks with a rather similar common lead composition at or prior to the commencement of the second stage (about 2500 m.y. ago), and have been subjected to an event at 1800—1900 m.y. ago with an incomplete homogenization which had partially remobilized or mixed some of the common lead components in these rocks. The scattering on a single line for rock samples 1-7, 3-8, 3-7 may indicate a spread of initial lead ratios at or prior to the second stage.

CHAPTER 6 COMPARISON WITH OTHER AREAS

The present study is a small part of a long-term project on the Precambrian Shield in Northeastern Alberta. Geochronological study has been carried out so far under the joint effort of Drs. Baadsgaard and Godfrey. The writer therefore takes advantage of some of their published and unpublished results, together with some other information, and attempt to achieve an overall viewpoint on the complex porblem and draw some concluding remarks.

The preliminary work on the Andrew Lake area by Baadsgaard and Godfrey (1967) has clarified some of the problems and initiated a general approach towards a better understanding of the area. Their results can be outlined as follows:

(1) K-Ar dates on micas of different rock types indicate a metamorphic event at about 1800 m.y. ago. The event apparently updated the micas, but did not affect hornblendes which give a somewhat older age (about 1900 m.y.).

(2) Whole rock Rb-Sr and U-Pb zircon-diffusion dates indicate a magmatic event at about 1900 m.y. This is the time when gneissic rocks were converted from older gneissic and sedimentary materials and were incorporated in the basement complex, and when the gneiss-in-gneiss inclusions were formed.

(3) An older "mixed" date of about 2250 m.y. is obtained for mainly gneissic materials (including one "late" granite)

which represent sedimentary materials from sources of different age (older age).

- (4) A general history derived from their results is:
- A) accumulation of materials >2250 m.y. old either via sedimentation or through (as yet) undiscovered older igneous intrusion;
 - B) two periods of gneissic formation, the later of which is closely associated in time with the intrusion of the late granites at about 1900 m.y. ago;
 - C) mineralization (involving at least Mo, U and Pb) that is essentially coeval with the formation of the late granites;
 - D) a final, probably regional, metamorphism at about 1800 m.y. ago (low biotite schist to greenschist grade?)

Since the above pioneer attempt, further work by different radiometric methods on whole rock and mineral samples from the area have been carried out by Dr. Baadsgaard during the period of 1968 — 1971. A brief outline of some of these results is given as follows:

(1) K-Ar dates on rock samples from the Charles Lake area (only the results for the same rock samples as this work are quoted):

Sample	Age(m.y.)	Sample	Age(m.y.)
Biotite 1-1	1760	Muscovite 3-6	1830
Biotite 1-5A	1720	Biotite 3-7	1780
" 1-5B	1800	" 3-7B	1700
Hornblende 1-7	1920	Biotite 3-8	1690
Hornblende 2-3	1850	Biotite 4-1	1820

(2) K-Ar dates on other different rock types including basement gneisses, biotite schist, amphibolite, "younger" granites and pegmatites all closely group around 1800 m.y.

(3) Rb-Sr mineral isochron dates on 12 whole rock and apatite pairs for all rock types give a mean age of 1760 m.y.

(4) Pb isotope interpretation of whole rock analyses for six "younger" granites give an age of about 1730 ± 30 m.y. with a slope of $0.104 \pm .002$.

(5) U-Pb whole rock isochron dates for six "younger" granites indicate a magmatic event of 1900 ± 30 m.y. with exclusion of two rock samples (63-628-6, 63-99-5) in ^{206}Pb - ^{238}U system, and one rock sample (63-94-2) in ^{207}Pb - ^{235}U system, respectively.

(6) Additional U-Pb zircon diffusion dates on one "younger" granite (Granite E, sample 63-99-4) and two granite gneisses (samples 63-105-11, 63-104-1) have further confirmed the deduction previously made by Baadsgaard and Godfrey (1967) that two groups of zircons, one 1900 m.y. old and the other 2250 m.y. or older can be distinguished. In fact the granite gneiss zircon data have enlarged the approximate primary age limit of 2250 m.y. to about 2400 m.y. and thus require a 2500 m.y. continuous diffusion interpretation.

(7) Rb-Sr whole rock dates on six pegmatites intruded in "older" granites of the Charles Lake area indicate a very old age of 2550 m.y. with an initial $^{87}\text{Sr}/^{86}\text{Sr}$ ratio of 0.703. Some pegmatites intruded in metasedimentary rocks

are somewhat scattered and plot above the 2550 m.y. isochron. The simplest implication is that relative daughter gain in Rb/Sr system in pegmatites occurred as a result of contamination with older materials when these pegmatites intruded the metasediments.

Besides the above outlined results, Koster and Baadsgaard (1970) have reported on the geochronology of the Tazin Lake region, N.W. Saskatchewan, about 70 miles east of the present Charles Lake area. They obtained K-Ar dates for 20 rocks from a "Northeastern basement complex" (mainly syn-to-late tectonic granodiorite-diorite series) which give a mean age of 2370 ± 40 m.y., with some biotite dates up to 2450 m.y., indicating that the emplacement age might be older than this date.

CHAPTER 7 SUMMARY AND CONCLUSION

SUMMARY

Different treatment of the U, Th and Pb isotopic analyses have been made to document possible U-Th-Pb variations in mineral-rock systems during their past history.

Firstly, U-Th-Pb systematics in zircon and apatite samples is considered. The following points are derived from a combined episodic and continuous diffusion Pb loss interpretation.

(1) Zircon samples 3-8 and 4-1 plot on a 1900 m.y. diffusion curve together with other zircons and uraninite of "younger" granites, and they are considered at present as admixtures of magmatic, older zircons and authigenic zircons which have been subjected to recrystallization during metamorphism.

(2) Zircon 1-7 is interpreted as a 2500 m.y. old zircon which episodically lost its lead during the 1900 m.y. diastrophic event. No continuous diffusion Pb loss before or after the event is inferred.

(3) Zircons 1-5 and 2-3 are considered as 2500 m.y. old zircons which variably lost Pb by episodic diffusion at the 1900 m.y. event, and they lost their leads by continuous diffusion before and after the event. Zircons of the basement gneisses display a similar Pb loss mechanism.

(4) Apatite 1-5 falls on the concordia indicating its last emplacement was about 1800 m.y. ago, while apatite 2-3 plots slightly below the concordia with a younger age of 1610 m.y.

(5) Apatites 1-7, 3-8 and 4-1 fall within the combined diffusion-episodic bounded area; the former two plot on a 1900 m.y. diffusion curve indicating that they have been affected by the last major episodic loss of Pb; apatite 4-1 falls inside the bounded area, and thus a combined effect of episodic-diffusion Pb loss is implied.

Secondly, from apatite-rock isochron and apatite Pb isotope interpretations, the following results are obtained:

(1) Apatites 1-5 and 3-8 are concordant in both U-Pb and Pb-Pb systems, indicating that these apatites have been stable in terms of U and Pb migration since their formation at the Hudsonian time.

(2) Apatite 2-3 gives a young age of about 1600 m.y. in both U-Pb and Pb-Pb systems, and thus is considered to be reset at this time when open system effect in Pb and U systems occurred.

(3) Apatites 1-7 and 4-1 both behave differently in U-Pb and Pb-Pb systems, and they are considered to be subjected to varying degrees of U addition or Pb diffusion loss effect after their formation at the Hudsonian.

(4) A Pb-Pb isochron for apatite, feldspar and rock samples gives a slope age of 1905 ± 40 m.y. with a slope of $0.11468 \pm .00200$. An internal and partial phase conta-

mination of lead (in mineral phases) within the whole rock system could have taken place around this time.

Thirdly, interpretations of K-feldspar leads and feldspar-rock isochrons reveal the following points:

(1) From the intercept of the anomalous K-feldspar leads with a primary growth curve of $\mu = 8.8$, a metamorphic age of 1775 ± 100 m.y. and a primary age of 2500 m.y. are obtained. All feldspar samples except 1-7 were affected by metamorphism 1800 m.y. ago when partial remobilization of radiogenic lead had caused variable extent of radiogenic lead addition. Feldspar 1-7 was the least affected, and feldspar 4-1 was greatly affected. Three "intermediate" feldspars (1-5, 2-3, 3-8) appear to be admixtures of the above two types.

(2) Two whole rock isochrons in both U-Pb systems for rock samples 1-5, 2-3 and 4-1 give a mean age of 2487 ± 26 m.y. Rock samples 1-7 and 3-8 deviate from the linear relationship observed for the above three rocks, and an intense open system effect of U and Th after the rock formation is indicated.

(3) Feldspar-rock isochrons in U-Pb and Th-Pb systems give ages that are discordant and deviate significantly from the 1800 — 1900 m.y. age range. The variations are considered to be mainly caused by open system behaviour of whole rocks in terms of U and Th transfer (gain or loss) during or after the Hudsonian event, and probably by the

fact that feldspar leads have not been subjected to the same degree of remobilization or remixing by metamorphism.

Fourthly, in a modified concordia plot for rock leads assuming a two-stage model, the writer checked the validity of this model and found that the whole rock system deviates from a closed system condition and thus a multistage history for the rock system is inferred. The following intercept time values are derived:

(1) An upper intercept of a best fit line through all scattered points with the concordia curve is interpreted as the age of the earth, and a value of 4530 ± 50 m.y. is obtained.

(2) A lower intercept with the concordia is interpreted as the time of commencement of the second stage, and the inferred age is 2500 ± 50 m.y. This might represent the time of isolation of the U-Pb system which is the immediate source of the rock leads.

(3) Calculated $^{238}\text{U}/^{204}\text{Pb}$ ratios for the first stage (normalized to $t_0 = 4550$ m.y.) for all rock samples do not show a good "normal" uniformity as in the case of well-established two-stage model data, and this is considered to be due to the inadequacy of these rock samples for a two-stage model. However, an overall average of $8.69 \pm .94$ ($> 10\%$ variation) might be compared to the average value of $8.70 \pm .12$ (1.4% variation) for 41 rock samples by Russell et al (1968).

In the final section, a three-stage model interpretation has been applied to the Pb isotopic compositions of whole rock and K-feldspar samples. In situ radiogenic Pb correction to 1850 m.y. (taken as the mean age of major event of metamorphism-intrusion) for whole rock and K-feldspar samples were made and it was found that initial Pb homogeneity at or prior to 1850 m.y. ago did exist between K-feldspar and whole rock in four rock samples, except rock-feldspar pair 1-7 which shows an extreme discrepancy in Pb isotopic compositions at or prior to 1850 m.y. ago. This is interpreted as a result of either initial isotopic variation or Pb remobilization by open system effect. With this finding in mind, the writer interprets the data according to a three-stage model and the following inferred time values are obtained:

(1) A best estimate for the time of the commencement of the second stage, i.e., the maximum age of the formation of the common lead in the source rock system (or the crust) is 2500 ± 50 m.y. ago.

(2) The maximum age of the final emplacement of the anomalous leads is estimated to be 1860 ± 70 m.y. ago. This value represents an upper limit to the time of separation of the radiogenic lead component from its source rocks (i.e., metamorphic age).

An anomalous lead line drawn through estimated initial lead ratios, three K-feldspar lead points (1-5, 2-3, 3-8), a young galena lead point, and a rock lead point (basement

gneiss) intersects the primary growth curve at two points, which define the upper and the lower limit for the second stage; the upper limit is 3000 m.y. ago, and the lower limit is 1800 m.y. ago. The 3000 m.y. age value might be an overestimation. If the common lead incorporation into the crust occurred as recently as possible, then the reasonable time of crustal formation in the region is around 2550 m.y. ago or older.

CONCLUSIONS

On the basis of the present results, a three-stage history of the rock samples under study may be summarized as follows:

(1) First stage — from 4550 m.y. ago to approximately 2550 m.y. ago; this is the primary system for U and Pb and is characteristic of a present $^{238}\text{U}/^{204}\text{Pb}$ ratio of 8.7 to 8.8. Between (probably?) 3000 m.y. and 2550 m.y. ago the first crustal material formed in this region and common lead incorporation in the crust occurred at the end of this stage.

(2) Second stage — from 2550 m.y. to 1900 m.y. ago; the present U-Pb system was probably isolated at the beginning of this stage, and common lead components probably developed in a crustal environment during this stage.

(3) Third stage — from 1900 m.y. ago to the present; Pb remixing occurred (anomalous lead formed) within the rock system at the beginning or slightly prior to this

stage. During the similar period U-Th-Pb systems in zircons were also disturbed. Lead incorporation or resetting in apatites probably occurred around 1800 m.y. ago. Initial Pb homogeneity between K-feldspar and whole rock was established at the beginning of this stage for the present rock samples (with the exception of sample 1-7).

Several concluding remarks on the rock samples under study may be made as follows:

(1) Grey hornblende granite (sample 68-2-3) and Foliated hornblende granite (sample 68-1-7) are possibly parts of the basement complex formed as a result of multiple intrusion at about 2500 m.y. ago.

(2) Granite F (sample 68-4-1) was probably produced by granitization of older basement materials around late Archean.

(3) Biotite "q" granite (sample 68-1-5 and sample 68-3-8), locating to the east of the Allan Fault zone (mylonite zone), might represent the early Hudsonian intrusion which involved contamination with older Archean basement materials through partial melting during the intrusion. Sample 1-5 also might be an Archean rock granitized at the early Hudsonian Orogeny.

(4) The diastrophic event of early Hudsonian (1800 — 1900 m.y. ago) has greatly disturbed rock sample 1-7 and partial lead remobilization in this rock is possible.

(5) U-Pb whole rock-mineral isochrons, U-Th-Pb

systematics of zircons and apatites, and Rb-Sr whole rock-apatite isochrons all display some variations in response to 1800 m.y. metamorphism in the different rock types. This might imply a long retrograde metamorphism (slow cooling?) which has affected variably (both spatially and temporally) different rocks and different mineral phases.

LITERATURE CITED

- Ahrens, L.H. (1955 a) The convergent lead ages of the oldest monazites and uraninites (Rhodesia, Manitoba, Madagascar, and Transvaal). *Geochim. Cosm. Acta.* 7, 294-300.
- Ahrens, L.H. (1955 b) Implications of the Rhodesia age pattern. *Geochim. Cosm. Acta.* 8, 1-15.
- Baadsgaard, H. (1965) Geochronology. *Medds. fra Dansk. Geol. Foren.* 16, 1-48.
- Baadsgaard, H. and Godfrey, J.D. (1967) Geochronology of the Canadian Shield in N.E. Alberta, I, Andrew Lake Area. *Can. J. Earth Sci.* 4, 541-563.
- Catanzaro, E.J. and Gast, P.W. (1960) Isotopic composition of lead in pegmatitic feldspars. *Geochim. Cosm. Acta.* 19, 113-126.
- Catanzaro, E.J. and Kulp, J.L. (1964) Discordant zircons from the Little Belt (Montana), Beartooth (Montana) and Santa Catalina (Arizona) Mountains. *Geochim. Cosm. Acta.* 28, 87-124.
- Compston, W. and Oversby, V.M. (1969) Lead isotopic analysis using a double-spike. *J. Geophys. Res.* 74, No. 17.
- Cooper, J.A., Reynolds, P.H., and Richards, J.R. (1969) Double-spike calibration of the Broken Hill standard lead. *Earth Planet. Sci. Lett.* 6, 467-478.

- Cumming, G.L., Tsong, F., and Gudjurgis, P.J. (1970) Fractional removal of lead from rocks by volatilization. *Earth Planet. Sci. Lett.* 9, 49-54.
- Dearnley, R. (1966) Orogenic fold-belts and a hypothesis of earth evolution, in "Physics and chemistry of the earth" vol. 7, 10.
- Doe, B.R. (1962) Relationships of lead isotopes among granites, pegmatites, and sulfide ore near Balmat, N.Y. *J. Geophys. Res.* 67, 2895-2906.
- Doe, B.R. and Hart, S.R. (1963) The effect of contact metamorphism of lead in K-feldspars near the Eldora Stock, Colorado. *J. Geophys. Res.* 68, 3521-3530.
- Doe, B.R., Tilton, G.R., and Hopson, C.A. (1965) Lead isotopes in feldspars from selected granitic rocks associated with regional metamorphism. *J. Geophys. Res.* 70, 1947-1968.
- Farquharson, R.B. (1968) Whole-rock isotopic studies in the region of Mount Isa, Queensland. Unpub. Ph.D. thesis, Australian National Univ., Australia.
- Gast, P.W. (1969) Reply to: Comments on paper by P.W.Gast: "The isotopic composition of lead from St. Helena and Ascension Islands" by M.Tatsumoto. *Earth Planet. Sci. Lett.* 7, 227.
- Gerling, E.K. and Shukolyukov, Yu.A. (1962) Age calculations for the Pb/U method using radioactive minerals containing common lead. *Geochemistry (Translation)* No. 5, 458.

- Godfrey, J.D. (1961) Geology of the Andrew Lake, North District, Alberta. Res. Council Alta. Prelim. Rept. 58-3.
- Godfrey, J.D. (1963) Geology of the Andrew Lake, South District, Alberta. Res. Council Alta. Prelim. Rept. 61-2.
- Godfrey, J.D. (1964) Geology of the Colin Lake district, Alberta. Res. Council Alta. Prelim. Rept. 62-2.
- Godfrey, J.D. (1966) Geology of the Bayonet, Ashton, Potts and Charles Lake District, Alberta. Res. Council Alta. Prelim. Rept. 65-6.
- Godfrey, J.D. and Baadsgaard, H. (1962) Structural pattern of the Precambrian Shield in N.E. Alberta and mica age-dates from the Andrew Lake District. Roy. Soc. Can. Spec. Publication IV, 30.
- Godfrey, J.D. and Peikert, E.W. (1963) Geology of the St. Agnes Lake district, Alberta. Res. Council Alta. Prelim. Report 62-1.
- Hamilton, E.I. (1966) The isotopic composition of lead in igneous rocks. Earth Planet. Sci. Lett. 1, 30-37.
- Kanasewich, E.R. (1962) Quantitative interpretations of anomalous lead isotope abundances. Unpub. Ph.D. thesis, Univ, British Columbia, Vancouver, B.C.
- Kanasewich, E.R. and Slawson, W.F. (1964) Precision inter-comparisons of lead isotope ratios: Ivigtut, Greenland. Geochim. Cosm. Acta. 28, 541-550.
- Koster, F. and Baadsgaard, H. (1970) On the geology and geochronology of N.W. Saskatchewan, I. Tazin Lake region. Can. J. Earth Sci. 7, 919-930.

- Murthy, V.R. and Patterson, C.C. (1962) Primary isochron of zero age for meteorites and the earth. *J. Geophys. Res.* 67, 1161.
- Nicolaysen, L.O. (1961) Graphic interpretation of discordant age measurements of metamorphic rocks. *Ann. N.Y. Acad. Sci.* 91, 198-206.
- O'Nions, R.K. (1969) Geochronology of the Bamble Sector of the Baltic Shield, South Norway. Unpub. Ph.D. thesis, Univ. of Alberta, Edmonton, Alberta.
- Ostic, R.G., Russell, R.D., and Reynolds, P.H. (1963) *Nature* 199, 1150.
- Ostic, R.G., Russell, R.D., and Stanton, R.L. (1967) Additional measurements of the isotopic composition of lead from stratiform deposits. *Can. J. Earth Sci.* 4, 245.
- Ozard, J.M. (1970) Solid source lead isotope studies with application to rock samples from the Superior geological province. Unpub. Ph.D. thesis, UBC, Vancouver, B.C.
- Ozard, J.M. and Russell, R.D. (1971) Lead isotope studies of rock samples from the Superior geological province. *Can. J. Earth Sci.* 8, 444-454.
- Patterson, C.C. (1956) Age of meteorites and the earth. *Geochim. Cosm. Acta.* 10, 230.
- Rankama, K. (1954) "Isotope Geology" p.384. Pergamon Press.
- Reynolds, P.H. (1971) A U-Th-Pb isotope study of rocks and ores from Broken Hill, Australia. *Earth Planet. Sci. Lett.* 12, 215-223.
- Riley, G.C. (1960) Geology, Fort Fitzgerald, Alberta. *Geol.*

- Survey of Canada Map 12, (1960).
- Rosholt, J.N. and Bartel, A.J. (1969) U, Th and Pb systematics in Granite Mountains, Wyoming. *Earth Planet. Sci. Lett.* 7, 141-147.
- Russell, R.D. and Ahrens, L.H. (1957) Additional regularities among discordant Pb-U ages. *Geochim. Cosm. Acta.* 11, 213-218.
- Russell, R.D. and Farquhar, R.M. (1960) "Lead isotopes in geology", Chapter 5. Interscience Publishers, N.Y.
- Russell, R.D., Slawson, W.F., Ulrych, T.J., and Reynolds, P.H. (1968) Further applications of concordia plots to rock lead isotope abundances. *Earth Planet. Sci. Lett.* 3, 284-288.
- Silver, L.T. (1970) U-Th-Pb isotope relations in lunar materials. *Science* 167, 468-471.
- Sinha, A.K. (1969) Removal of radiogenic Pb from K-feldspars by volatilization. *Earth Planet. Sci. Lett.* 7, 109-115.
- Stacey, J.S., Delevaux, M., and Ulrych, T.J. (1969) Some triple filament Pb isotope analyses and absolute parameters for single stage leads. *Earth Planet. Sci. Lett.* 6, 15-25.
- Steiger, R.H., and Wasserburg, G.J. (1966) Systematics of the Pb^{208} - Th^{232} , Pb^{207} - U^{235} , and Pb^{206} - U^{238} systems. *J. Geophys. Res.* 71, 6065-6090.
- Stockwell, C.H., McGlynn, J.C., Emslie, R.F., Stanford, B.V., Norris, A.W., Donaldson, J.A., Fahrig, W.F., and Currie, K.L. (1970) Geology of the Canadian Shield, Chapter IV, in "Geology and Economic Minerals of Canada", G.S.C.
- Tatsumoto, M. (1966) Isotopic composition of lead in volcanic rocks from Hawaii, Iwo Jima, and Japan. *J. Geophys. Res.*

- 71, 1721-1734.
- Tatsumoto, M. (1969) Comments on paper by P.W.Gast: "The isotopic composition of lead from St. Helena and Ascension Islands". *Earth Planet. Sci. Lett.* 7, 224-226.
- Tatsumoto, M. and Rosholt, J.N. (1970) Age of the moon: an isotopic study of uranium-thorium-lead systematics of lunar samples. *Science* 167, 461-463.
- Tilton, G.R. (1960) Volume diffusion as a mechanism for discordant lead ages. *J.Geophys. Res.* 65, 2933-2945.
- Tyrrell, J.B. (1896) Report on the country between Athabasca Lake and Churchill River. *Geol. Surv. Can. Annual Rept. (New Ser.)* 8, Part D, 1895.
- Ulrych, T.J. (1964) The anomalous nature of Ivigtut lead. *Geochim. Cosm. Acta.* 28, 1389-1396.
- Ulrych, T.J. (1967) Oceanic basalt leads: A new interpretation and an independent age for the earth. *Science* 158, 252-256.
- Ulrych, T.J. (1969) A comment on the concordia method of interpreting whole-rock U/Pb ratios. *Earth Planet. Sci. Lett.* 7, 116-118.
- Ulrych, T.J., and Reynolds, P.H. (1966) Whole-rock and mineral leads from the Llano Uplift, Texas. *J. Geophys. Res.* 71, 3089-3094.
- Ulrych, T.J., Burger, A., and Nicolaysen, L.O. (1967) Least radiogenic terrestrial leads. *Earth Planet. Sci. Lett.* 2, 179-184.
- Van Niekerk, C.B., and Burger, A. (1968) Pb-isotope dating

- of Zeotlief System, South Africa. *Earth Planet. Sci. Lett.* 4, 211-218.
- Wampler, J.M., and Kulp, J.L. (1964) An isotopic study of lead in sedimentary pyrite. *Geochim. Cosm. Acta.* 28, 1419-1458.
- Wasserburg, G.J. (1963) Diffusion processes in lead-uranium systems. *J. Geophys. Res.* 68, 4823-4846.
- Watanabe, R.Y. (1961) Geology of the Waugh Lake metasedimentary complex, N.E. Alberta. Unpub, M.Sc. thesis, Univ. of Alberta, Edmonton, Alberta.
- Watanabe, R.Y. (1966) Petrology of cataclastic rocks of N.E. Alberta. Unpub. Ph.D. thesis, Univ. of Alberta, Edmonton, Alberta.
- Wetherill, G.W. (1956) Discordant uranium-lead ages, 1. *Trans. Am. Geophys. Union* 37, 320-326.
- Wetherill, G.W. (1963) Discordant uranium-lead ages, 2. Discordant ages resulting from diffusion of lead and uranium. *J. Geophys. Res.* 68, 2957-2965.
- Yoder, H.S. and Eugster, H.P. (1954) Phlogopite synthesis and stability range. *Geochim. Cosm. Acta.* 6, 157-185.
- Zartman, R.E. (1965) The isotopic composition of lead in microclines from the Llano Uplift, Texas. *J. Geophys. Res.* 70, 965-976.
- Zartman, R.E. and Wasserburg, G.J. (1969) The isotopic composition of lead in potassium feldspars from some 1.0 b.y. old North American igneous rocks. *Geochim. Cosm. Acta.* 33, 901-942.

APPENDIX A

THIN SECTION OBSERVATIONS OF 5 ROCK SAMPLES

(1) Foliated hornblende granite (sample 68-1-7)

The rock is cataclastic, contains abundant K-feldspar and lesser plagioclase (some smaller plagioclase grains with altered core and fresh rim are enclosed in K-feldspar); also contains some perthite and microcline. The rock generally shows a partial "mortar" texture in which larger porphyroblasts are surrounded by crushed matrix of crushed quartz bands, fewer dark minerals (hornblende, biotite, with the former a little more abundant than the latter) and small amounts of magnetite. The rock as a whole is more felsic than typical quartz monzonite, strongly strained, and is considered to be a cataclastic or foliated biotite-hornblende granite.

(2) Biotite granite F (sample 68-4-1)

The rock is massive, porphyroblastic in texture. Anhedral to subhedral megacrysts of plagioclase are common and they contain inclusions of biotite. Along corroded margins of some of the plagioclase megacrysts, myrmekitic texture is commonly observed. A slight degree of sericitization is also observed in some plagioclase megacrysts. Some microcline is present. The main dark mineral is biotite which is partly chloritized and forms reddish flakes indicating a somewhat higher temperature (?). The matrix consists of medium grained (< 1 mm.) plagioclase, highly strained and polycrystalline

quartz, biotite, chlorite and muscovite, with little apatite and zircon inclusions in biotite. The rock may have been derived from originally different materials (?). It is considered to be a (cataclastic) biotite-granodiorite.

(3) Grey hornblende granite (sample 68-2-3)

The rock is characterized by large spherical porphyroclasts of perthite and microcline, with subhedral to anhedral plagioclase being the most abundant mineral. The K-feldspar megacrysts contain inclusions of epidote, biotite, apatite, plagioclase and some hornblende. The hornblende is generally chloritized and its original character is hardly recognizable. The matrix is medium-grained, granoblastic and composed of quartz, plagioclase, microcline, biotite, hornblende and epidote. Some plagioclase grains show a distinct undulatory extinction. The rock is considered to be hornblende granodiorite. Watanabe (1966) has mentioned that the rock from this location has not been affected by post-crystalline deformation.

(4) Biotite "q" granite (samples 68-1-5, 68-3-8)

Sample 68-1-5

Abundant porphyroblasts (ranging from 1 to 3 mm.) of rounded to lenticular K-feldspar (mainly orthoclase and microcline) together with a slightly lesser amount of subhedral porphyroblasts of plagioclase are present in a clearly foliated and deformed matrix consisting of wavy

bands of crushed quartz and chloritized biotite which surround the porphyroblasts. Biotite bands commonly enclose small grains of epidote and apatite and could have been hornblende-rich bands. Other constituent minerals of the matrix are magnetite, pyrite, feldspar and muscovite. In both porphyroblasts of K-feldspar and plagioclase, microcrystalline inclusions of the same minerals are common; plagioclase generally shows distinct twinning, and some rimming of feldspar is observed. The rock is considered as (cataclastic) biotite quartz monzonite.

Sample 68-3-8

The rock is mainly composed of large feldspar porphyroclasts in which K-feldspar is slightly in excess or equal to plagioclase in amount. Long strings of brown and green biotite, partly altered to chlorite, fill interstices or are enclosed in the porphyroclasts. The matrix is composed of wavy bands of crushed quartz and chlorite-rich bands which surround the elliptical to augen-shaped feldspar porphyroclasts. As accessory minerals, there are apatite, a little sphene, zircon and, apparently, leucoxene. On close examination leucoxene is found to be fine-grained sphene which appears white in reflected light. The rock is considered as a cataclastic biotite quartz monzonite.

APPENDIX B

THIN SECTION OBSERVATIONS OF 3 ADDITIONAL ROCK SAMPLES

(1) Biotite granite gneiss (sample 68-1-1)

The rock is equigranular, well-foliated in texture, and contains quite abundant amounts of plagioclase, K-feldspar and quartz. The main mafic mineral is biotite. Plagioclase is slightly sericitized, and generally forms anhedral to subhedral porphyroblasts. Mermekitic texture showing intergrowth of quartz with plagioclase (replaced albite) is observed. Microcline, sometimes microcline perthite, is relatively abundant and forms augen-shaped porphyroblasts 0.5 to 1 mm. in diameter. Quartz forms polycrystalline lenticles and rounded inclusions in plagioclase and microcline porphyroblasts. It also shows wavy extinction indicating dynamic compression or shearing. Biotite generally forms greenish brown flakes, commonly chloritized along cleavage planes. Some anhedral to subhedral laths of hornblende are present and they are enclosed as relict grains by chlorite. Accessary minerals mainly consist of apatite, sphene and magnetite.

(2) Leucocratic granite (?) (sample 68-3-6)

This is a much "silicified" rock; most of the quartz is considered to be introduced during deformation. Plagioclase phenocrysts are abundant and comprise about half of the rock. The most common mineral other than the above two is muscovite, some chlorite (most probably altered from

biotite) and a few biotite flakes. Biotite flakes occur together with muscovite as "bridges" across each other (forming the so-called birds-eye aggregates of flakes). These biotite and muscovite are more or less deformed and crumpled. Quartz forms small veins in or replacing the biotite. A little microcline is also seen. The original texture of the rock is destroyed and can hardly be traced. It is almost certain that this is not a normal granite because of its high percentage of plagioclase. It is possibly a simple pegmatite or a mixed pegmatitic-quartzitic rock.

(3) Biotite "q" granite (sample 68-3-7)

The rock is generally strained, contains predominantly subhedral to anhedral porphyroclasts of microcline, with fewer subhedral porphyroclasts of plagioclase showing distinct albite and pericline twinning. (Microcline is about twice as abundant as plagioclase). Most of the dark mineral is chloritized biotite, some chlorite, epidote, little muscovite, opaque minerals (magnetite, hematite), altered allanite (?), occasionally fluorite and accessory minerals (apatite, zircon). The matrix is filled up by polycrystalline quartz aggregates, plagioclase patches, biotite and other opaque minerals. This rock is deformed but not to the extent of sample 1-5 (which is considered to be quartz monzonite), and since it has more (about twice) K-feldspar than plagioclase, it is probably just on

the boundary of quartz monzonite and granite. It is thus considered as a strained biotite granite or biotite quartz monzonite.

Note: The presence of allanite, fluorite, coexistence of muscovite and biotite may indicate that this rock is pegmatite or has associated with pegmatites. According to Yoder and Eugster (1954), the coexistence of biotite and muscovite indicates that crystallization took place between 650 — 825°C and at about 1700 — 4000 atmospheres of water-vapour pressure.

APPENDIX C

CRYSTAL MORPHOLOGY OF ZIRCON SAMPLES

(1) Zircon 68-1-5

Euhedral to anhedral (subrounded) grains of various crystal sizes, the amounts of larger and smaller grains are about equal. Pinkish to reddish brown. Elongation ratio is about 1/3 to 1/4. Some zoned grains with few cracks are present and may contain some acicular inclusions. Smaller subhedral grains may be multifaceted zircons (?). As a whole, this zircon population shows simple crystal habits. Outgrowth or overgrowth is not detected.

(2) Zircon 68-1-7

(1-7A) — mainly large euhedral grains with very few rounded to subrounded grains. Color is pinkish white to translucent. Larger grains appear to contain inclusions and cracks. Few zoned crystals and very few outgrowths are present. Simple crystal habit. Elongation ratio ranges from 1/2 (few large grains), 1/3 (intermediate grains, majority), to $> 1/3$ (thinner and smaller, few).

(1-7B) — slightly smaller than above, same color, excellent euhedral large and small grains. Abundant cracks are visible in most grains but no inclusions present. Very few subhedral grains. Elongation ratio is about 1/4.

(1-7C) — similar in size as 1-7B, mainly euhedral grains which contain some acicular inclusions (obvious when pinkish

inclusions are present in transparent grains). Some grains have rounded cores. Very few smaller subhedral grains are detected. No overgrowth or outgrowth is detected in this fraction.

(3) Zircon 68-2-3

Mainly euhedral small grains (pinkish white) with few slightly larger grains (brownish). Smaller amounts of rounded grains. May include very small amounts of outgrown grains, but no overgrowth is observed. Elongation ratio is about 1/3.

(4) Zircon 68-3-8

(3-8A) — similar amounts of euhedral and anhedral (subrounded to rounded) grains; light brownish white, transparent and red grains. All grains have abundant cracks and appear to contain rounded cores and inclusions. Overgrowth or outgrowth is not detected. Elongation ratio ranges from 1/5 to 1/3.

(3-8B) — similar in size and color as 3-8A; more euhedral grains than sunhedral to rounded grains. Contains abundant inclusions and cracks, some with rounded cores. Zoned crystals are visible. No outgrowth or overgrowth is observable. Elongation ratio is 1/3 to 1/5.

(3-8C) — abundant smaller euhedral grains and few larger grains. Similar color as above. Larger grains contain cracks, rounded cores and acicular inclusions. Rounded grains (rounded to subrounded) consist about half the

sample. Variable crystal size. No zoned or overgrown grains are present. Elongation ratio ranges from 1/3 to 1/4.

(5) Zircon 68-4-1

Small in size, more small subhedral (malformed ?) to rounded crystals than excellently euhedral (larger) crystals. Light brownish white to translucent, few zoned crystals with rounded cores are detected. Acicular inclusions are mainly found in translucent grains. No outgrowth or overgrowth is detectable. Variable crystal size. Elongation ratio ranges from 1/3 to 1/5. This zircon population may be classified into two different types: dark, stumpy multifaceted (malformed ?) zircons; and clear, prismatic zircons with simple sharp bipyramid terminations (also with inclusions and rounded cores).

APPENDIX D

EXTRACTION PROCEDURE OF LEAD

An aliquot of the sample solution was extracted with dilute (0.01% — 0.001%) diphenylthiocarbozone (dithizone) solution and ammonium citrate at a pH of 8 — 9. After back-extracting with 2% HNO_3 and washing with chloroform, the solution containing lead was extracted with dithizone in the presence of 2% potassium cyanide at pH = 8 — 9. The lead was transferred back into an acid phase, and the solution adjusted to pH = 4.5.

Finally, lead was precipitated as PbS with H_2S . The precipitate was centrifuged down, and loaded on an outgassed single Tantalum filament for isotopic measurement.

APPENDIX E

EXTRACTION PROCEDURE OF URANIUM AND THORIUM

A sample solution (or aliquot in the case of zircon) was mixed with a double-spike isotope dilutant of ^{235}U and ^{230}Th , then uranium and thorium hydroxides were precipitated together with R_2O_3 by adding ammonium hydroxide (NH_4OH). The centrifuged precipitate was then dissolved in 10 ml. 6N HNO_3 , and added to a 14 x 1.2 cm. Dowex 1-x8 anion exchange resin column which was preset and cleaned with 0.5M HNO_3 and washed with 40 ml. 6M HNO_3 .

Uranium was eluted from the column with 40 ml. 6M HNO_3 after eluting 75 ml. 6M HNO_3 through the column.

Thorium was then removed from the column by stripping with 40 ml. 0.5M HNO_3 after passing 80 ml. 6M HNO_3 through the column.

Uranium and thorium eluents were then evaporated to dryness, and stored for isotopic measurement.

B30013